



Search for charginos and neutralinos with $B - L$ R -parity violating decays in $\sqrt{s} = 13$ TeV and 13.6 TeV pp collisions with the ATLAS detector

The ATLAS Collaboration

A search is performed for the electroweak pair production of charginos and associated production of a chargino and neutralino, each of which decays through an R -parity-violating coupling into a lepton and a W , Z , or Higgs boson. This search targets the Higgs boson decay channel of the charginos and neutralinos, using events with three or more b -tagged jets and one or two electrons or muons. The analyzed data corresponds to an integrated luminosity of 140 fb^{-1} and 56 fb^{-1} of proton–proton collision data produced by the Large Hadron Collider at center-of-mass energies of $\sqrt{s} = 13$ TeV and $\sqrt{s} = 13.6$ TeV respectively, collected by the ATLAS experiment between 2015 and 2023. The data are found to be consistent with predictions from the Standard Model. The results are interpreted as limits at 95% confidence level on model-independent cross sections for processes beyond the Standard Model. Limits are also set on the production of charginos and neutralinos for a Minimal Supersymmetric Standard Model with an additional $B - L$ gauge symmetry that is spontaneously broken. Charginos and neutralinos with masses between 150 GeV and 1100 GeV are excluded at 95% confidence level for a scenario in which they decay via Higgs bosons, assuming equal decay branching fractions to each lepton flavor. Additional limits are derived for flavor-specific decay scenarios.

Contents

1	Introduction	2
2	ATLAS detector	4
3	Data and simulated samples	5
4	Object reconstruction	7
5	Event selection	9
	5.1 Analysis variables	9
	5.2 Region definitions	10
6	Background estimation	12
	6.1 Background-only fit results	13
7	Systematic uncertainties	14
8	Results	16
	8.1 Background-only fit results	17
	8.2 Model-independent results	17
	8.3 Model-dependent exclusion limits	18
9	Conclusion	20

1 Introduction

Supersymmetry (SUSY) is an extension of the Standard Model (SM) [1–6] that offers solutions to many open problems in particle physics, including the hierarchy problem [7–10]. However, the full SUSY model space allows for baryon number (B) and lepton number (L) violation. While this can lead to rapid proton decay or large flavor-changing neutral currents in processes like $\mu \rightarrow e\gamma$, these processes can be prevented by requiring conservation of R -parity [11], a multiplicative quantum number defined as $R = (-1)^{3(B-L)+2s}$, where s is the particle’s spin. Enforcing the conservation of R -parity (or equivalently, the quantity $B - L$) has additional phenomenological consequences for SUSY models. SM particles have $R = +1$, whereas their SUSY partner particles (“superpartners”) have $R = -1$. Therefore, in R -parity conserving SUSY models, superpartners must be pair-produced at the Large Hadron Collider (LHC) [12], and the lightest supersymmetric particle (LSP) must be stable.

R -parity conservation, however, is an ad hoc solution, and may be too restrictive; there are phenomenologically viable R -parity violating (RPV) SUSY theories. One such theory, known as the $B - L$ Minimal Supersymmetric Standard Model, introduces a $U(1)_{B-L}$ gauge symmetry in addition to the SM $SU(3)_C \times SU(2)_L \times U(1)_Y$ gauge group, along with right-handed sterile neutrinos [13–16]. When the superpartners to the right-handed neutrino fields obtain a vacuum expectation value, the $U(1)_{B-L}$ symmetry is spontaneously broken in a way that violates only lepton number, while providing a mechanism to give the left-handed Standard Model neutrinos their small masses. RPV couplings allow direct decay of superpartners to SM particles, including the decay of the LSP, producing signatures that are forbidden in

R -parity conserving theories. These couplings remain weak, so the production mechanisms of superpartners are not significantly affected.

A wino LSP and next-to-lightest supersymmetric particle (NLSP), superpartners to the electroweak bosons whose primary component comes from the W boson superpartners, provide a unique search scenario for this model due to the possibility of a charged LSP. The charged component, the chargino $\tilde{\chi}_1^\pm$, and the neutral component, the neutralino $\tilde{\chi}_1^0$, are expected to be nearly mass-degenerate, with less than 200 MeV mass difference [17, 18]. This small mass splitting suppresses R -parity conserving decays of the NLSP to the LSP. The chargino undergoes prompt RPV decays into a Higgs boson and a charged lepton ($\tilde{\chi}_1^\pm \rightarrow h\ell^\pm$), to a Z boson and a charged lepton ($\tilde{\chi}_1^\pm \rightarrow Z\ell^\pm$), or to a W boson and a neutrino ($\tilde{\chi}_1^\pm \rightarrow W^\pm\nu$). Similarly, the neutralino undergoes prompt decays into a Higgs boson and a neutrino ($\tilde{\chi}_1^0 \rightarrow h\nu$), to a Z boson and a neutrino ($\tilde{\chi}_1^0 \rightarrow Z\nu$), or to a W boson and a charged lepton ($\tilde{\chi}_1^0 \rightarrow W^\pm\ell^\mp$). While the proportion of these decays depends on parameters of the SUSY theory, the branching fractions for decays for $\tilde{\chi}_1^\pm \rightarrow h\ell^\pm$ and $\tilde{\chi}_1^0 \rightarrow h\nu$ are expected to be above 80% for most scenarios [18] and are therefore targeted in this search. The relative branching fractions of these decays for different lepton flavors depends on the neutrino mass hierarchy [18].

This paper presents a search for chargino-chargino pair production ($\tilde{\chi}_1^\pm\tilde{\chi}_1^\mp$) and chargino-neutralino production ($\tilde{\chi}_1^\pm\tilde{\chi}_1^0$) with RPV $\tilde{\chi}_1^\pm \rightarrow h\ell^\pm$ and $\tilde{\chi}_1^0 \rightarrow h\nu$ decays. The data was collected with the ATLAS detector in proton–proton (pp) collisions at the LHC and comprises 140 fb^{-1} at $\sqrt{s} = 13\text{ TeV}$ taken from 2015–2018 (Run 2) and 56 fb^{-1} at $\sqrt{s} = 13.6\text{ TeV}$ taken from 2022–2023 (partial Run 3). This analysis only considers the dominant decay of the Higgs boson into b -quarks ($\mathcal{B}(h \rightarrow b\bar{b}) = 58\%$). Higgs bosons are reconstructed from pairs of jets, and the selection requires at least three jets to be identified as originating from b -hadrons (b -tagged jets). Diagrams for the signal model are shown in Figure 1. In the case of $\tilde{\chi}_1^\pm\tilde{\chi}_1^\mp$ production, final states should contain two leptons with opposite-sign electric charge, while for $\tilde{\chi}_1^\pm\tilde{\chi}_1^0$ production, final states should contain one lepton and missing transverse momentum (\vec{p}_T^{miss} , with magnitude E_T^{miss}), due to the undetected neutrino. While τ -leptons are not explicitly targeted by this search, they are included in the signal sample generation and contribute to the sensitivity through their leptonic decays. The search strategy aims at reconstructing the mass of the chargino m_C from Higgs–lepton resonances and the transverse mass of the neutralino $m_{N,T}$ from a Higgs boson and the \vec{p}_T^{miss} .

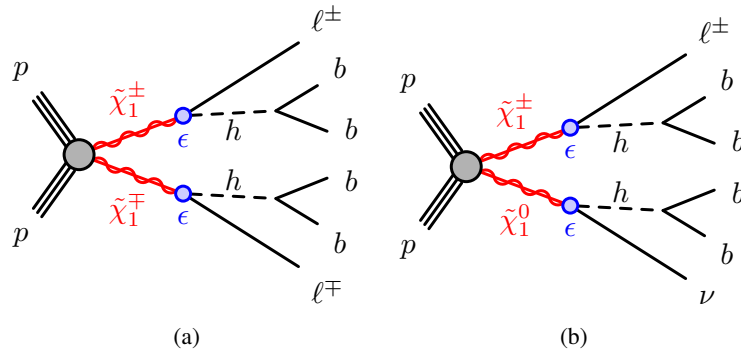


Figure 1: Representative diagrams of the signal model processes considered in this analysis with (a) the chargino–chargino process ($\tilde{\chi}_1^\pm\tilde{\chi}_1^\mp$) and (b) the chargino–neutralino process ($\tilde{\chi}_1^\pm\tilde{\chi}_1^0$). The RPV effective vertices are marked with the bilinear RPV coupling ϵ .

A previous ATLAS search for electroweakino pair production with RPV decays targeted chargino decays

into $Z\ell$ with subsequent $Z \rightarrow \ell\ell$ by searching for a trilepton resonance using the full Run 2 dataset [19]. The search described in this paper provides complementary sensitivity by targeting chargino and neutralino decays into Higgs bosons and leptons, making use of different regions of phase space.

A dedicated series of Run 2 searches for RPV $B - L$ scenarios has also been carried out considering the superpartner of the top quark to be the LSP [20, 21]. These were optimized for the pair production of top squarks with RPV decays into a bottom quark and charged lepton. The final state signature is a pair of resonances formed from a b -jet and a lepton, requiring ≥ 1 b -jets in the signal region.

This analysis benefits from developments in the capability of identifying jets originating from b -hadrons, namely the GN2 algorithm [22], which allows significantly better background reduction as compared with the previous algorithm. The analysis also benefits from strong background rejection due to the requirement of reconstructing two Higgs boson candidates. The sensitivity in the $\tilde{\chi}_1^\pm \tilde{\chi}_1^0$ channel is driven by low background due to tight selections, while the sensitivity in the $\tilde{\chi}_1^\pm \tilde{\chi}_1^\mp$ channel is due to good mass resolution for the chargino resonance from the reconstruction algorithms.

This paper is organized as follows. The ATLAS detector is described in Section 2. The data and simulated samples used are described in Section 3. Analysis objects are defined in Section 4. The definition of analysis regions and the background estimation strategy are described in Section 5 and Section 6 respectively. Systematic uncertainties are discussed in Section 7, and analysis results are shown in Section 8. Concluding remarks are made in Section 9.

2 ATLAS detector

The ATLAS experiment [23, 24] at the LHC is a multipurpose particle detector with a forward–backward symmetric cylindrical geometry and a near 4π coverage in solid angle.¹ It consists of an inner tracking detector (ID) surrounded by a thin superconducting solenoid providing a 2 T axial magnetic field, electromagnetic and hadronic calorimeters, and a muon spectrometer (MS). The inner tracking detector covers the pseudorapidity range $|\eta| < 2.5$. It consists of silicon pixel (including the insertable B-layer), silicon microstrip, and transition radiation tracking detectors. Lead/liquid-argon (LAr) sampling calorimeters provide electromagnetic (EM) energy measurements with high granularity within the region $|\eta| < 3.2$. A steel/scintillator-tile hadronic calorimeter covers the central pseudorapidity range ($|\eta| < 1.7$). The endcap and forward regions are instrumented with LAr calorimeters for EM and hadronic energy measurements up to $|\eta| = 4.9$. The muon spectrometer surrounds the calorimeters and is based on three large superconducting air-core toroidal magnets with eight coils each. The field integral of the toroids ranges between 2.0 and 6.0 T m across most of the detector. The muon spectrometer includes a system of precision tracking chambers up to $|\eta| = 2.7$ and fast detectors for triggering up to $|\eta| = 2.4$. The luminosity is measured mainly by the LUCID–2 detector that is located close to the beampipe. A two-level trigger system was used to select events [25, 26]. The first-level trigger is implemented in hardware and used a subset of the detector information to accept events at a rate close to 100 kHz. This is followed by a software-based trigger that reduced the accepted rate of complete events to 1.25 kHz and 3 kHz on average

¹ ATLAS uses a right-handed coordinate system with its origin at the nominal interaction point (IP) in the center of the detector and the z -axis along the beam pipe. The x -axis points from the IP to the center of the LHC ring, and the y -axis points upwards. Polar coordinates (r, ϕ) are used in the transverse plane, ϕ being the azimuthal angle around the z -axis. The pseudorapidity is defined in terms of the polar angle θ as $\eta = -\ln \tan(\theta/2)$ and is equal to the rapidity $y = \frac{1}{2} \ln \left(\frac{E+p_z}{E-p_z} \right)$ in the relativistic limit.

Angular distance is measured in units of $\Delta R \equiv \sqrt{(\Delta y)^2 + (\Delta\phi)^2}$.

in Run 2 and Run 3, respectively, depending on the data-taking conditions. A software suite [27] is used in data simulation, in the reconstruction and analysis of real and simulated data, in detector operations, and in the trigger and data acquisition systems of the experiment.

3 Data and simulated samples

This analysis is performed using pp collision data collected by the ATLAS experiment during Run 2 of the LHC from 2015 to 2018 and Run 3 of the LHC from 2022 to 2023. The LHC collided protons at a center-of-mass energy of $\sqrt{s} = 13$ TeV during Run 2 and $\sqrt{s} = 13.6$ TeV during Run 3. The data sample corresponds to a total integrated luminosity of 196 fb^{-1} , with 140 fb^{-1} from Run 2 and 56 fb^{-1} from Run 3. The uncertainty in the 2015–2018 (2022–2023) integrated luminosity is 0.83% [28] (2.0% [29]), obtained using the LUCID-2 detector [30] for the primary luminosity measurements, complemented by measurements using the inner detector and calorimeters. Data quality requirements are applied to ensure that only data with stable LHC beams and operational subdetectors are used [31]. Data were collected using triggers requiring the presence of an electron or a muon [26, 32, 33]. The triggers have varying requirements on the identification working point, isolation, and transverse momentum (p_T) thresholds of the leptons.

Monte Carlo (MC) simulations are used to model the signals and SM background processes for this analysis. All samples were produced with the ATLAS simulation framework [27, 34] based on GEANT4 [35]. The signal samples simulate $\tilde{\chi}_1^\pm \tilde{\chi}_1^\mp$ and $\tilde{\chi}_1^\pm \tilde{\chi}_1^0$ production at leading order (LO) with up to two additional partons in the matrix element. In the benchmark model considered, the masses of the chargino and neutralino are set to be equal. The production cross sections are computed at next-to-leading-order (NLO) plus next-to-leading-logarithm (NLL) precision in a limit of mass-degenerate wino $\tilde{\chi}_1^\pm$ and $\tilde{\chi}_1^0$, with all the other sparticles assumed to be heavy and decoupled [36–38]. These vary from about 2612 fb (5181 fb) for $\tilde{\chi}_1^\pm \tilde{\chi}_1^\mp$ ($\tilde{\chi}_1^\pm \tilde{\chi}_1^0$) production at a chargino and neutralino mass of 150 GeV to about 0.62 fb (1.34 fb) for $\tilde{\chi}_1^\pm \tilde{\chi}_1^\mp$ ($\tilde{\chi}_1^\pm \tilde{\chi}_1^0$) production at 1000 GeV for Run 2, with slightly higher cross sections for Run 3. The decay branching ratios are set to $\mathcal{B}(\tilde{\chi}_1^\pm \rightarrow h\ell^\pm) = 100\%$ and $\mathcal{B}(\tilde{\chi}_1^0 \rightarrow h\nu) = 100\%$, with equal branching fractions to each lepton generation. Samples were generated with MADGRAPH5_AMC@NLO 3.5.3 [39] with the NNPDF3.0NLO [40] parton distribution function (PDF). The parton shower, hadronization, and underlying event were modeled using PYTHIA 8.310 [41] with the A14 set of tuned parameters (tune) [42]. The MC setup for the signal, along with the SM background processes, is shown in Table 1.

The dominant background in this analysis is from top-quark pair production ($t\bar{t}$). The production of $t\bar{t}$ events was modeled using the POWHEG Box v2 [47–50] generator at NLO with the NNPDF3.0NLO PDF set and the h_{damp} parameter² set to $1.5 m_{\text{top}}$ [65]. The events were interfaced to PYTHIA 8.230(8.308) [51] for Run 2 (Run 3) to model the parton shower, hadronization, and underlying event, with parameters set according to the A14 tune and using the NNPDF2.3LO set of PDFs [66].

These $t\bar{t}$ events are separated by particle flavor into $t\bar{t}$ with additional light-flavor jets ($t\bar{t} + \text{light}$), c -jets ($t\bar{t} + \geq 1c$), or b -jets ($t\bar{t} + \geq 1b$). This classification uses generator-level jets, which are reconstructed from stable particles using the anti- k_r algorithm [67, 68] with a radius parameter of $R = 0.4$. The filtering classifies the flavor of generator-level jets by using a ΔR matching with heavy-flavor hadrons (excluding

² The h_{damp} parameter is a resummation damping factor and one of the parameters that controls the matching of POWHEG matrix elements to the parton shower. It thus effectively regulates the high- p_T radiation against which the $t\bar{t}$ system recoils.

Table 1: Details of the MC simulation for each physics process, including the calculations used for normalization, the generator used for the parton shower (PS) and hadronization, the PS parameter tunes, and the order in α_s of the production cross-section calculations. NLO stands for next-to-leading-order, NNLO stands for next-to-next-to-leading-order, NLL stands for next-to-leading-logarithm, and NNLL stands for next-to-next-to-leading-logarithm. The default table values are for Run 2, with Run 3 in parentheses if they differ.

Process	Event generator	PS and hadronization	PS tune	Cross section accuracy
$\tilde{\chi}_1^\pm \tilde{\chi}_1^\mp$ and $\tilde{\chi}_1^\pm \tilde{\chi}_1^0$	MADGRAPH5_AMC@NLO 3.5.3 [39]	PYTHIA 8.310 [41]	A14 [42]	NLO+NNL
$t\bar{t}b\bar{b}$	POWHEG BOX RES [43] and OPENLOOPS [44–46]	PYTHIA 8.309(8.312)	A14	NLO
$t\bar{t}$	POWHEG BOX v2 [47–50]	PYTHIA 8.230(8.308) [51]	A14	NNLO+NNLL [52–58]
$t\bar{t}h$	POWHEG BOX v2	PYTHIA 8.230(8.308)	A14	NLO [59]
$t\bar{t}W$	SHERPA2.2.14 [60]	SHERPA2.2.14	Default	NLO [59]
$t\bar{t}Z$	MADGRAPH5_AMC@NLO 2.8.1(3.5.1)	PYTHIA 8.210(8.309)	A14	NLO [59]
Single-top (s/t -channel)	POWHEG BOX v2	PYTHIA 8.230(8.308)	A14	NNLO [61]
Single-top (Wt)	POWHEG BOX v2	PYTHIA 8.309(8.308)	A14	NNLO+NNLL [62, 63]
Diboson	SHERPA2.2	SHERPA2.2	Default	NLO
V +jets	SHERPA2.2.11(2.2.14)	SHERPA2.2.11(2.2.14)	Default	NNLO [64]

hadrons with the top quark or W boson as parent particles). Generator-level jets with $p_T > 15$ GeV and $|\eta| < 2.5$ are labeled b -flavored if they are matched within $\Delta R = 0.4$ to a b -hadron with $p_T > 5$ GeV, and events containing at least one such jet are labeled $t\bar{t} + \geq 1b$ events. Jets that are not matched to a b -hadron but are matched to a c -hadron with $p_T > 5$ GeV within $\Delta R = 0.4$ are labeled c -flavored, and events containing at least one such jet and no b -flavored jets are labeled $t\bar{t} + \geq 1c$ events. All $t\bar{t}$ events that do not contain a b -flavored or c -flavored jet are classified as $t\bar{t}$ + light events. The $t\bar{t} + \geq 1b$ events are removed from the inclusive $t\bar{t}$ sample and are instead modeled with dedicated $t\bar{t}b\bar{b}$ samples. The $t\bar{t} + \geq 1c$ and $t\bar{t}$ + light events are removed from the $t\bar{t}b\bar{b}$ samples. These $t\bar{t}b\bar{b}$ events were produced using the POWHEG BOX RES [43] generator at NLO and OPENLOOPS [44–46], and the NNPDF3.1_{NLO} [69] PDF set. The events were interfaced to PYTHIA 8.309(8.312) in Run 2 (Run 3) using the A14 set of tuned parameters and using the NNPDF2.3_{LO} set of PDFs. The four-flavor scheme was used with the b -quark mass set to 4.95 GeV.

The production of $t\bar{t}h$ events was modeled using the POWHEG BOX v2 [70] generator at NLO with the NNPDF3.0_{NLO} PDF set. The production of $t\bar{t}Z$ events was modeled using the MADGRAPH5_AMC@NLO 2.8.1 (3.5.1) generator at NLO with the NNPDF3.0_{NLO} PDF in Run 2 (Run 3). The production of $t\bar{t}W$ events was modeled using SHERPA 2.2.14 [60] with up to one additional parton at NLO and two additional partons at LO and the NNPDF3.0_{NNLO} [40] PDF set. Events from the $t\bar{t}h$, $t\bar{t}Z$, and $t\bar{t}W$ processes are collectively labeled $t\bar{t}X$.

Single-top s - and t -channel production were modeled using the POWHEG BOX v2 [50] generator at NLO in QCD in the five-flavor scheme with the NNPDF3.0_{NLO} PDF set, while Wt samples were generated using POWHEG BOX v2 at NLO interfaced with PYTHIA 8.309 (PYTHIA 8.308) for Run 2 (Run 3). The Wt samples used the diagram removal scheme [71]. Diboson production was modeled using the SHERPA 2.2.14 or 2.2.16 generator depending on the process, including off-shell effects and Higgs boson contributions, where appropriate. Fully leptonic final states and semileptonic final states were generated using matrix elements at NLO accuracy in QCD for up to one additional parton and at LO accuracy for up to three additional parton emissions. Samples for $gg \rightarrow VV$ were generated for Run 2 using SHERPA 2.2.2 with LO-accurate matrix elements for up to one additional parton emission for both the cases of fully leptonic and semileptonic final states. The NNPDF3.0_{NNLO} PDF set was used for all diboson samples. The production of V +jets was modeled using SHERPA 2.2.14 in Run 3 as well as in Run 2 $Z \rightarrow \tau\tau$, and SHERPA 2.2.11 for the remainder of Run 2 processes, with up to two additional partons at NLO and up to five additional partons at LO.

The virtual QCD corrections were provided by the OPENLOOPS library. The NNPDF3.0_{NLO} PDF set was used.

For all samples using SHERPA, the matrix elements were merged with the parton shower using the MEPS@NLO prescription [72–75]. For all samples using PYTHIA for the parton shower model, the decays of bottom and charm hadrons were simulated using EVTGEN [76]. The effect of multiple interactions in the same and neighboring bunch crossings (pileup) was modeled by overlaying [77] the simulated hard-scattering event with inelastic pp events generated from a mix of EPOS 2.0.1.4 [78] and PYTHIA 8.308. The EPOS events were generated with the EPOS LHC tune [79] and the PYTHIA events with the A3 tune [80] and the NNPDF2.3_{LO} set of PDFs. PYTHIA pileup events include either a high- p_T jet, a prompt photon, or a lepton from a b -hadron decay, while EPOS was filtered to simulate all remaining pileup events in the overlay sample. The individual simulations were first reweighted to ensure a smooth connection across jet p_T then the combination reweighted to match the distribution of the actual number of interactions per bunch crossing (μ) measured in data.

4 Object reconstruction

Charged-particle tracks are required to have $p_T > 0.5$ GeV [81–83]. Primary vertex candidates are reconstructed from at least two charged-particle tracks [84]. To identify the hard-scattering interaction, the event’s primary vertex is chosen as the vertex with the largest sum of the squared track p_T ($\sum p_{T,\text{track}}^2$).

Electrons, muons, and jets are defined for this analysis at two levels: “baseline” and “signal-quality”. Baseline objects are used as inputs to the \vec{p}_T^{miss} calculation and overlap removal, while signal-quality objects are used for event selections. A summary of the p_T and η requirements on signal-quality objects is shown in Table 2. Electrons are reconstructed as described in Ref. [85] and are calibrated based on the procedure and results described in Refs. [85, 86]. For Run 3, there are additional corrections on the insitu scale and resolution corrections that account for small differences in the ATLAS reconstruction software, increased uncertainties to reflect the Run 3 pileup conditions, and a change in optimal filtering coefficients for the LAr calorimeter readout. Baseline electrons are required to satisfy the *Loose* likelihood identification criteria with at least one B-layer hit [87] and have $p_T > 10$ GeV, $|\eta| < 2.47$, and a selection of $|z_0 \sin(\theta)| < 0.5$ mm on the longitudinal impact parameter z_0 . Baseline electrons that survive the overlap removal procedure described at the end of this section, satisfy the *Loose (Tight)* isolation requirements [87] in Run 2 (Run 3), satisfy the *Tight* identification criteria, have $p_T > 40$ GeV, and have a transverse impact parameter significance $|d_0|/\sigma(d_0) < 5$ are labeled as signal-quality electrons. The large p_T threshold is used to suppress jets and photons misidentified as electrons.

Muons are identified using tracks in the ID and MS, and are calibrated to match data [88, 89]. Baseline muons are required to satisfy the *Medium* identification requirement [90] and have $p_T > 10$ GeV, $|\eta| < 2.7$, and a selection of $|z_0 \sin(\theta)| < 0.5$ mm. For Run 3, baseline muons are also required to have $|\eta| < 2.5$. Other selections and requirements match those used in Run 2. Muons with transverse impact parameter $|d_0| \geq 0.2$ mm or longitudinal impact parameter $|z_0| \geq 1$ mm are removed to reject muons originating from cosmic-ray interactions, and events containing baseline muons flagged as bad due to misalignments between the inner detector and muon spectrometer are vetoed. Baseline muons that survive overlap removal, satisfy the *Loose* isolation working point, satisfy the *HighPt* identification criteria [90], have $p_T > 40$ GeV, and have transverse impact parameter significance $|d_0|/\sigma(d_0) < 3$ are labeled signal-quality muons. Events with signal-quality muons flagged as bad are again removed, as the criteria are different for the *HighPt* working point. The large p_T threshold is used to suppress objects misidentified as muons.

Table 2: Summary of the p_T and η requirements for signal-quality objects. Signal-quality electrons and jets use the same requirements in Run 2 and Run 3.

Signal-quality Object	p_T [GeV]	$ \eta $
Electrons	> 40	< 2.47
Muons (Run 2)	> 40	< 2.7
Muons (Run 3)	> 40	< 2.5
Jets	> 20	< 2.8

Jets are reconstructed using the anti- k_t algorithm [67, 68] with a radius parameter of $R = 0.4$. This uses particle-flow objects [91] as inputs, which are formed using calorimeter energy clusters [92] and ID tracks. Calibrations are applied for the jet energy scale and jet energy resolution, and include components derived both from simulation and *in situ* measurements [93]. Events containing jets from non-collision backgrounds are vetoed [94]. Baseline jets are required to have $p_T > 20$ GeV and $|\eta| < 2.8$. Baseline jets are used in the overlap removal described below. Baseline jets that survive overlap removal are subjected to jet vertex tagger (JVT) requirements to suppress pileup, with remaining jets labeled signal-quality jets. Jets with $p_T < 60$ GeV and $|\eta| < 2.5$ are subjected to the *FixedEffPt* JVT working point [95] while jets with $p_T < 60$ GeV and $|\eta| > 2.5$ use the *Loose* forward jet vertex tagger (fJVT) working point [96].

Jets containing b -hadrons (b -jets) are identified using the GN2 tagger at a working point corresponding to 77% efficiency as measured in $t\bar{t}$ events [22]. The tagger uses a transformer-based model utilizing information about secondary vertices and other jet and track properties to identify b -jets.

Baseline photons are reconstructed as described in Ref. [85]. They are required to satisfy the *Tight* identification working point [85, 87] and have $p_T > 25$ GeV and $|\eta| < 2.37$. The *Tight* identification working point removes photons in the crack region of the detector, $1.37 < |\eta| < 1.52$. Baseline photons are used in the \vec{p}_T^{miss} calculation, but not in the overlap removal procedure described below nor in any analysis selections.

The missing transverse momentum \vec{p}_T^{miss} , with magnitude E_T^{miss} , is defined as the negative vector sum of the p_T of all selected and calibrated baseline physics objects in the event, with an extra term added to account for soft energy in the event that is not associated with any of the selected objects [97]. This soft term is calculated from inner detector tracks matched to the primary vertex to make it more resilient to pileup contamination. Jets that fail to meet the JVT requirement are not considered in the \vec{p}_T^{miss} calculation, while jets that fail to meet the fJVT requirement are considered.

A procedure is applied to remove overlaps between baseline electrons, muons, and jets. First, any muon that is identified using the calorimeter and shares an ID track with an electron is rejected. Next, any electron sharing an ID track with a remaining muon is removed. If a jet is found to be within $\Delta R = 0.2$ of a remaining electron, the jet is removed. If an electron is found to be within $\Delta R = 0.4$ from a remaining jet, the electron is removed. Next, any jet with an associated muon ID track or a muon within $\Delta R = 0.2$ of its axis is removed if the jet has less than three tracks. Lastly, any muon is removed if it is found to be within $\Delta R = 0.4$ from any remaining jet.

5 Event selection

The event selection for $\tilde{\chi}_1^\pm \tilde{\chi}_1^\mp \rightarrow h\ell^\pm h\ell^\mp \rightarrow b\bar{b}\ell^\pm b\bar{b}\ell^\mp$ and $\tilde{\chi}_1^\pm \tilde{\chi}_1^0 \rightarrow h\ell h\nu \rightarrow b\bar{b}\ell b\bar{b}\nu$ requires events to have at least four jets, at least two of which must be identified as b -jets, and have at least one electron or muon. If there are two or more electrons or muons in an event, the two leading leptons are required to have opposite charge. Reconstructed signal-quality leptons, defined in Section 4, have tighter identification working point requirements than applied at online level to ensure high trigger efficiency for selected events. Events are required to have at least one reconstructed signal-quality lepton that activated one of the triggers and has an offline p_T higher than a trigger-dependent offline threshold. The lowest p_T thresholds are 27 GeV (27.3 GeV) for electrons (muons) in 2015–2018, while for 2022–2023 they are 27 GeV (25.2 GeV).

5.1 Analysis variables

Higgs boson candidates are reconstructed using four jets. If there are four or more b -jets in an event, the four with the highest p_T are used. If there are fewer than four b -jets, all of the b -jets in the event are used, with the highest p_T non- b -tagged jets used for the remaining Higgs boson candidate jets. The jets are paired to form two Higgs boson candidates by looking for pairs of jets with a small opening angle $\Delta R_{jj}(h)$, where $\Delta R_{jj}(h)$ is the angular distance between the two jets from the decay of the Higgs boson h and is calculated for each possible pairing. The jet pairing that minimizes $\max(\Delta R_{jj}(h_1), \Delta R_{jj}(h_2))$ is chosen. Studies on generator-level signal MC simulations show that this algorithm makes the correct assignment around 40% of the time for low chargino masses, rising to 95% of the time for high chargino masses. The highest p_T Higgs boson candidate is labeled h_1 and the other is labeled h_2 . The reconstructed masses of the Higgs boson candidates are referred to as m_{h_1} and m_{h_2} , respectively.

Higgs boson candidates, electrons, muons, and \vec{p}_T^{miss} are used to reconstruct chargino and neutralino candidates. First, the four-momentum of each Higgs boson candidate is rescaled by the factor required to yield an invariant mass of 125 GeV to improve the mass resolution of the reconstructed charginos and neutralinos, as studied in signal MC simulation. This correction is only applied for the chargino and neutralino reconstruction. In events with two or more charged leptons, the two Higgs boson candidates and the two leading leptons are used to reconstruct two chargino candidates by pairing each Higgs boson candidate with one lepton. Both possible pairings are tested, and the pairing with the minimum mass asymmetry is selected. The mass asymmetry is defined as

$$A_C = \frac{|m_{C1} - m_{C2}|}{m_{C1} + m_{C2}}, \quad (1)$$

where the m_{C1} is the mass of the chargino candidate with the higher reconstructed mass and m_{C2} is the mass of the chargino candidate with the lower reconstructed mass. The alternative jet pairing with the maximum mass asymmetry is used to define the variable m_{C2}^{rej} , which corresponds to the lower of the two reconstructed chargino candidate masses in that “rejected” pairing. In events with only one charged lepton, one Higgs boson candidate is paired with the lepton to form a chargino candidate, while the other is paired with the \vec{p}_T^{miss} (representing the neutrino in the signal model) to form a neutralino candidate. The 1-lepton channel is optimized to search for high-mass charginos and neutralinos, which tend to each decay into a back-to-back Higgs boson and lepton. The pairing that maximizes the ΔR between the Higgs boson candidate and the charged lepton is therefore used. As only the transverse component of the neutrino momentum is available (from \vec{p}_T^{miss}), the mass of the neutralino cannot be fully reconstructed. Instead, the

neutralino’s transverse mass $m_{N,T} = m_T(h, \vec{p}_T^{\text{miss}})$ is used. The transverse mass of objects i, j is calculated as

$$m_T(i, j) = \sqrt{m_i^2 + m_j^2 + 2(E_{T,i}E_{T,j} - p_{T,i}p_{T,j} \cos(\Delta\phi_{ij}))}, \quad (2)$$

where $\Delta\phi_{ij}$ is the transverse angular separation between the objects and $E_{T,i} = \sqrt{m_i^2 + p_{T,i}^2}$. The \vec{p}_T^{miss} is assumed to come from a massless neutrino. For both 1-lepton and 2-lepton regions, H_T is defined as the scalar sum of p_T of the four jets and 1–2 charged leptons used in the chargino and neutralino reconstruction.

5.2 Region definitions

Two signal regions (SRs) are defined for this analysis, SR2 ℓ and SR1 ℓ . These regions are used to search for new physics in a simultaneous fit, described in more detail in Sections 6 and 8. Their definitions, as well as those of the control and validation regions described in Section 6, are shown in Table 3 and Table 4 respectively. Each region has a Run 2 and a Run 3 counterpart, using the same definitions.

SR2 ℓ targets $\tilde{\chi}_1^\pm \tilde{\chi}_1^\mp$ production in events with two leptons (2 ℓ). The reconstructed Higgs boson masses, m_{h_1} and m_{h_2} are required to be close to the Higgs boson mass of 125 GeV. The m_{h_2} requirements are shifted to lower masses as muons and neutrinos from b -hadron decays can lead to an underestimate of the Higgs boson mass. The H_T selection is used to reject lower-energy background processes, while the requirement that the dilepton invariant mass $m_{\ell\ell}$ is at least 15 GeV higher than the Z boson mass is used to reject processes with leptonic Z decays including $t\bar{t}Z$, Z +jets, and diboson production. The A_C requirement rejects background processes by ensuring that the two reconstructed chargino masses are consistent. The $m_{C_2}^{\text{rej}}$ selection reduces $t\bar{t}$ backgrounds. SR2 ℓ is binned in m_{C_1} , using eight bins with lower bin edges of [125, 175, 225, 300, 400, 500, 600, 700] GeV, where the last bin includes all events with $m_{C_1} > 700$ GeV. The bins start at 125 GeV as the chargino must be heavier than the Higgs boson. The bins are narrower at low masses to capture features of the distribution and wider at high masses to avoid creating bins with very low event counts. The expected pre-fit distribution of m_{C_1} in Run 2 SR2 ℓ using this binning is shown in Figure 2(a).

SR1 ℓ targets $\tilde{\chi}_1^\pm \tilde{\chi}_1^0$ production in events with one lepton (1 ℓ). This region makes use of the higher cross section relative to $\tilde{\chi}_1^\pm \tilde{\chi}_1^\mp$ to provide increased signal yields for high-mass signals. Similarly to SR2 ℓ , the two reconstructed Higgs boson candidates are required to have masses consistent with the Higgs boson mass. The H_T selection of 800 GeV is tighter than for SR2 ℓ , as SR1 ℓ is optimized for higher mass signals that yield higher H_T values. The minimum transverse mass of the \vec{p}_T^{miss} and any of the three leading b -jets is labeled $m_{T,\text{min}}^{b\text{-jets}}$, computed with the b -jet mass set to 0 GeV. For $t\bar{t}$ events with a single leptonic W -boson decay, $m_{T,\text{min}}^{b\text{-jets}}$ has an upper bound of $\sqrt{m_t^2 - m_W^2} \approx 150$ GeV and is used to further reduce the semileptonic $t\bar{t}$ background. Events with low E_T^{miss} are rejected as signals have high E_T^{miss} values due to the energetic neutrino from the neutralino decay. The transverse mass of the lepton and \vec{p}_T^{miss} (m_T^ℓ , see Equation 2) is required to be above the W boson mass to reject events with leptonic W boson decays from processes such as $t\bar{t}$, $t\bar{t}W$, single-top (including Wt), and diboson production. SR1 ℓ uses a single bin due to the low predicted event count. The expected pre-fit distribution of $m_{N,T}$ in Run 2 SR1 ℓ is shown in Figure 2(b).

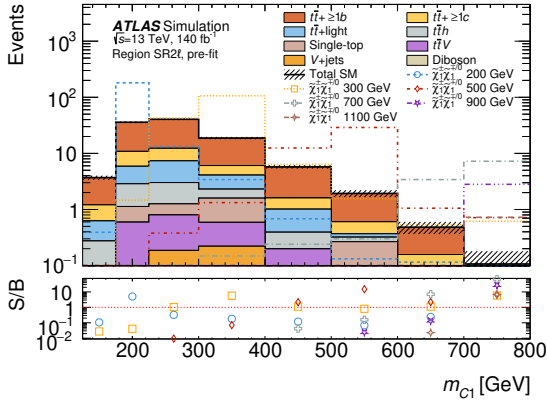
Four regions, referred to as “discovery regions”, are used to obtain results on new physics, independent of a specific signal hypothesis. The first two, SR2 ℓ and SR1 ℓ , are single-bin regions matching the definitions for the SRs in Tables 3 and 4. In addition, SR2 ℓ 700 is defined as SR2 ℓ with an additional requirement

Table 3: Summary of the signal, control, and validation regions used for the 2-lepton analysis regions targeting $\tilde{\chi}_1^\pm \tilde{\chi}_1^\mp$ signals. All regions require at least four jets and two oppositely charged leptons. Each region has both a Run 2 and a Run 3 version, which use the same definition.

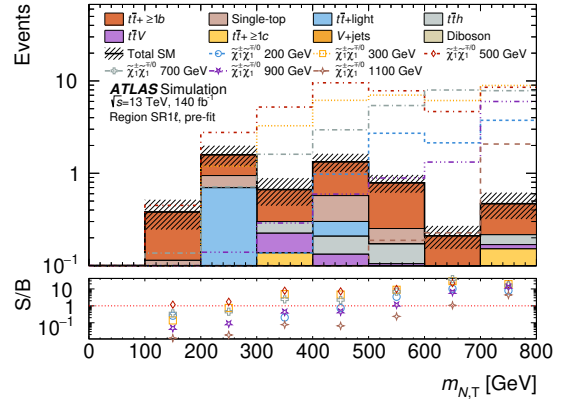
Region	$N_{b\text{-jet}}$	m_{h1} [GeV]	m_{h2} [GeV]	H_T [GeV]	$m_{\ell\ell}$ [GeV]	A_C	m_{C2}^{rej} [GeV]	m_{C1} [GeV]
SR2 ℓ	≥ 3	$\in [100, 150]$	$\in [85, 135]$	> 400	> 106.2	< 0.2	> 200	—
CR2 ℓ 2b	2	$\in [100, 150]$	$\in [85, 135]$	—	> 106.2	< 0.2	< 200	< 500
CR2 ℓ 3b	≥ 3	$\notin [100, 150]$	$\notin [85, 135]$	> 400	> 106.2	> 0.2	—	< 700
VR2 ℓ 2b	2	$\in [100, 150]$	$\in [85, 135]$	—	> 106.2	< 0.2	> 200	< 500
VR2 ℓ 3b	≥ 3	$\notin [100, 150]$	$\in [85, 135]$	> 400	> 106.2	> 0.2	—	—

Table 4: Summary of the signal, control, and validation regions used for the 1-lepton analysis regions targeting $\tilde{\chi}_1^\pm \tilde{\chi}_1^0$ signals. All regions require at least four jets and one lepton. Each region has both a Run 2 and a Run 3 version, which use the same definition.

Region	$N_{b\text{-jet}}$	m_{h1} [GeV]	m_{h2} [GeV]	H_T [GeV]	$m_{T,\text{min}}^{b\text{-jets}}$ [GeV]	E_T^{miss} [GeV]	m_T^ℓ [GeV]
SR1 ℓ	≥ 3	$\in [100, 150]$	$\in [85, 135]$	> 800	> 80	> 150	> 100
CR1 ℓ 3b	≥ 3	$\notin [100, 150]$	$\notin [85, 135]$	> 800	> 80	> 150	≤ 100
VR1 ℓ 3b1	≥ 3	$\notin [100, 150]$	$\in [85, 135]$	> 800	> 80	> 150	≤ 100
VR1 ℓ 3b2	≥ 3	$\notin [100, 150]$	$\notin [85, 135]$	> 800	> 80	> 150	> 100



(a)



(b)

Figure 2: Expected Run 2 pre-fit distributions for signal and background samples for (a) the higher mass of the two reconstructed chargino candidates m_{C1} in SR2 ℓ and (b) the transverse mass of the neutralino $m_{N,T}$ in SR1 ℓ . The lower panels show the signal to background ratios. The hatching shows the MC statistical uncertainty in the predicted background yields. The sum of the signal contributions from $\tilde{\chi}_1^\pm \tilde{\chi}_1^\mp$ and $\tilde{\chi}_1^\pm \tilde{\chi}_1^0$ is shown, assuming $\mathcal{B}(\tilde{\chi}_1^\pm \rightarrow h\ell^\pm) = 100\%$ and $\mathcal{B}(\tilde{\chi}_1^0 \rightarrow h\nu) = 100\%$, with equal decay branching fractions to each lepton flavor. The generator-level signal masses are shown in the legend. Overflow is included in the last bin.

of $m_{C1} > 700$ GeV and is equivalent to the last bin of SR2 ℓ . Finally, SR1 ℓ 600 is defined as SR1 ℓ with an additional requirement on the transverse mass of the neutralino $m_{N,T} > 600$ GeV. Each of these four

regions is defined for both Run 2 and Run 3 as they cannot be combined in a model-independent way due to the different center-of-mass energies.

6 Background estimation

The background is estimated by using the MC simulation samples described in Section 3. The main backgrounds are from $t\bar{t}$ ($t\bar{t} + \geq 1b$, $t\bar{t} + \geq 1c$, and $t\bar{t} + \text{light}$) production, and are normalized to data in control regions (CRs). Separate normalizations are used for the 1-lepton and 2-lepton regions due to the different phase space. The largest contribution in the SRs is given by $t\bar{t} + \geq 1b$ production. Smaller backgrounds that are present in this search are $t\bar{t}h$, $t\bar{t}Z$, $t\bar{t}W$, single-top, Z +jets, W +jets, and diboson production. These backgrounds, referred to as minor backgrounds, collectively constitute less than 10% of the pre-fit expected background in $\text{SR}2\ell$ and less than a third of the pre-fit expected background in $\text{SR}1\ell$.

Two CRs, $\text{CR}2\ell 2b$ and $\text{CR}2\ell 3b$ are used to measure the normalizations of dileptonic $t\bar{t}$ backgrounds. Separate normalizations are determined for Run 2 and Run 3 due to differences in the experimental setup and simulations. These CRs are defined in Table 3. $\text{CR}2\ell 3b$ is constructed by inverting the $\text{SR}2\ell$ selections on m_{h1} , m_{h2} , and A_C to select a region with low signal contribution while removing the requirements on m_{C2}^{rej} to further reduce signal contamination and lower the statistical uncertainty. An additional requirement is placed on m_{C1} to prevent contributions from signals with large chargino masses. This region is used to measure a common normalization factor for $t\bar{t} + \geq 1b$ and $t\bar{t} + \geq 1c$ production, referred to as $t\bar{t}$ +HF (heavy-flavor). MC simulation predicts similar relative contributions from $t\bar{t} + \geq 1b$ and $t\bar{t} + \geq 1c$ in $\text{CR}2\ell 3b$ and $\text{SR}2\ell$, allowing a joint measurement with smaller statistical uncertainty. The $t\bar{t} + \text{HF}$ purity in this region is over 80%. The expected signal contributions are found to be less than 8% of the pre-fit expected background for any signal mass hypothesis.

$\text{CR}2\ell 2b$ is used to measure the $t\bar{t} + \text{light}$ normalization. This uses events with only two b -jets, as $t\bar{t}b\bar{b}$ events have four true b -jets and $t\bar{t} + \geq 1c$ events are more likely than $t\bar{t} + \text{light}$ events to have a third reconstructed b -jet due to the higher charm mis-tagging rate compared to light jets. Contributions from signals are limited by inverting the $\text{SR}2\ell$ selection on m_{C2}^{rej} and removing the requirement on H_T . An upper bound is placed on m_{C1} to prevent contributions from signals with large chargino masses. $\text{CR}2\ell 2b$ has a $t\bar{t} + \text{light}$ purity of approximately 80%. The expected signal contributions are found to be less than 2% of the pre-fit expected background for any signal mass hypothesis.

$\text{CR}1\ell 3b$ is used to measure the normalization of semileptonic $t\bar{t}$ backgrounds. Separate normalizations are determined for Run 2 and Run 3. This measures a common normalization factor for all semileptonic $t\bar{t}$ backgrounds ($t\bar{t} + \geq 1b$, $t\bar{t} + \geq 1c$, and $t\bar{t} + \text{light}$), jointly referred to as $t\bar{t} 1\ell$. These are measured jointly to lower the statistical uncertainty, as the $t\bar{t} + \geq 1c$ and $t\bar{t} + \text{light}$ backgrounds are expected to contribute a total of less than one event in $\text{SR}1\ell$ and therefore do not require separate measurements. The dominant background component in $\text{SR}1\ell$ and $\text{CR}1\ell 3b$ is $t\bar{t} + \geq 1b$. $\text{CR}1\ell 3b$ is defined in Table 4 and is constructed by inverting the $\text{SR}1\ell$ requirements on m_{h1} , m_{h2} , and m_T^ℓ to reduce signal contributions. The $t\bar{t} 1\ell$ purity in this region is over 80%, while the expected signal contributions are found to be less than 1% of the pre-fit expected background for any signal mass hypothesis.

Validation regions (VRs) are constructed to test the extrapolation of the background model from the CRs to the SRs. These regions are defined to fall in the phase space between their corresponding CR and SR, as shown in Tables 3 and 4. $\text{VR}2\ell 2b$ and $\text{VR}2\ell 3b$ test the extrapolations over m_{C2}^{rej} and m_{h2} respectively, while $\text{VR}1\ell 3b1$ and $\text{VR}1\ell 3b2$ test the extrapolations over m_{h2} and m_T^ℓ respectively. The expected signal

contributions are found to be less than 12% of the pre-fit expected background in each VR for any signal mass hypothesis.

The agreement between data and predicted backgrounds for different variables are checked in each CR and VR except VR1 ℓ 3b2. This region is only checked in a single bin as it has high signal contamination in some kinematic regimes. Reconstructed chargino and Higgs boson masses are shown for the VRs in Figure 3, where good modeling of the SM background is seen.

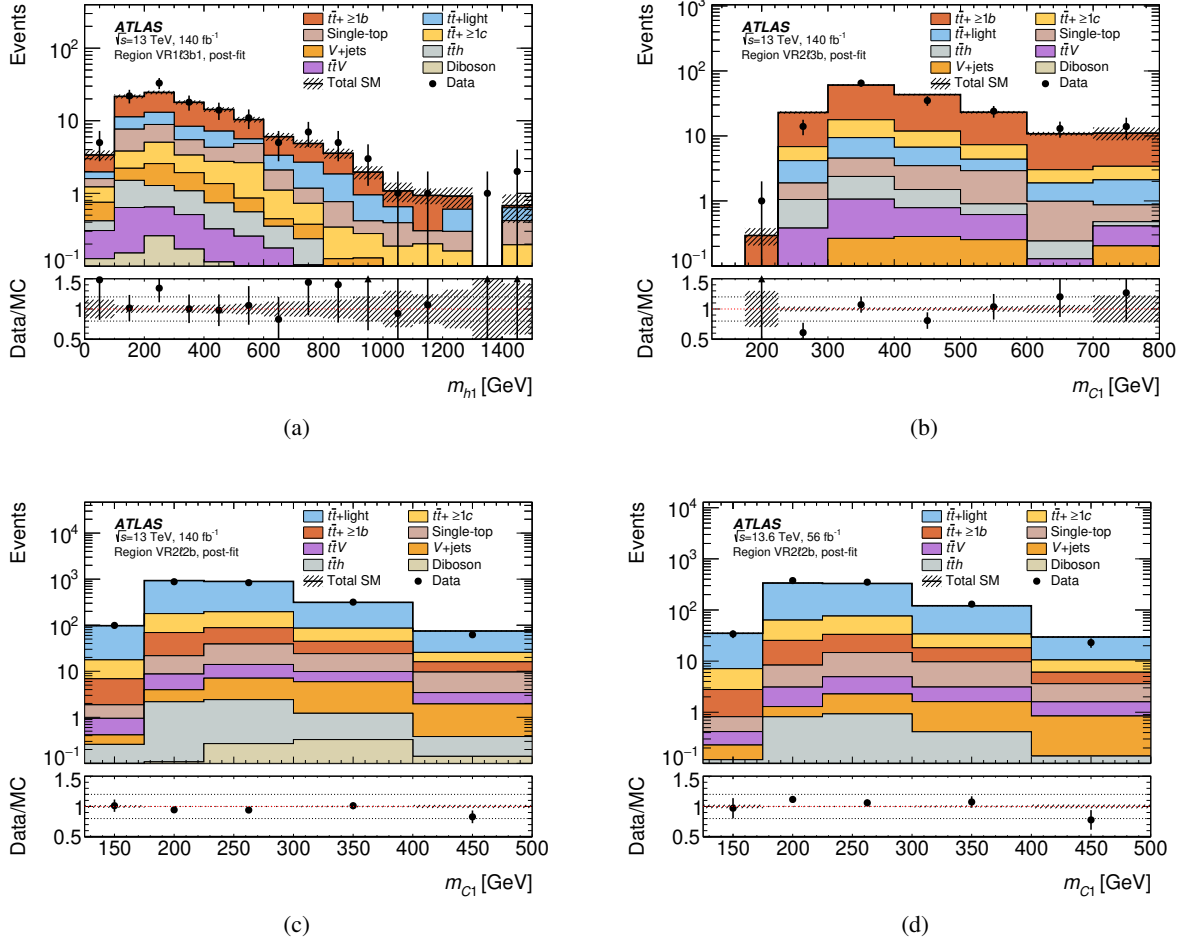


Figure 3: Data and background distributions in the validation regions for (a) the m_{h_1} distribution in Run 2 VR1 ℓ 3b1, (b) the m_{C_1} distribution in Run 2 VR2 ℓ 3b, (c) the m_{C_1} distribution in Run 2 VR2 ℓ 2b, and (d) the m_{C_1} distribution in Run 3 VR2 ℓ 2b. The backgrounds are calculated using pre-fit values but with the normalization factors measured from the CR background-only fit applied. The hatching shows the MC statistical uncertainty in the predicted background yields. The lower panels show the ratio of data to predicted background. Overflow is included in the last bin.

6.1 Background-only fit results

Profile-likelihood fits are performed to measure the agreement between data and predicted background. There are six free-floating background normalization factors in total. Each Run has two normalization factors for $\bar{t}t + \text{HF}$ and $\bar{t}t + \text{light}$ flavor production in 2-lepton regions and one normalization factor for $\bar{t}t$

production in 1-lepton regions. The MC statistical uncertainties and the systematic uncertainties described in Section 7 are treated as nuisance parameters. Unless otherwise noted, all fits use these six normalization factors and both 1-lepton and 2-lepton regions in both Run 2 and Run 3. All fits are performed using the PYHF framework [98, 99].

A background-only fit is performed in the CRs using a single bin for each region. The measured normalization factors are shown in Table 5.

Table 5: Fit results for normalization factors from the background-only fit in the CRs. The first listed uncertainties are from the fit using all systematic and statistical uncertainties, while the values in parentheses are determined from the fit using only statistical uncertainties. Due to correlations between the normalization factors and systematic uncertainties, the relative uncertainties in the predicted backgrounds yields may be smaller than those on the normalization factors.

Process (Channel)	Run 2 Norm. Factor	Run 3 Norm. Factor
$t\bar{t} + \text{HF} (2\ell)$	1.16 ± 0.46 (± 0.06 stat.)	1.08 ± 0.42 (± 0.10 stat.)
$t\bar{t} + \text{light} (2\ell)$	0.93 ± 0.20 (± 0.03 stat.)	0.85 ± 0.20 (± 0.05 stat.)
$t\bar{t} (1\ell)$	0.88 ± 0.33 (± 0.06 stat.)	1.01 ± 0.45 (± 0.08 stat.)

Results from the background-only fit are extrapolated to the VRs, with the agreement between data and the post-fit background prediction shown in Figure 4. No significant mismodeling is observed. The largest deviation in yield between data and predicted background is 1.2σ , which is seen in Run 3 VR2 ℓ 2b.

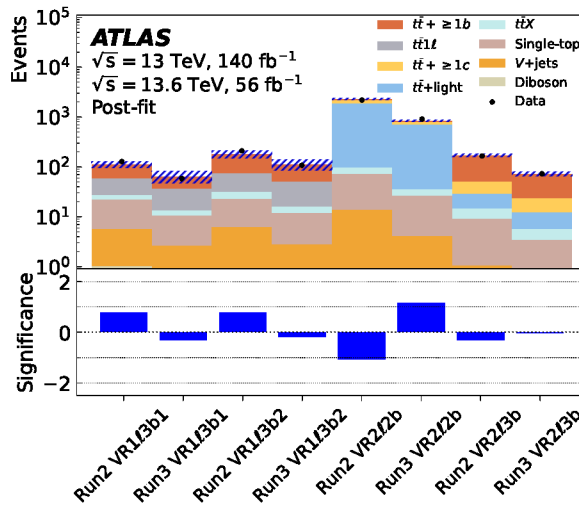


Figure 4: Data and post-fit background yields as determined from the background-only fit extrapolated to the validation regions. The hatching shows the uncertainty in the predicted yields from MC statistical and systematic effects. The lower panel shows the significance of the deviations between data and predicted background. The $t\bar{t} 1\ell$ category includes all $t\bar{t} + \geq 1c$ and $t\bar{t} + \text{light}$ production with one reconstructed lepton. $t\bar{t}X$ includes $t\bar{t}h$, $t\bar{t}Z$, and $t\bar{t}W$ production. Significances are calculated following the method in Ref. [100].

7 Systematic uncertainties

Predicted signal and background MC simulation yields are subject to uncertainties. Three types of uncertainties are applied: experimental uncertainties, theoretical uncertainties, and MC statistical uncer-

tainties.

Experimental uncertainties account for systematic effects in ATLAS calibration procedures and efficiency measurements and are applied to all signal and background MC simulations. Experimental jet uncertainties are applied on the jet energy scale and resolution [91–93], JVT [95] and fJVT [96], and flavor tagging efficiencies [22]. Experimental muon uncertainties include uncertainties on the muon isolation, reconstruction, and trigger efficiency correction factors [26, 33, 88–90]. Additional systematic uncertainties affect the muon momenta due to variations in the momentum scale, track resolution, and charge-dependent corrections. For electrons, experimental uncertainties are applied on the identification, isolation, reconstruction, and trigger efficiency correction factors, as well as on the energy scale and resolution [26, 32, 87, 101]. Scale and resolution uncertainties are applied on the E_T^{miss} soft term [97, 102]. Further experimental uncertainties considered are on the pileup conditions [103] and luminosity [28, 29]. Luminosity uncertainties are not applied to $t\bar{t}$ and $t\bar{t}b\bar{b}$ backgrounds as they rely on data-driven normalization measurements. Uncertainties related to electrons, E_T^{miss} , and most of the jet energy scale and resolution components are correlated between Run 2 and Run 3, while the remaining uncertainties are not correlated between Runs. The largest experimental uncertainties are related to the jet energy resolution. As measured using the background-only fit extrapolated to the signal regions, these are collectively 1.3% (3.5%) of the post-fit yields in Run 2 (Run 3) SR2 ℓ and 23% (35%) of the post-fit yields in the Run 2 (Run 3) SR1 ℓ .

Theoretical uncertainties are applied to the background and signal MC samples. These uncertainties are evaluated by comparing simulations using nominal values of theory parameters with alternative or reweighted samples using variations on these parameters. Uncertainties in the matrix element, parton shower model, factorization and renormalization scales, modeling of initial and final-state radiation, parton distribution functions, and strong coupling constant are applied to the $t\bar{t} + \geq 1b$, $t\bar{t} + \geq 1c$, and $t\bar{t} + \text{light}$ backgrounds. The matrix element and parton shower uncertainties are calculated by comparing the nominal samples to samples generated with the PYTHIA 8 $p_{T,\text{hard}}$ parameter set to 1.0 and with the HERWIG 7 parton shower model [104–107] respectively. In addition, uncertainties on the h_{damp} parameter are applied to the $t\bar{t} + \geq 1c$ and $t\bar{t} + \text{light}$ backgrounds by comparing the nominal samples to samples produced with the h_{damp} parameter set to $3.0 m_{\text{top}}$. A 50% normalization uncertainty is applied to each of the remaining background samples ($t\bar{t}h$, $t\bar{t}V$, single- t , V +jets, and diboson). As the background is dominated by $t\bar{t}$ and $t\bar{t}b\bar{b}$ and the analysis is statistically limited, the uncertainties on these minor backgrounds have no significant impact on the results. Background theoretical uncertainties are correlated between Run 2 and Run 3, but are not correlated between 1-lepton and 2-lepton regions due to the different phase space. The largest theoretical uncertainties in SR2 ℓ are from the parton shower model. As measured using the background-only fit extrapolated to the signal regions, these are collectively 4.2%–6.0% of the post-fit yields in the 2-lepton SRs, depending on the Run. The largest theoretical uncertainties in SR1 ℓ are from the modeling of final-state radiation and the parton shower modeling. As measured using the background-only fit extrapolated to the signal regions, these are each 3%–20% of the post-fit yields in the 1-lepton SRs, depending on the uncertainty and Run. For signal samples, uncertainties on the factorization and renormalization scales, merging scale, parton shower tuning, parton distribution function, and α_s are considered. The factorization and renormalization scale uncertainties are the largest of these, ranging from 6.1%–11% for $\tilde{\chi}_1^\pm \tilde{\chi}_1^\mp$ signals in SR2 ℓ and 8.4%–12.6% for $\tilde{\chi}_1^\pm \tilde{\chi}_1^0$ signals in SR1 ℓ , depending on the mass point.

The effects of different sources of uncertainties on the SR2 ℓ and SR1 ℓ post-fit background yields are shown in Figure 5. Background theory uncertainties are larger than experimental uncertainties in Run 2, while for Run 3 experimental uncertainties are larger than theoretical uncertainties in SR1 ℓ and some bins of SR2 ℓ . MC statistical uncertainties are smaller than both background theory and experimental uncertainties. The

high- m_{C1} bins in SR2 ℓ have low MC event statistics, making the systematic estimates prone to statistical fluctuations.

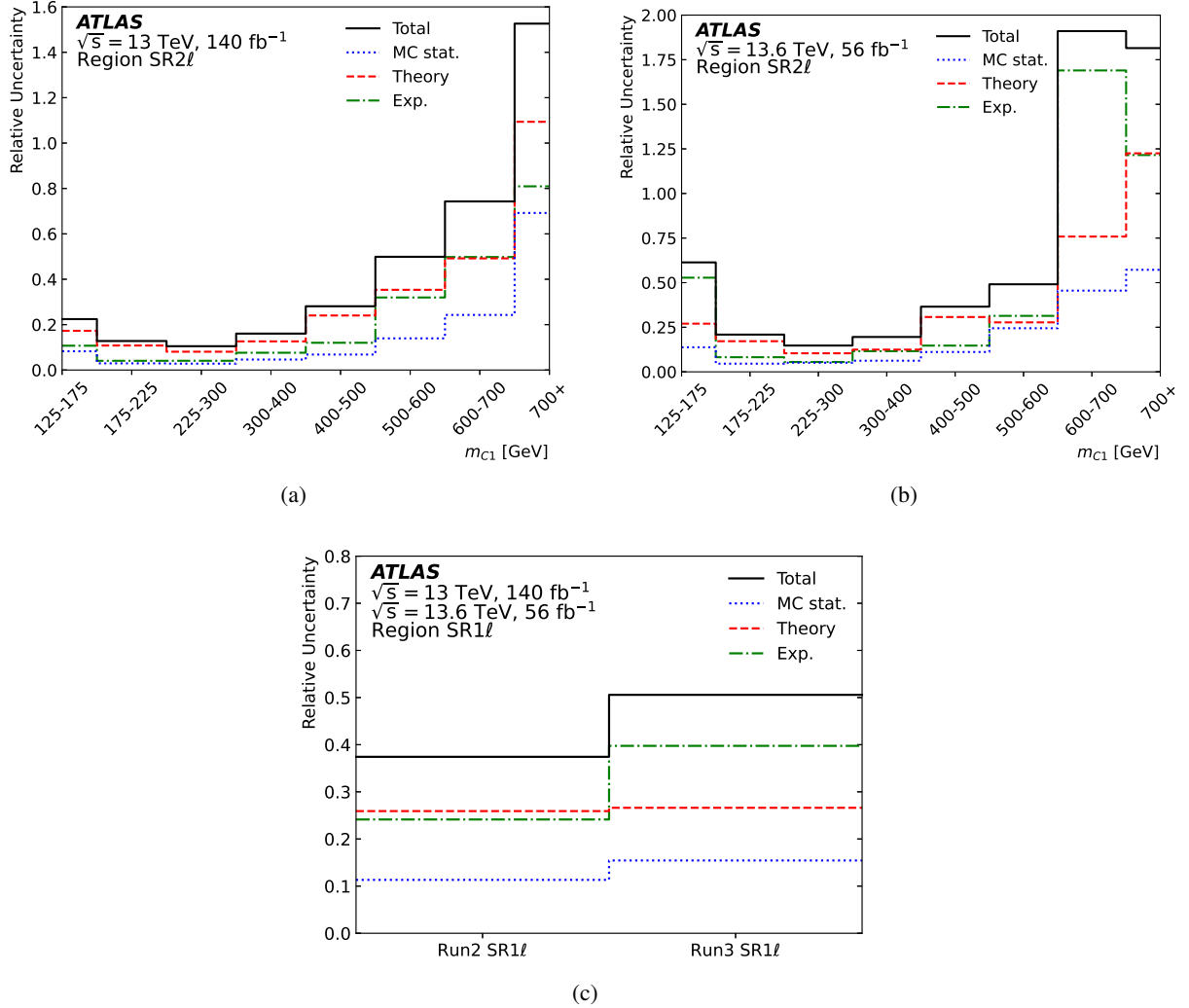


Figure 5: Background uncertainties as a fraction of total post-fit yields as determined from the background-only fit extrapolated to the signal regions for (a) Run 2 SR2 ℓ , (b) Run 3 SR2 ℓ , and (c) Run 2 and Run 3 SR1 ℓ . Exp. stands for the experimental uncertainty while MC stat. stands for MC statistical uncertainty. The total uncertainty includes systematic and MC statistical uncertainties. The total uncertainty is not necessarily equal to the quadrature sum of the individual uncertainties due to correlations.

8 Results

Results are obtained using three types of fits. First, the results of the background-only fit described in Section 6 are extrapolated to the SRs to show the level of agreement between data and predicted background. Second, fits are performed in each discovery region to search for evidence for and set constraints on new physics in a model-independent manner. Third, an exclusion fit is performed in the SRs to set limits on the simplified model described in Section 1.

Table 6: Results for the model-independent discovery regions. The second column shows the number of observed events (N_{obs}), while the third column shows the post-fit number of predicted events obtained using a background-only fit (N_{pred}). The fourth column shows the 95% CL observed upper limit on the efficiency times cross section of beyond-the-SM processes ($\langle\epsilon\sigma\rangle_{\text{obs}}^{95}$ [fb]). The fifth and sixth columns show the 95% CL observed (S_{obs}^{95}) and expected (S_{exp}^{95}) upper limits on the number of events from processes beyond the SM, with the $\pm 1\sigma$ uncertainty included with the expected limit. Uncertainties in S_{exp}^{95} less than 0.05 are reported as 0.0 due to rounding. The seventh column shows CL_b , the confidence level observed for the background-only hypothesis. The final column shows the discovery p -value ($p(s=0)$) and its significance. The p -value is not calculated but instead set to 0.5 for regions with a deficit relative to the post-fit background prediction. SR2 ℓ and SR1 ℓ are the same regions used for exclusions.

Region	N_{obs}	N_{pred}	$\langle\epsilon\sigma\rangle_{\text{obs}}^{95}$ [fb]	S_{obs}^{95}	S_{exp}^{95}	CL_b	$p(s=0)$
Run 2 SR2 ℓ	117	120 \pm 10	0.24	33	31 $^{+12}_{-8}$	0.58	0.50 (0.00)
Run 2 SR2 ℓ 700	0	0.11 \pm 0.17	0.022	3.1	3.0 $^{+0.1}_{-0.0}$	0.08	0.50 (0.00)
Run 2 SR1 ℓ	4	5.0 \pm 1.9	0.048	6.7	6.7 $^{+2.6}_{-1.6}$	0.50	0.50 (0.00)
Run 2 SR1 ℓ 600	1	0.62 \pm 0.51	0.031	4.3	3.3 $^{+1.3}_{-0.1}$	0.78	0.13 (1.14)
Run 3 SR2 ℓ	40	46.4 \pm 6.1	0.27	15	18.4 $^{+7.6}_{-5.2}$	0.30	0.50 (0.00)
Run 3 SR2 ℓ 700	0	0.023 \pm 0.041	0.053	3.0	3.0 $^{+0.0}_{-0.0}$	0.95	0.50 (0.00)
Run 3 SR1 ℓ	2	2.9 \pm 1.5	0.078	4.4	5.0 $^{+2.0}_{-1.2}$	0.36	0.50 (0.00)
Run 3 SR1 ℓ 600	0	0.35 \pm 0.36	0.054	3.0	3.0 $^{+0.6}_{-0.0}$	0.19	0.50 (0.00)

8.1 Background-only fit results

Results from the background-only fit performed in the CRs (described in Section 6) are extrapolated to the SRs. The agreement between data and the post-fit background prediction is shown for SR1 ℓ and each bin of SR2 ℓ in Figure 6. Note that the discovery region SR2 ℓ 700 is defined as the last bin of SR2 ℓ . No significant excess is observed. The largest excess observed is in the 125 GeV–175 GeV bin of Run 3 SR2 ℓ , with four observed events and 1.24 ± 0.76 predicted background events. This corresponds to a local significance of 1.5σ . The largest deficit occurs in the 400 GeV–500 GeV bin of Run 3 SR2 ℓ , with zero observed events and 2.58 ± 0.94 predicted background events. This corresponds to a local significance of -2.1σ .

8.2 Model-independent results

Model-independent results are obtained for each discovery region of the analysis. A separate fit is performed for each discovery region. For a given fit, CRs and normalization factors corresponding to a different Run or number of leptons than the discovery region are not used. Significances and upper limits are determined respectively using the q_0 and \tilde{q}_μ test statistics [108] based on the profile likelihood ratio. The upper limits are set at 95% confidence level (CL) using the CL_s prescription [109]. Regions with non-zero observed events use 50,000 pseudoexperiments to calculate p -values, limits, and the confidence level observed for the background-only hypothesis, CL_b . Regions with zero observed events use 100,000 pseudoexperiments. It is assumed that no signal events enter the CRs. Results are shown in Table 6. No significant excess is observed, and limits are set on the yield and cross section of beyond-the-SM physics processes.

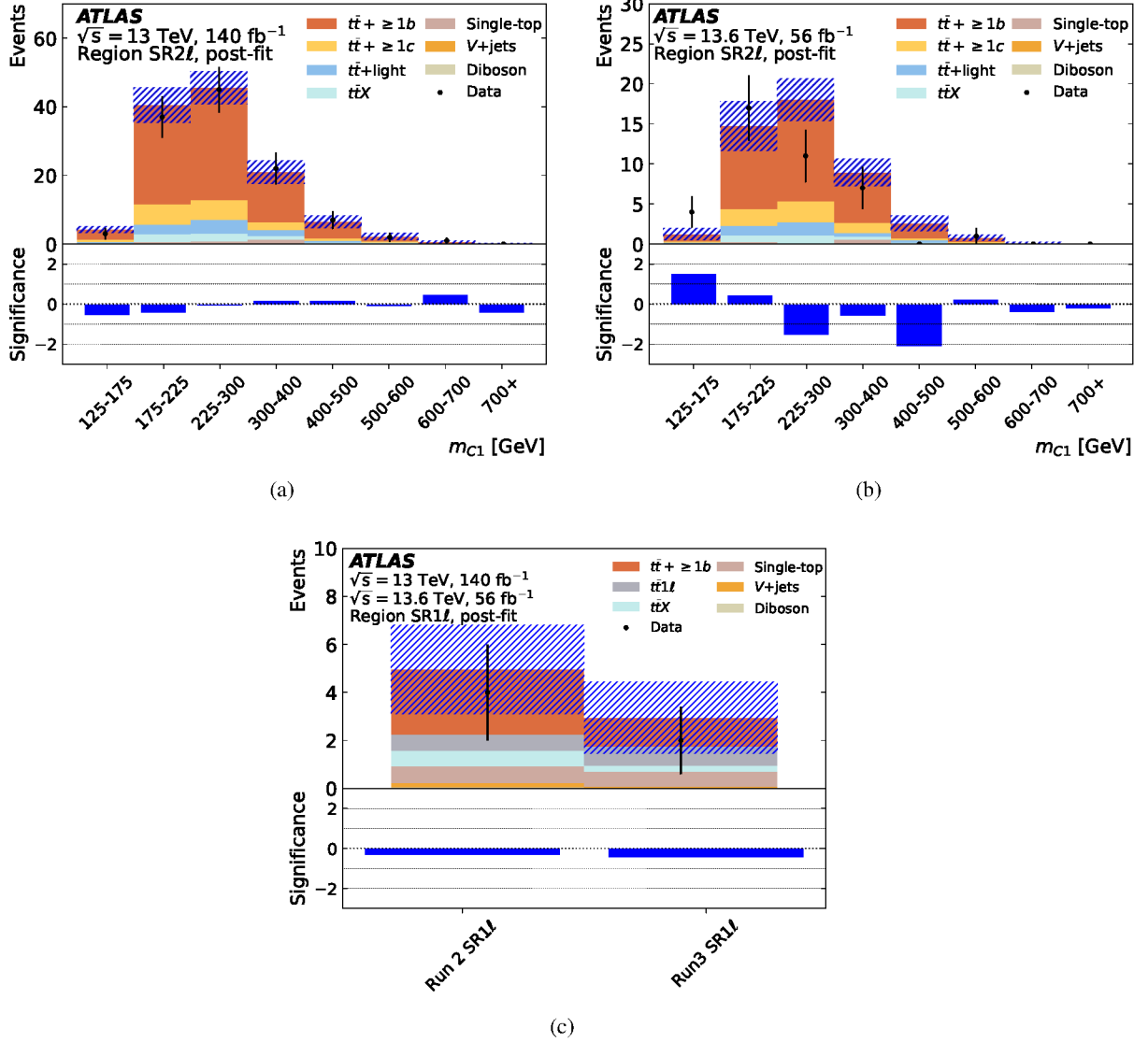


Figure 6: Data and post-fit background yields as determined from the background-only fit extrapolated to the signal regions for (a) Run 2 SR2 ℓ , (b) Run 3 SR2 ℓ , and (c) Run 2 and Run 3 SR1 ℓ . The hatching shows the uncertainty in the predicted yields from MC statistical and systematic effects. The lower panel shows the significance of the deviations between data and predicted background. The $t\bar{t} 1\ell$ category includes all $t\bar{t} + \geq 1c$ and $t\bar{t} + \text{light}$ production with one reconstructed lepton. $t\bar{t}X$ includes $t\bar{t}h$, $t\bar{t}Z$, and $t\bar{t}W$ production. Significances are calculated following the method in Ref. [100].

8.3 Model-dependent exclusion limits

As no significant excess is observed in the discovery regions, upper limits are set at 95% CL for the simplified signal model for $\tilde{\chi}_1^\pm \tilde{\chi}_1^\mp$ and $\tilde{\chi}_1^\pm \tilde{\chi}_1^0$ production with RPV decays $\tilde{\chi}_1^\pm \rightarrow h\ell^\pm$ and $\tilde{\chi}_1^0 \rightarrow h\nu$ described in Section 1. Other decay modes of the charginos and neutralinos are assumed to be negligible after selections and are not considered. The limits are determined for each mass point through signal-plus-background fits using all CRs, Run 2 and Run 3 SR1 ℓ , and Run 2 and Run 3 SR2 ℓ , with each SR2 ℓ binned in m_{C1} . The

Run 2 and Run 3 counterparts of each region are treated as separate regions. The \tilde{q}_μ test statistic [108] with the CL_s prescription [109] and the asymptotic approximation are used [108].

Results for the hypothesis where each flavor of charged lepton is equally likely are shown in Figure 7. SR2 ℓ provides most of the sensitivity to low chargino and neutralino masses ($\lesssim 500$ GeV), while SR1 ℓ and SR2 ℓ have similar sensitivity to high chargino and neutralino masses. For the branching fractions $\mathcal{B}(\tilde{\chi}_1^\pm \rightarrow h\ell^\pm) = 100\%$ and $\mathcal{B}(\tilde{\chi}_1^0 \rightarrow h\nu) = 100\%$, charginos and neutralinos with masses between 150 GeV and 1100 GeV are excluded. This has complementary sensitivity to the previous search for a tripleton resonance [19], which excludes charginos and neutralinos with masses between 100 GeV and 975 GeV for the alternate $\mathcal{B}(\tilde{\chi}_1^\pm \rightarrow Z\ell^\pm) = 100\%$ and $\mathcal{B}(\tilde{\chi}_1^0 \rightarrow Z\nu) = 100\%$ assumptions.

Results are also obtained for alternative flavor hypotheses. In addition to the usual SR requirements, the pure-electron (pure-muon) interpretation requires the reconstructed lepton in SR1 ℓ and two leading reconstructed leptons in SR2 ℓ to be electrons (muons). Figure 8(a) shows the upper limits for the hypothesis where the charged lepton from the decay is always an electron while Figure 8(b) shows the upper limits for the hypothesis where the charged lepton from the decay is always a muon. Charginos and neutralinos with masses between 150 GeV and 1225 GeV (150 GeV and 1150 GeV) are excluded for the pure-electron (pure-muon) interpretation. Figure 9 shows the upper limits for scenarios with $\mathcal{B}(\tilde{\chi}_1^\pm \rightarrow h\tau^\pm) = 100\%$, excluding charginos and neutralinos with masses between 450 GeV and 750 GeV. The pure-electron and pure-muon interpretations have greater sensitivity than the pure- τ scenario because the analysis does not reconstruct hadronically-decaying τ -leptons. In addition, only part of the energy from leptonically-decaying τ -leptons is retained by the daughter electron or muon, which can cause the lepton p_T to be below the 40 GeV threshold as well as lead to misreconstruction of the chargino pairs. This also causes the pure-electron and pure-muon scenarios to have higher sensitivity than the equal electron, muon, and τ -lepton scenario. The pure-electron scenario has slightly higher sensitivity than the pure-muon scenario due to a higher electron reconstruction efficiency.

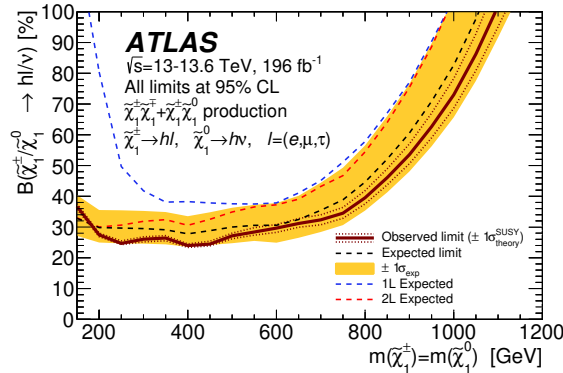


Figure 7: 95% CL upper limits on $\mathcal{B}(\tilde{\chi}_1^\pm \rightarrow h\ell^\pm)$ and $\mathcal{B}(\tilde{\chi}_1^0 \rightarrow h\nu)$, which are assumed to be equal, for the hypothesis where the charginos are equally likely to decay into each flavor of charged lepton. The expected and observed limits are shown by the dashed and solid lines respectively. The shaded bands around the expected limit show the $\pm 1\sigma$ variations due to statistical and systematic uncertainties, while the dotted bands around the observed limit show the $\pm 1\sigma$ variations from the theoretical uncertainty on the signal cross section. The expected limits using only 1-lepton (2-lepton) regions are shown by the dashed blue and dashed red lines respectively.

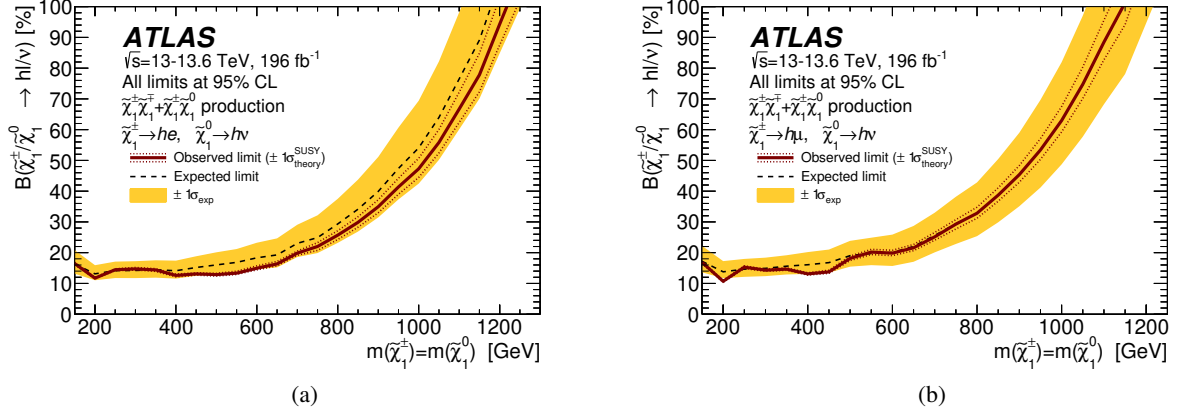


Figure 8: 95% CL upper limits on $\mathcal{B}(\tilde{\chi}_1^\pm \rightarrow h\ell^\pm)$ and $\mathcal{B}(\tilde{\chi}_1^0 \rightarrow h\nu)$, which are assumed to be equal, for (a) the hypothesis where the charged lepton from the decay is always an electron and (b) the hypothesis where the charged lepton from the decay is always a muon. The expected and observed limits are shown by the dashed and solid lines respectively. The shaded bands around the expected limit show the $\pm 1\sigma$ variations due to statistical and systematic uncertainties, while the dotted bands around the observed limit show the $\pm 1\sigma$ variations from the theoretical uncertainty on the signal cross section.

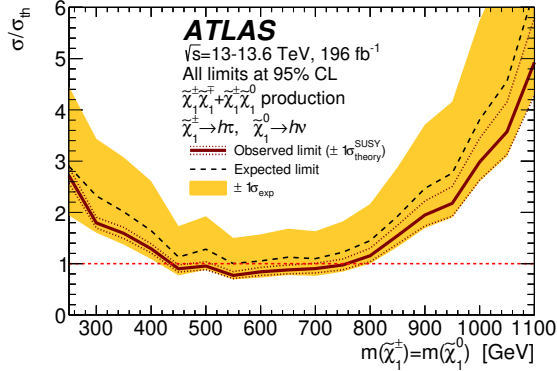


Figure 9: 95% CL upper limits on the cross section times branching ratio for $\tilde{\chi}_1^\pm\tilde{\chi}_1^\mp$ and $\tilde{\chi}_1^\pm\tilde{\chi}_1^0$ production normalized to the theoretical prediction, assuming $\mathcal{B}(\tilde{\chi}_1^\pm \rightarrow h\tau^\pm) = 100\%$. The expected and observed limits are shown by the dashed and solid lines respectively. The shaded bands around the expected limit show the $\pm 1\sigma$ variations due to statistical and systematic uncertainties, while the dotted bands around the observed limit show the $\pm 1\sigma$ variations from the theoretical uncertainty on the signal cross section.

9 Conclusion

A search for $\tilde{\chi}_1^\pm\tilde{\chi}_1^\mp$ and $\tilde{\chi}_1^\pm\tilde{\chi}_1^0$ production where each chargino and neutralino decays into a Higgs boson and a lepton was performed in a final state with one or two charged leptons and at least four jets, with at least three identified b -jets. This search complements a previous search for RPV chargino decays into a Z boson and a lepton in a channel with three or more leptons, and provides the first constraints on the simplified signal model for charginos with high decay branching fractions to Higgs bosons and leptons. The data correspond to an integrated luminosity of 196 fb^{-1} of proton–proton collision data produced at

center-of-mass energies of $\sqrt{s} = 13$ TeV and $\sqrt{s} = 13.6$ TeV, collected by the ATLAS experiment at the LHC between 2015 and 2023.

No significant excess above the SM prediction was observed. Model-independent limits are set at 95% CL on the visible cross section for new physics processes. Charginos and neutralinos with masses between 150 GeV and 1100 GeV are excluded at 95% CL for the $\mathcal{B}(\tilde{\chi}_1^\pm \rightarrow h\ell^\pm) = 100\%$ and $\mathcal{B}(\tilde{\chi}_1^0 \rightarrow h\nu) = 100\%$ hypothesis, where each flavor of charged lepton (electron, muon, and τ -lepton) is equally likely to be produced. Lower limits of 1225 GeV and 1150 GeV are also set on the chargino and neutralino masses for the $\mathcal{B}(\tilde{\chi}_1^\pm \rightarrow h e^\pm) = 100\%$ and $\mathcal{B}(\tilde{\chi}_1^\pm \rightarrow h\mu^\pm) = 100\%$ hypotheses respectively.

Acknowledgments

We thank CERN for the very successful operation of the LHC and its injectors, as well as the support staff at CERN and at our institutions worldwide without whom ATLAS could not be operated efficiently.

The crucial computing support from all WLCG partners is acknowledged gratefully, in particular from CERN, the ATLAS Tier-1 facilities at TRIUMF/SFU (Canada), NDGF (Denmark, Norway, Sweden), CC-IN2P3 (France), KIT/GridKA (Germany), INFN-CNAF (Italy), NL-T1 (Netherlands), PIC (Spain), RAL (UK) and BNL (USA), the Tier-2 facilities worldwide and large non-WLCG resource providers. Major contributors of computing resources are listed in Ref. [110].

We gratefully acknowledge the support of ANPCyT, Argentina; YerPhI, Armenia; ARC, Australia; BMWFW and FWF, Austria; ANAS, Azerbaijan; CNPq and FAPESP, Brazil; NSERC, NRC and CFI, Canada; CERN; ANID, Chile; CAS, MOST and NSFC, China; Minciencias, Colombia; MEYS CR, Czech Republic; DNRF and DNSRC, Denmark; IN2P3-CNRS and CEA-DRF/IRFU, France; SRNSFG, Georgia; BMFTR, HGF and MPG, Germany; GSRI, Greece; RGC and Hong Kong SAR, China; ICHEP and Academy of Sciences and Humanities, Israel; INFN, Italy; MEXT and JSPS, Japan; CNRST, Morocco; NWO, Netherlands; RCN, Norway; MNiSW, Poland; FCT, Portugal; MNE/IFA, Romania; MSTDI, Serbia; MSSR, Slovakia; ARIS and MVZI, Slovenia; DSI/NRF, South Africa; MICIU/AEI, Spain; SRC and Wallenberg Foundation, Sweden; SERI, SNSF and Cantons of Bern and Geneva, Switzerland; NSTC, Taipei; TENMAK, Türkiye; STFC/UKRI, United Kingdom; DOE and NSF, United States of America.

Individual groups and members have received support from BCKDF, CANARIE, CRC and DRAC, Canada; CERN-CZ, FORTE and PRIMUS, Czech Republic; COST, ERC, ERDF, Horizon 2020 and Marie Skłodowska-Curie Actions, European Union; Investissements d’Avenir Labex, Investissements d’Avenir IDEX and ANR, France; DFG and AvH Foundation, Germany; Herakleitos, Thales and Aristeia programmes co-financed by EU-ESF and the Greek NSRF, Greece; BSF-NSF and MINERVA, Israel; NCN and NAWA, Poland; La Caixa Banking Foundation, CERCA and AGAUR programs from Generalitat de Catalunya and PROMETEO and GenT Programmes Generalitat Valenciana, Spain; Göran Gustafssons Stiftelse, Sweden; The Royal Society and Leverhulme Trust, United Kingdom; Eric and Wendy Schmidt Fund for Strategic Innovation, United States of America.

In addition, individual members wish to acknowledge support from Chile: Agencia Nacional de Investigación y Desarrollo (ANID FONDECYT reg. 1230987, FONDECYT 1230812, FONDECYT 1240864, Fondecyt 3240661, Fondecyt Regular 1240721); China: Chinese Ministry of Science and Technology (MOST-2023YFA1605700, MOST-2023YFA1609300), National Natural Science Foundation of China (NSFC 12275265, NSFC-W2543005); Czech Republic: Czech Science Foundation (GACR - 24-11373S), Ministry

of Education Youth and Sports (ERC-CZ-LL2327, FORTE CZ.02.01.01/00/22_008/0004632), PRIMUS Research Programme (PRIMUS/21/SCI/017); EU: H2020 European Research Council (ERC - 101002463); European Union: European Research Council (BARD No. 101116429, ERC - 101219398, ERC - 948254, ERC 101089007), European Regional Development Fund (HE COFUND GA No.101081355, ERDF), Marie Skłodowska-Curie Actions (GAP-101168829); France: Agence Nationale de la Recherche (ANR-21-CE31-0013, ANR-22-EDIR-0002, ANR-24-CE31-0504-01); Germany: Deutsche Forschungsgemeinschaft (DFG - 469666862); China: Research Grants Council (GRF); Italy: Istituto Nazionale di Fisica Nucleare (LHC-MIUR - 28003/2025), Ministero dell'Università e della Ricerca (NextGenEU I53D23000820006 M4C2.1.1, SOE2024_0000023); Japan: Japan Society for the Promotion of Science (JSPS KAKENHI JP25H0063, JSPS KAKENHI JP22H01227, JSPS KAKENHI JP22H04944, JSPS KAKENHI JP22KK0227, JSPS KAKENHI JP24K23939, JSPS KAKENHI JP24KK0251, JSPS KAKENHI JP25H00650, JSPS KAKENHI JP25H01291, JSPS KAKENHI JP25K01011, JSPS KAKENHI JP25K01023); Poland: Polish National Science Centre (NCN 2021/42/E/ST2/00350, NCN OPUS 2023/51/B/ST2/02507, NCN OPUS nr 2022/47/B/ST2/03059, NCN UMO-2019/34/E/ST2/00393, UMO-2022/47/O/ST2/00148, UMO-2023/49/B/ST2/04085, UMO-2023/51/B/ST2/00920, UMO-2024/53/N/ST2/00869); Spain: Agència de Gestió d'Ajuts Universitaris i de Recerca. (AGAUR - 2023 BP 00141), Ministry of Science and Innovation (RYC2019-028510-I, RYC2020-030254-I, RYC2021-031273-I, RYC2022-038164-I), Ministerio de Ciencia, Innovación y Universidades/Agencia Estatal de Investigación (EU NextGenerationEU (PRTR-C17.I1), PID2022-142604OB-C22); Sweden: Carl Trygger Foundation (Carl Trygger Foundation CTS 22:2312), Swedish Research Council (Swedish Research Council 2023-04654, VR 2021-03651, VR 2022-03845, VR 2022-04683, VR 2023-03403, VR 2024-05451, VR 2025-05940), Knut and Alice Wallenberg Foundation (KAW 2023.0366); Switzerland: Swiss National Science Foundation (SNSF - PCEFP2_194658); United Kingdom: The Binks Trust, Royal Society (NIF-R1-231091); United States of America: U.S. Department of Energy (ECA DE-AC02-76SF00515), John Templeton Foundation (John Templeton Foundation 63206), Neubauer Family Foundation.

References

- [1] Y. Gol'fand and E. Likhtman, *Extension of the Algebra of Poincare Group Generators and Violation of P Invariance*, [JETP Lett. **13** \(1971\) 323](#), [[Pisma Zh. Eksp. Teor. Fiz. **13** \(1971\) 452](#)].
- [2] D. V. Volkov and V. P. Akulov, *Is the neutrino a goldstone particle?* [Phys. Lett. B **46** \(1973\) 109](#).
- [3] J. Wess and B. Zumino, *Supergauge transformations in four dimensions*, [Nucl. Phys. B **70** \(1974\) 39](#).
- [4] J. Wess and B. Zumino, *Supergauge invariant extension of quantum electrodynamics*, [Nucl. Phys. B **78** \(1974\) 1](#).
- [5] S. Ferrara and B. Zumino, *Supergauge invariant Yang-Mills theories*, [Nucl. Phys. B **79** \(1974\) 413](#).
- [6] A. Salam and J. Strathdee, *Super-symmetry and non-Abelian gauges*, [Phys. Lett. B **51** \(1974\) 353](#).
- [7] N. Sakai, *Naturalness in supersymmetric GUTS*, [Z. Phys. C **11** \(1981\) 153](#).
- [8] S. Dimopoulos, S. Raby, and F. Wilczek, *Supersymmetry and the scale of unification*, [Phys. Rev. D **24** \(1981\) 1681](#).
- [9] L. E. Ibáñez and G. G. Ross, *Low-energy predictions in supersymmetric grand unified theories*, [Phys. Lett. B **105** \(1981\) 439](#).
- [10] S. Dimopoulos and H. Georgi, *Softly broken supersymmetry and SU(5)*, [Nucl. Phys. B **193** \(1981\) 150](#).
- [11] G. R. Farrar and P. Fayet, *Phenomenology of the production, decay, and detection of new hadronic states associated with supersymmetry*, [Phys. Lett. B **76** \(1978\) 575](#).
- [12] L. Evans and P. Bryant, *LHC Machine*, [JINST **3** \(2008\) S08001](#).
- [13] Z. Marshall, B. A. Ovrut, A. Purves, and S. Spinner, *Spontaneous R-Parity Breaking, Stop LSP Decays and the Neutrino Mass Hierarchy*, [Phys. Lett. B **732** \(2014\) 325](#), [arXiv: 1401.7989 \[hep-ph\]](#).
- [14] R. Deen, B. A. Ovrut, and A. Purves, *The minimal SUSY B – L model: simultaneous Wilson lines and string thresholds*, [JHEP **07** \(2016\) 043](#), [arXiv: 1604.08588 \[hep-ph\]](#).
- [15] P. Fileviez Perez, *New Paradigm for Baryon and Lepton Number Violation*, [Phys. Rept. **597** \(2015\) 1](#), [arXiv: 1501.01886 \[hep-ph\]](#).
- [16] B. A. Ovrut, A. Purves, and S. Spinner, *The minimal SUSY B – L model: from the unification scale to the LHC*, [JHEP **06** \(2015\) 182](#), [arXiv: 1503.01473 \[hep-ph\]](#).
- [17] S. Dumitru, B. A. Ovrut, and A. Purves, *The R-parity Violating Decays of Charginos and Neutralinos in the B – L MSSM*, [JHEP **02** \(2019\) 124](#), [arXiv: 1810.11035 \[hep-ph\]](#).
- [18] S. Dumitru, B. A. Ovrut, and A. Purves, *R-parity Violating Decays of Wino Chargino and Wino Neutralino LSPs and NLSPs at the LHC*, [JHEP **06** \(2019\) 100](#), [arXiv: 1811.05581 \[hep-ph\]](#).
- [19] ATLAS Collaboration, *Search for trilepton resonances from chargino and neutralino pair production in $\sqrt{s} = 13$ TeV pp collisions with the ATLAS detector*, [Phys. Rev. D **103** \(2021\) 112003](#), [arXiv: 2011.10543 \[hep-ex\]](#).

- [20] ATLAS Collaboration, *Search for $B - L$ R -parity-violating top squarks in $\sqrt{s} = 13$ TeV pp collisions with the ATLAS experiment*, *Phys. Rev. D* **97** (2018) 032003, arXiv: 1710.05544 [hep-ex].
- [21] ATLAS Collaboration, *Search for R -parity violating supersymmetric decays of the top squark to a b -jet and a lepton in $\sqrt{s} = 13$ TeV pp collisions with the ATLAS detector*, *Phys. Rev. D* **110** (2024) 092004, arXiv: 2406.18367 [hep-ex].
- [22] ATLAS Collaboration, *Transforming jet flavour tagging at ATLAS*, *Nature Commun.* **17** (2026) 541, arXiv: 2505.19689 [hep-ex].
- [23] ATLAS Collaboration, *The ATLAS Experiment at the CERN Large Hadron Collider*, *JINST* **3** (2008) S08003.
- [24] ATLAS Collaboration, *The ATLAS experiment at the CERN Large Hadron Collider: a description of the detector configuration for Run 3*, *JINST* **19** (2024) P05063, arXiv: 2305.16623 [physics.ins-det].
- [25] ATLAS Collaboration, *Performance of the ATLAS trigger system in 2015*, *Eur. Phys. J. C* **77** (2017) 317, arXiv: 1611.09661 [hep-ex].
- [26] ATLAS Collaboration, *The ATLAS trigger system for LHC Run 3 and trigger performance in 2022*, *JINST* **19** (2024) P06029, arXiv: 2401.06630 [hep-ex].
- [27] ATLAS Collaboration, *Software and computing for Run 3 of the ATLAS experiment at the LHC*, *Eur. Phys. J. C* **85** (2025) 234, arXiv: 2404.06335 [hep-ex], Erratum: *Eur. Phys. J. C* **85** (2025) 907.
- [28] ATLAS Collaboration, *Luminosity determination in pp collisions at $\sqrt{s} = 13$ TeV using the ATLAS detector at the LHC*, *Eur. Phys. J. C* **83** (2023) 982, arXiv: 2212.09379 [hep-ex].
- [29] ATLAS Collaboration, *Preliminary analysis of the luminosity calibration for the ATLAS 13.6 TeV data recorded in 2023*, ATL-DAPR-PUB-2024-001, 2024, URL: <https://cds.cern.ch/record/2900949>.
- [30] G. Avoni et al., *The new LUCID-2 detector for luminosity measurement and monitoring in ATLAS*, *JINST* **13** (2018) P07017.
- [31] ATLAS Collaboration, *ATLAS data quality operations and performance for 2015–2018 data-taking*, *JINST* **15** (2020) P04003, arXiv: 1911.04632 [physics.ins-det].
- [32] ATLAS Collaboration, *Performance of electron and photon triggers in ATLAS during LHC Run 2*, *Eur. Phys. J. C* **80** (2020) 47, arXiv: 1909.00761 [hep-ex].
- [33] ATLAS Collaboration, *Performance of the ATLAS muon triggers in Run 2*, *JINST* **15** (2020) P09015, arXiv: 2004.13447 [physics.ins-det].
- [34] ATLAS Collaboration, *The ATLAS Simulation Infrastructure*, *Eur. Phys. J. C* **70** (2010) 823, arXiv: 1005.4568 [physics.ins-det].
- [35] S. Agostinelli et al., *GEANT4 – a simulation toolkit*, *Nucl. Instrum. Meth. A* **506** (2003) 250.
- [36] B. Fuks, M. Klasen, D. R. Lamprea, and M. Rothering, *Gaugino production in proton-proton collisions at a center-of-mass energy of 8 TeV*, *JHEP* **10** (2012) 081, arXiv: 1207.2159 [hep-ph].

- [37] B. Fuks, M. Klasen, D. R. Lamprea, and M. Rothering, *Precision predictions for electroweak superpartner production at hadron colliders with RESUMMINO*, *Eur. Phys. J. C* **73** (2013) 2480, arXiv: [1304.0790 \[hep-ph\]](#).
- [38] J. Fiaschi, B. Fuks, M. Klasen, and A. Neuwirth, *Electroweak superpartner production at 13.6 TeV with Resummino*, *Eur. Phys. J. C* **83** (2023) 707, arXiv: [2304.11915 \[hep-ph\]](#).
- [39] J. Alwall et al., *The automated computation of tree-level and next-to-leading order differential cross sections, and their matching to parton shower simulations*, *JHEP* **07** (2014) 079, arXiv: [1405.0301 \[hep-ph\]](#).
- [40] NNPDF Collaboration, R. D. Ball, et al., *Parton distributions for the LHC run II*, *JHEP* **04** (2015) 040, arXiv: [1410.8849 \[hep-ph\]](#).
- [41] C. Bierlich et al., *A comprehensive guide to the physics and usage of PYTHIA 8.3*, *SciPost Phys. Codebases* (2022) 8, arXiv: [2203.11601 \[hep-ph\]](#).
- [42] ATLAS Collaboration, *ATLAS Pythia 8 tunes to 7 TeV data*, ATL-PHYS-PUB-2014-021, 2014, URL: <https://cds.cern.ch/record/1966419>.
- [43] T. Ježo, J. M. Lindert, N. Moretti, and S. Pozzorini, *New NLOPS predictions for $t\bar{t} + b$ -jet production at the LHC*, *Eur. Phys. J. C* **78** (2018) 502, arXiv: [1802.00426 \[hep-ph\]](#).
- [44] F. Buccioni et al., *OpenLoops 2*, *Eur. Phys. J. C* **79** (2019) 866, arXiv: [1907.13071 \[hep-ph\]](#).
- [45] F. Cascioli, P. Maierhöfer, and S. Pozzorini, *Scattering Amplitudes with Open Loops*, *Phys. Rev. Lett.* **108** (2012) 111601, arXiv: [1111.5206 \[hep-ph\]](#).
- [46] A. Denner, S. Dittmaier, and L. Hofer, *COLLIER: A fortran-based complex one-loop library in extended regularizations*, *Comput. Phys. Commun.* **212** (2017) 220, arXiv: [1604.06792 \[hep-ph\]](#).
- [47] S. Frixione, G. Ridolfi, and P. Nason, *A positive-weight next-to-leading-order Monte Carlo for heavy flavour hadroproduction*, *JHEP* **09** (2007) 126, arXiv: [0707.3088 \[hep-ph\]](#).
- [48] P. Nason, *A new method for combining NLO QCD with shower Monte Carlo algorithms*, *JHEP* **11** (2004) 040, arXiv: [hep-ph/0409146](#).
- [49] S. Frixione, P. Nason, and C. Oleari, *Matching NLO QCD computations with parton shower simulations: the POWHEG method*, *JHEP* **11** (2007) 070, arXiv: [0709.2092 \[hep-ph\]](#).
- [50] S. Alioli, P. Nason, C. Oleari, and E. Re, *A general framework for implementing NLO calculations in shower Monte Carlo programs: the POWHEG BOX*, *JHEP* **06** (2010) 043, arXiv: [1002.2581 \[hep-ph\]](#).
- [51] T. Sjöstrand et al., *An introduction to PYTHIA 8.2*, *Comput. Phys. Commun.* **191** (2015) 159, arXiv: [1410.3012 \[hep-ph\]](#).
- [52] M. Beneke, P. Falgari, S. Klein, and C. Schwinn, *Hadronic top-quark pair production with NNLL threshold resummation*, *Nucl. Phys. B* **855** (2012) 695, arXiv: [1109.1536 \[hep-ph\]](#).

- [53] M. Cacciari, M. Czakon, M. Mangano, A. Mitov, and P. Nason, *Top-pair production at hadron colliders with next-to-next-to-leading logarithmic soft-gluon resummation*, [Phys. Lett. B **710** \(2012\) 612](#), arXiv: [1111.5869 \[hep-ph\]](#).
- [54] P. Bärnreuther, M. Czakon, and A. Mitov, *Percent-Level-Precision Physics at the Tevatron: Next-to-Next-to-Leading Order QCD Corrections to $q\bar{q} \rightarrow t\bar{t} + X$* , [Phys. Rev. Lett. **109** \(2012\) 132001](#), arXiv: [1204.5201 \[hep-ph\]](#).
- [55] M. Czakon and A. Mitov, *NNLO corrections to top-pair production at hadron colliders: the all-fermionic scattering channels*, [JHEP **12** \(2012\) 054](#), arXiv: [1207.0236 \[hep-ph\]](#).
- [56] M. Czakon and A. Mitov, *NNLO corrections to top pair production at hadron colliders: the quark-gluon reaction*, [JHEP **01** \(2013\) 080](#), arXiv: [1210.6832 \[hep-ph\]](#).
- [57] M. Czakon, P. Fiedler, and A. Mitov, *Total Top-Quark Pair-Production Cross Section at Hadron Colliders Through $O(\alpha_S^4)$* , [Phys. Rev. Lett. **110** \(2013\) 252004](#), arXiv: [1303.6254 \[hep-ph\]](#).
- [58] M. Czakon and A. Mitov, *Top++: A program for the calculation of the top-pair cross-section at hadron colliders*, [Comput. Phys. Commun. **185** \(2014\) 2930](#), arXiv: [1112.5675 \[hep-ph\]](#).
- [59] D. de Florian et al., *Handbook of LHC Higgs Cross Sections: 4. Deciphering the Nature of the Higgs Sector*, (2017), arXiv: [1610.07922 \[hep-ph\]](#).
- [60] E. Bothmann et al., *Event generation with Sherpa 2.2*, [SciPost Phys. **7** \(2019\) 034](#), arXiv: [1905.09127 \[hep-ph\]](#).
- [61] ATLAS and CMS Collaborations, *Reference Single Top-Quark Cross-Sections for ATLAS and CMS Analyses*, ATL-PHYS-PUB-2025-035, 2025, URL: <https://cds.cern.ch/record/2942746>.
- [62] N. Kidonakis, *Two-loop soft anomalous dimensions for single top quark associated production with a W^- or H^-* , [Phys. Rev. D **82** \(2010\) 054018](#), arXiv: [1005.4451 \[hep-ph\]](#).
- [63] N. Kidonakis, “Top Quark Production,” *Proceedings, Helmholtz International Summer School on Physics of Heavy Quarks and Hadrons (HQ2013)* (JINR, Dubna, Russia, July 15–28, 2013) 139, arXiv: [1311.0283 \[hep-ph\]](#).
- [64] C. Anastasiou, L. Dixon, K. Melnikov, and F. Petriello, *High-precision QCD at hadron colliders: Electroweak gauge boson rapidity distributions at next-to-next-to leading order*, [Phys. Rev. D **69** \(2004\) 094008](#), arXiv: [hep-ph/0312266](#).
- [65] ATLAS Collaboration, *Studies on top-quark Monte Carlo modelling for Top2016*, ATL-PHYS-PUB-2016-020, 2016, URL: <https://cds.cern.ch/record/2216168>.
- [66] NNPDF Collaboration, R. D. Ball, et al., *Parton distributions with LHC data*, [Nucl. Phys. B **867** \(2013\) 244](#), arXiv: [1207.1303 \[hep-ph\]](#).
- [67] M. Cacciari, G. P. Salam, and G. Soyez, *The anti- k_t jet clustering algorithm*, [JHEP **04** \(2008\) 063](#), arXiv: [0802.1189 \[hep-ph\]](#).
- [68] M. Cacciari, G. P. Salam, and G. Soyez, *FastJet user manual*, [Eur. Phys. J. C **72** \(2012\) 1896](#), arXiv: [1111.6097 \[hep-ph\]](#).

- [69] R. D. Ball et al., *Parton distributions from high-precision collider data*, *Eur. Phys. J. C* **77** (2017) 663, arXiv: [1706.00428 \[hep-ph\]](#).
- [70] H. B. Hartanto, B. Jäger, L. Reina, and D. Wackerroth, *Higgs boson production in association with top quarks in the POWHEG BOX*, *Phys. Rev. D* **91** (2015) 094003, arXiv: [1501.04498 \[hep-ph\]](#).
- [71] S. Frixione, E. Laenen, P. Motylinski, C. White, and B. R. Webber, *Single-top hadroproduction in association with a W boson*, *JHEP* **07** (2008) 029, arXiv: [0805.3067 \[hep-ph\]](#).
- [72] S. Höche, F. Krauss, M. Schönherr, and F. Siegert, *A critical appraisal of NLO+PS matching methods*, *JHEP* **09** (2012) 049, arXiv: [1111.1220 \[hep-ph\]](#).
- [73] S. Höche, F. Krauss, M. Schönherr, and F. Siegert, *QCD matrix elements + parton showers. The NLO case*, *JHEP* **04** (2013) 027, arXiv: [1207.5030 \[hep-ph\]](#).
- [74] S. Catani, F. Krauss, B. R. Webber, and R. Kuhn, *QCD Matrix Elements + Parton Showers*, *JHEP* **11** (2001) 063, arXiv: [hep-ph/0109231](#).
- [75] S. Höche, F. Krauss, S. Schumann, and F. Siegert, *QCD matrix elements and truncated showers*, *JHEP* **05** (2009) 053, arXiv: [0903.1219 \[hep-ph\]](#).
- [76] D. J. Lange, *The EvtGen particle decay simulation package*, *Nucl. Instrum. Meth. A* **462** (2001) 152.
- [77] ATLAS Collaboration, *Emulating the impact of additional proton–proton interactions in the ATLAS simulation by presampling sets of inelastic Monte Carlo events*, *Comput. Softw. Big Sci.* **6** (2022) 3, arXiv: [2102.09495 \[hep-ex\]](#).
- [78] K. Werner, F.-M. Liu, and T. Pierog, *Parton ladder splitting and the rapidity dependence of transverse momentum spectra in deuteron–gold collisions at the BNL Relativistic Heavy Ion Collider*, *Phys. Rev. C* **74** (2006) 044902, arXiv: [hep-ph/0506232](#).
- [79] T. Pierog, I. Karpenko, J. M. Katzy, E. Yatsenko, and K. Werner, *EPOS LHC: Test of collective hadronization with data measured at the CERN Large Hadron Collider*, *Phys. Rev. C* **92** (2015) 034906, arXiv: [1306.0121 \[hep-ph\]](#).
- [80] ATLAS Collaboration, *The Pythia 8 A3 tune description of ATLAS minimum bias and inelastic measurements incorporating the Donnachie–Landshoff diffractive model*, ATL-PHYS-PUB-2016-017, 2016, URL: <https://cds.cern.ch/record/2206965>.
- [81] ATLAS Collaboration, *Performance of the ATLAS track reconstruction algorithms in dense environments in LHC Run 2*, *Eur. Phys. J. C* **77** (2017) 673, arXiv: [1704.07983 \[hep-ex\]](#).
- [82] ATLAS Collaboration, *Software Performance of the ATLAS Track Reconstruction for LHC Run 3*, *Comput. Softw. Big Sci.* **8** (2024) 9, arXiv: [2308.09471 \[hep-ex\]](#).
- [83] ATLAS Collaboration, *Track and Vertex Reconstruction with the ATLAS Inner Detector*, (2026), arXiv: [2605.07585 \[physics.ins-det\]](#).
- [84] ATLAS Collaboration, *Vertex Reconstruction Performance of the ATLAS Detector at $\sqrt{s} = 13$ TeV*, ATL-PHYS-PUB-2015-026, 2015, URL: <https://cds.cern.ch/record/2037717>.

- [85] ATLAS Collaboration, *Electron and photon performance measurements with the ATLAS detector using the 2015–2017 LHC proton–proton collision data*, [JINST **14** \(2019\) P12006](#), arXiv: [1908.00005 \[hep-ex\]](#).
- [86] ATLAS Collaboration, *Electron and photon energy calibration with the ATLAS detector using LHC Run 2 data*, [JINST **19** \(2024\) P02009](#), arXiv: [2309.05471 \[hep-ex\]](#).
- [87] ATLAS Collaboration, *Electron and photon efficiencies in LHC Run 2 with the ATLAS experiment*, [JHEP **05** \(2024\) 162](#), arXiv: [2308.13362 \[hep-ex\]](#).
- [88] ATLAS Collaboration, *Studies of the muon momentum calibration and performance of the ATLAS detector with pp collisions at $\sqrt{s} = 13$ TeV*, [Eur. Phys. J. C **83** \(2023\) 686](#), arXiv: [2212.07338 \[hep-ex\]](#).
- [89] ATLAS Collaboration, *Muon reconstruction performance of the ATLAS detector in proton–proton collision data at $\sqrt{s} = 13$ TeV*, [Eur. Phys. J. C **76** \(2016\) 292](#), arXiv: [1603.05598 \[hep-ex\]](#).
- [90] ATLAS Collaboration, *Muon reconstruction and identification efficiency in ATLAS using the full Run 2 pp collision data set at $\sqrt{s} = 13$ TeV*, [Eur. Phys. J. C **81** \(2021\) 578](#), arXiv: [2012.00578 \[hep-ex\]](#).
- [91] ATLAS Collaboration, *Jet reconstruction and performance using particle flow with the ATLAS Detector*, [Eur. Phys. J. C **77** \(2017\) 466](#), arXiv: [1703.10485 \[hep-ex\]](#).
- [92] ATLAS Collaboration, *Topological cell clustering in the ATLAS calorimeters and its performance in LHC Run 1*, [Eur. Phys. J. C **77** \(2017\) 490](#), arXiv: [1603.02934 \[hep-ex\]](#).
- [93] ATLAS Collaboration, *Jet energy scale and resolution measured in proton–proton collisions at $\sqrt{s} = 13$ TeV with the ATLAS detector*, [Eur. Phys. J. C **81** \(2021\) 689](#), arXiv: [2007.02645 \[hep-ex\]](#).
- [94] ATLAS Collaboration, *Selection of jets produced in 13 TeV proton–proton collisions with the ATLAS detector*, ATLAS-CONF-2015-029, 2015, URL: <https://cds.cern.ch/record/2037702>.
- [95] ATLAS Collaboration, *Performance of pile-up mitigation techniques for jets in pp collisions at $\sqrt{s} = 8$ TeV using the ATLAS detector*, [Eur. Phys. J. C **76** \(2016\) 581](#), arXiv: [1510.03823 \[hep-ex\]](#).
- [96] ATLAS Collaboration, *Identification and rejection of pile-up jets at high pseudorapidity with the ATLAS detector*, [Eur. Phys. J. C **77** \(2017\) 580](#), arXiv: [1705.02211 \[hep-ex\]](#), Erratum: [Eur. Phys. J. C **77** \(2017\) 712](#).
- [97] ATLAS Collaboration, *The performance of missing transverse momentum reconstruction and its significance with the ATLAS detector using 140fb^{-1} of $\sqrt{s} = 13$ TeV pp collisions*, [Eur. Phys. J. C **85** \(2025\) 606](#), arXiv: [2402.05858 \[hep-ex\]](#).
- [98] L. Heinrich, M. Feickert, and G. Stark, *pyhf: v0.7.6*, version 0.7.6, <https://github.com/scikit-hep/pyhf/releases/tag/v0.7.6>, URL: <https://doi.org/10.5281/zenodo.1169739>.

- [99] L. Heinrich, M. Feickert, G. Stark, and K. Cranmer, *pyhf: pure-Python implementation of HistFactory statistical models*, *Journal of Open Source Software* **6** (2021) 2823.
- [100] ATLAS Collaboration, *Formulae for Estimating Significance*, ATL-PHYS-PUB-2020-025, 2020, URL: <https://cds.cern.ch/record/2736148>.
- [101] ATLAS Collaboration, *Electron and photon energy calibration with the ATLAS detector using LHC Run 1 data*, *Eur. Phys. J. C* **74** (2014) 3071, arXiv: 1407.5063 [hep-ex].
- [102] W. Balunas et al., *A Flexible and Efficient Approach to Missing Transverse Momentum Reconstruction*, *Comput. Softw. Big Sci.* **8** (2024) 2, arXiv: 2308.15290 [hep-ex].
- [103] ATLAS Collaboration, *Measurement of the Inelastic Proton–Proton Cross Section at $\sqrt{s} = 13$ TeV with the ATLAS Detector at the LHC*, *Phys. Rev. Lett.* **117** (2016) 182002, arXiv: 1606.02625 [hep-ex].
- [104] M. Bähr et al., *Herwig++ physics and manual*, *Eur. Phys. J. C* **58** (2008) 639, arXiv: 0803.0883 [hep-ph].
- [105] J. Bellm et al., *Herwig 7.0/Herwig++ 3.0 release note*, *Eur. Phys. J. C* **76** (2016) 196, arXiv: 1512.01178 [hep-ph].
- [106] J. Bellm et al., *Herwig 7.1 Release Note*, (2017), arXiv: 1705.06919 [hep-ph].
- [107] J. Bellm et al., *Herwig 7.2 release note*, *Eur. Phys. J. C* **80** (2020) 452, arXiv: 1912.06509 [hep-ph].
- [108] G. Cowan, K. Cranmer, E. Gross, and O. Vitells, *Asymptotic formulae for likelihood-based tests of new physics*, *Eur. Phys. J. C* **71** (2011) 1554, arXiv: 1007.1727 [physics.data-an], Erratum: *Eur. Phys. J. C* **73** (2013) 2501.
- [109] A. L. Read, *Presentation of search results: the CL_s technique*, *J. Phys. G* **28** (2002) 2693.
- [110] ATLAS Collaboration, *ATLAS Computing Acknowledgements*, ATL-SOFT-PUB-2026-001, 2026, URL: <https://cds.cern.ch/record/2952666>.

The ATLAS Collaboration

G. Aad ¹⁰², E. Aakvaag ¹⁷, B. Abbott ¹²¹, S. Abdelhameed ^{83b}, K. Abeling ⁵⁴, N.J. Abicht ⁴⁸, S.H. Abidi ³⁰, M. Aboeela ⁴⁴, A. Aboulhorma ^{36e}, H. Abramowicz ¹⁵⁴, B.S. Acharya ^{68a,68b,m}, A. Ackermann ^{62a}, J. Ackerschott ⁵⁵, C. Adam Bourdarios ⁴, L. Adamczyk ^{85a}, S.V. Addepalli ¹⁴⁶, M.J. Addison ¹⁰¹, J. Adelman ¹¹⁷, A. Adiguzel ^{22c}, T. Adye ¹³⁵, A.A. Affolder ¹³⁷, Y. Afik ³⁹, M.N. Agaras ¹³, A. Aggarwal ¹⁰⁰, C. Agheorghiesei ^{28c}, A. Ahmad ^{83a}, F. Ahmadov ^{38,ad}, S. Ahuja ⁹⁵, S. Ahuja ¹⁶⁵, X. Ai ^{113c}, G. Aielli ^{75a,75b}, A. Aikot ¹⁶⁵, M. Ait Tamlihat ^{36e}, T.P.A. Åkesson ⁹⁸, D. Akiyama ¹⁷⁰, N.N. Akolkar ²⁵, S. Aktas ¹⁶⁸, G.L. Alberghi ^{24b}, J. Albert ¹⁶⁷, U. Alberti ²⁰, P. Albicocco ⁵², S. Alderweireldt ⁵¹, Z.L. Alegria ¹²², M. Aleksa ³⁷, I.N. Aleksandrov ³⁸, C. Alexa ^{28b}, T. Alexopoulos ¹⁰, F. Alfonsi ^{24b}, M. Algren ⁵⁵, M. Alhroob ¹⁶⁹, B. Ali ¹³³, H.M.J. Ali ^{91,v}, S. Ali ³², S.W. Alibocus ⁹², M. Aliev ^{34c}, G. Alimonti ^{70a}, C. Allaire ⁶⁵, B.M.M. Allbrooke ¹⁴⁹, D.R. Allen ¹²², J.S. Allen ¹⁰¹, J.F. Allen ⁵¹, C.S. Alley ¹, E.R. Almazan ¹³⁷, A. Aloisio ^{71a,71b}, F. Alonso ⁹⁰, C. Alpigliani ¹⁴⁰, A. Alvarez Fernandez ¹⁰⁰, M. Alves Cardoso ⁵⁵, M.G. Alviggi ^{71a,71b}, M. Aly ¹⁰¹, Y. Amaral Coutinho ^{81b}, C. Amelung ³⁷, M. Amerl ¹⁰¹, T. Amezza ¹²⁸, B. Amini ⁵³, K. Amirie ¹⁵⁸, A. Amirkhanov ³⁸, D. Amperidou ¹⁵⁵, S. An ⁸², C. Anastopoulos ¹⁴², T. Andeen ¹¹, J.K. Anders ⁹², A.C. Anderson ⁵⁸, A. Andreazza ^{70a,70b}, S. Angelidakis ⁹, A. Angerami ⁴¹, A.V. Anisenkov ³⁸, A. Annovi ^{73a}, C. Antel ³⁷, E. Antipov ¹⁴⁸, M. Antonelli ⁵², F. Anulli ^{74a}, M. Aoki ⁸², T. Aoki ¹⁵⁶, M.A. Aparo ¹³, L. Aperio Bella ⁴⁷, M. Apicella ³¹, C. Appelt ¹⁵⁴, A. Apyan ²⁷, M. Arampatzi ¹⁰, S.J. Arbiol Val ⁸⁶, C. Arcangeletti ⁵², A.T.H. Arce ⁵⁰, M. Arcuri ^{43b,43a}, J-F. Arguin ¹⁰⁸, S. Argyropoulos ¹⁵⁵, J.-H. Arling ⁴⁷, O. Arnaez ⁴, H. Arnold ¹⁴⁸, G. Artoni ^{74a,74b}, H. Asada ¹¹¹, S. Asatryan ¹⁷⁵, N.A. Asbah ³⁷, R.A. Ashby Pickering ¹⁶⁹, A.M. Aslam ⁹⁵, J. Assahsah ^{36d}, K. Assamagan ³⁰, R. Astalos ^{29a}, K.S.V. Astrand ⁹⁸, S. Atashi ¹⁶², R.J. Atkin ^{34a}, H. Atmani ^{36f}, P.A. Atmasiddha ¹²⁹, K. Augsten ¹³³, A.D. Auriol ⁴⁰, V.A. Austrup ¹⁰¹, A.S. Avad ⁹⁴, G. Avolio ³⁷, A. Azzam ¹³, D. Babal ^{29b}, H. Bachacou ¹³⁶, K. Bachas ^{155,p}, A. Bachiu ³⁵, E. Bachmann ⁴⁹, M.J. Backes ^{62a}, A. Badea ³⁹, T.M. Baer ¹⁰⁶, M. Bahmani ¹⁹, D. Bahner ⁵³, K. Bai ¹²⁴, L. Baines ⁹⁴, O.K. Baker ¹⁷⁴, D. Bakshi Gupta ⁸, L.E. Balabram Filho ^{81b}, V. Balakrishnan ¹²¹, R. Balasubramanian ⁴, P. Balek ^{85a}, E. Ballabene ^{24b,24a}, F. Balli ¹³⁶, L.M. Bales ^{62a}, W.K. Balunas ¹²⁷, I. Bamwidhi ^{83c}, E. Banas ⁸⁶, M. Bandieramonte ¹³⁰, S. Bansal ²⁵, L. Barak ¹⁵⁴, M. Barakat ⁴⁷, E.L. Barberio ¹⁰⁵, D. Barberis ^{18b}, M. Barbero ¹⁰², M.Z. Barel ¹¹⁶, T. Barillari ¹¹⁰, M-S. Barisits ³⁷, T. Barklow ¹⁴⁶, P. Baron ¹³⁴, D.A. Baron Moreno ¹⁰¹, A. Baroncelli ⁶¹, A.J. Barr ^{127,g}, J.D. Barr ⁹⁶, F. Barreiro ⁹⁹, J. Barreiro Guimarães da Costa ¹⁴, M.G. Barros Teixeira ^{131a}, F. Bartels ³⁷, R. Bartoldus ¹⁴⁶, A.E. Barton ⁹¹, P. Bartos ^{29a}, M. Baselga ⁴⁸, S. Bashiri ⁸⁶, A. Bassalat ^{65,b}, M.J. Basso ^{159a}, S. Bataju ⁴⁴, R. Bate ¹⁶⁶, R.L. Bates ⁵⁸, M. Battaglia ¹³⁷, D. Battulga ¹⁹, M. Bauce ^{74a,74b}, L. Bauckhage ⁴⁷, P. Bauer ²⁵, L.T. Bayer ⁴⁷, L.T. Bazzano Hurrell ³¹, T. Beau ¹²⁸, J.Y. Beaucamp ⁹⁰, S. Beauceron ¹²⁸, P.H. Beauchemin ¹⁶¹, P. Bechtel ²⁵, H.P. Beck ^{20,o}, K. Becker ¹⁶⁹, A.J. Beddall ⁸⁰, V.A. Bednyakov ³⁸, C.P. Bee ¹⁴⁸, L.J. Beemster ¹⁶, M. Begalli ^{81d}, M. Begel ³⁰, J.K. Behr ⁴⁷, J.F. Beirer ³⁷, F. Beisiegel ²⁵, I.B. Belean ^{28d}, M. Belfkir ^{83c}, G. Bella ¹⁵⁴, L. Bellagamba ^{24b}, A. Bellerive ³⁵, C.D. Bellgraph ⁶⁷, P. Bellos ²¹, I. Benaoumeur ²¹, D. Benckroun ^{36a}, F. Bendebba ^{36a}, Y. Benhammou ¹⁵⁴, K.C. Benkendorfer ¹⁶⁷, L. Beresford ⁴⁷, M. Beretta ⁵², E. Bergeas Kuutmann ¹⁶³, N. Berger ⁴, B. Bergmann ¹³³, J. Beringer ^{18a}, M. Berkat ¹³⁶, G. Bernardi ⁵, C. Bernius ¹⁴⁶, F.U. Bernlochner ²⁵, A. Berrocal Guardia ¹³, T. Berry ⁹⁵, P. Berta ¹³⁴, A. Bertl ^{131a}, R. Bertrand ¹⁰², S. Bethke ¹¹⁰, A. Betti ^{74a,74b}, T.F. Beumker ¹⁷³,

A.J. Bevan ⁹⁴, L. Bezio ⁵⁵, N.K. Bhalla ⁵³, S. Bharthuar ¹¹⁰, S. Bhatta ¹⁴⁸, P. Bhattarai ¹⁴⁶,
 Z.M. Bhatti ¹¹⁸, K.D. Bhide ¹⁶⁴, V.S. Bhopatkar ¹²², R.M. Bianchi ¹³⁰, G. Bianco ^{24b,24a},
 O. Biebel ¹⁰⁹, M. Biglietti ^{76a}, P. Bijl ⁵³, C.S. Billingsley ⁴⁴, Y. Bimgdi ^{36f}, M. Bindi ⁵⁴,
 A. Bingham ¹⁷³, A. Bingul ^{22b}, C. Bini ^{74a,74b}, M. Biros ¹³⁴, S. Biryukov ¹⁴⁹, T. Bisanz ⁴⁸,
 E. Bisceglie ^{24b,24a}, J.P. Biswal ¹³⁵, D. Biswas ¹⁴⁴, M. Biyabi ¹⁴, I. Bloch ⁴⁷, A. Blue ⁵⁸,
 U. Blumenschein ⁹⁴, V.S. Bobrovnikov ³⁸, L. Boccardo ^{56b,56a}, M. Boehler ⁵³, B. Boehm ¹⁶⁸,
 D. Bogavac ¹³, L.S. Boggia ¹²⁸, V. Boisvert ⁹⁵, P. Bokan ¹⁶³, T. Bold ^{85a}, M. Bomben ⁵,
 M. Bona ⁹⁴, M. Boonekamp ¹³⁶, A.G. Borbély ⁵⁸, G. Borissov ⁹¹, A. Borkar ¹⁶⁸,
 D. Bortoletto ¹²⁷, M. Borysova ¹⁷¹, D. Boscherini ^{24b}, M. Bosman ¹³, K. Bouaouda ^{36a},
 L. Boudet ¹³⁶, J. Boudreau ¹³⁰, E.V. Bouhova-Thacker ⁹¹, D. Boumediene ⁴⁰, R. Bouquet ^{56b,56a},
 A. Boveia ¹²⁰, D. Boye ³⁰, I.R. Boyko ³⁸, L. Bozianu ⁵⁵, J. Bracini ²¹, N. Brahim ⁴,
 G. Brandt ¹⁷³, O. Brandt ³³, B. Brau ¹⁰³, R. Brenner ¹⁷¹, L. Brenner ¹¹⁶, R. Brenner ¹⁶³,
 S. Bressler ¹⁷¹, M. Brettell ⁹⁶, G. Brianti ¹¹⁶, D. Britton ⁵⁸, D. Britzger ¹¹⁰, I. Brock ²⁵,
 R. Brock ¹⁰⁷, H. Bronson ¹²⁹, G. Brooijmans ⁴¹, A.J. Brooks ⁶⁷, E.M. Brooks ^{159b}, E. Brost ³⁰,
 L.M. Brown ^{167,159a}, L.E. Bruce ⁶⁰, T.L. Bruckler ¹²⁷, P.A. Bruckman de Renstrom ⁸⁶,
 B. Brüers ⁴⁷, A. Bruni ^{24b}, G. Bruni ^{24b}, D. Brunner ^{46a,46b}, M. Bruschi ^{24b}, N. Brusino ^{74a,74b},
 T. Buanes ¹⁷, Q. Buat ¹⁴⁰, D. Buchin ¹¹⁰, A.G. Buckley ⁵⁸, J. Bucko ¹³⁴, M. Bühring ⁴⁹,
 O. Bulekov ⁸⁰, B.A. Bullard ¹⁴⁶, T.O. Buratovich ⁹⁰, S. Burdin ⁹², C.D. Burgard ⁴⁸,
 A.M. Burger ⁸⁹, B. Burghgrave ⁸, O. Burlayenko ⁵³, J. Burleson ¹⁶⁴, J.C. Burzynski ¹²¹,
 V. Büscher ¹⁰⁰, P.J. Bussey ⁵⁸, O. But ²⁵, J.M. Butler ²⁶, C.M. Buttar ⁵⁸, J.M. Butterworth ⁹⁶,
 P. Butti ³⁷, W. Buttinger ¹³⁵, C.J. Buxo Vazquez ¹⁰⁷, A.R. Buzykaev ³⁸, S. Cabrera Urbán ¹⁶⁵,
 L. Cadamuro ⁶⁵, H. Cai ³⁷, Y. Cai ^{24b,112c,24a}, Y. Cai ^{112a}, M.A. Cairo ¹²⁹, V.M.M. Cairo ³⁷,
 O. Cakir ^{3a}, N. Calace ³⁷, P. Calafiura ^{18a}, G. Calderini ¹²⁸, P. Calfayan ³⁵, L. Calic ⁹⁸,
 G. Callea ⁵⁸, L.P. Caloba ^{81b}, D. Calvet ⁴⁰, S. Calvet ⁴⁰, R. Camacho Toro ¹²⁸, S. Camarda ³⁷,
 D. Camarero Munoz ²⁷, P. Camarri ^{75a,75b}, C. Camincher ³⁷, M. Campanelli ⁹⁶, A. Camplani ⁴²,
 V. Canale ^{71a,71b}, A.C. Canbay ^{3a}, E. Canonero ⁹⁵, J. Cantero ¹⁶⁵, F. Capocasa ²⁷, P. Cappelli ²⁷,
 M. Capua ^{43b,43a}, A. Carbone ^{70a,70b}, R. Cardarelli ^{75a}, J.C.J. Cardenas ⁸, M.P. Cardiff ²⁷,
 G. Carducci ^{43b,43a}, T. Carli ³⁷, G. Carlino ^{71a}, J.I. Carlotto ¹³, B.T. Carlson ^{130,q},
 E.M. Carlson ¹⁶⁷, L. Carminati ^{70a,70b}, A. Carnelli ⁴, M. Carnesale ³⁷, S. Caron ¹¹⁵,
 E. Carquin ^{138g}, I.B. Carr ¹⁰⁵, S. Carrá ^{72a,72b}, G. Carratta ^{24b,24a}, C. Carrion Martinez ¹⁶⁵,
 A.M. Carroll ¹²⁴, N. Cartalade ⁴⁰, M.P. Casado ^{13,h}, P. Casolaro ^{71a,71b}, M. Caspar ⁴⁷,
 F. Cassinese ⁹⁰, F. Castiglioni ^{73a,73b}, W.R. Castiglioni ³⁹, F.L. Castillo ⁴, V. Castillo Gimenez ¹⁶⁵,
 N.F. Castro ^{131a,131e}, A. Catinaccio ³⁷, J.R. Catmore ¹²⁶, T. Cavaliere ⁴, V. Cavaliere ³⁰,
 E. Celebi ⁸⁰, S. Cella ³⁰, V. Cepaitis ⁵⁵, K. Cerny ¹²³, A.S. Cerqueira ^{81a}, A. Cerri ^{73a,ap},
 L. Cerrito ^{75a,75b}, F. Cerutti ^{18a}, B. Cervato ^{70a,70b}, A. Cervelli ^{24b}, G. Cesarini ⁵², S.A. Cetin ⁸⁰,
 V.C. Chabalala ^{34j}, P.M. Chabrilat ¹²⁸, R. Chakkappai ⁶⁵, S. Chakraborty ¹⁶⁹, A. Chambers ⁶⁰,
 J. Chan ^{18a}, J.D. Chapman ³³, E. Chapon ¹³⁶, D.G. Charlton ²¹, C. Chauhan ¹³², Y. Che ^{112a},
 S. Chekanov ⁶, G.A. Chelkov ^{38,a}, H. Chen ³⁰, J. Chen ^{141a}, J. Chen ¹⁴⁵, M. Chen ⁵⁹,
 S. Chen ⁸⁷, S.J. Chen ^{112a}, X. Chen ^{141a}, X. Chen ^{15,ai}, Z. Chen ⁶¹, C.L. Cheng ¹⁷²,
 H.C. Cheng ^{63a}, S. Cheong ¹⁴⁶, A. Cheplakov ³⁸, E. Cherepanova ¹¹⁶, E. Cheu ⁷, K. Cheung ⁶⁴,
 L. Chevalier ¹³⁶, G. Chiarelli ^{73a}, G. Chiodini ^{69a}, A.S. Chisholm ²¹, J.L. Chisholm ¹⁶⁶,
 A. Chitan ^{28b}, M. Chitishvili ¹⁶⁵, M.V. Chizhov ^{38,r}, K. Chmiel ^{76a,76b}, K. Choi ¹¹, Y. Chou ¹⁴⁰,
 E.Y.S. Chow ¹¹⁵, G. Christou ⁵¹, K.L. Chu ¹⁷¹, M.C. Chu ^{63a}, Z. Chubinidze ⁵², J. Chudoba ¹³²,
 J.J. Chwastowski ⁸⁶, D. Cieri ¹¹⁰, K.M. Ciesla ^{85a}, V. Cindro ⁹³, A. Ciocio ^{18a}, F. Ciotto ^{71a,71b},
 Z.H. Citron ¹⁷¹, M. Citterio ^{70a}, D.A. Ciubotaru ^{28b}, A. Clark ⁵⁵, P.J. Clark ⁵¹, N. Clarke Hall ⁹⁶,
 C. Clarry ¹⁵⁸, S.E. Clawson ⁴⁷, C. Clement ^{46a,46b}, L. Clissa ^{24b,24a}, Y. Coadou ¹⁰²,
 M. Cobal ^{68a,68c}, A. Coccaro ^{56b}, M.G. Cochran Branson ¹⁴⁰, R.F. Coelho Barrue ^{131a},

R. Coelho Lopes De Sa ¹⁰³, S. Coelli ^{70a}, M.M. Cohen ¹²⁹, L.S. Colangeli ¹⁵⁸, B. Cole ⁴¹, P. Collado Soto ⁹⁹, J. Collot ⁵⁹, M.R. Coluccia ^{69a}, I. Combes ⁶⁵, P. Conde Muiño ^{131a,131g}, L.H.J. Condren ¹⁶², M.P. Connell ^{34c}, S.H. Connell ^{34c}, E.I. Conroy ¹²⁷, M. Contreras Cossio ¹¹, F. Conventi ^{71a,ak}, A.M. Cooper-Sarkar ¹²⁷, L. Corazzina ^{74a,74b}, F.A. Corchia ^{24b,24a}, A. Cordeiro Oudot Choi ¹⁴⁰, L.D. Corpe ⁴⁰, M. Corradi ^{74a,74b}, F. Corriveau ^{104,ab}, A. Cortes-Gonzalez ¹⁵⁶, M.J. Costa ¹⁶⁵, F. Costanza ⁴, D. Costanzo ¹⁴², J. Couthures ⁴, G. Cowan ⁹⁵, K. Cranmer ¹⁷², L. Cremer ⁴⁸, D. Cremonini ^{24b,24a}, S. Crépe-Renaudin ⁵⁹, F. Crescioli ¹²⁸, T. Cresta ^{72a,72b}, M. Cristinziani ¹⁴⁴, M. Cristoforetti ^{77a,77b}, T.M. Critchley ⁵⁵, E. Critelli ⁹⁶, A. Cueto ⁹⁹, H. Cui ⁹⁶, Z. Cui ⁷, B.M. Cunnett ¹⁴⁹, W.R. Cunningham ⁵⁸, E. Cuppini ¹¹⁰, F. Curcio ¹⁶⁵, J.R. Curran ⁵¹, M.J. Da Cunha Sargedas De Sousa ^{56b,56a}, J.V. Da Fonseca Pinto ^{81b}, C. Da Via ¹⁰¹, W. Dabrowski ^{85a}, T. Dado ³⁷, S. Dahbi ¹⁵¹, T. Dai ¹⁰⁶, D. Dal Santo ²⁰, C. Dallapiccola ¹⁰³, M. Dam ⁴², G. D'amen ³⁰, V. D'Amico ¹⁰⁹, J.R. Dandoy ³⁵, M. D'Andrea ^{56b,56a}, D. Dannheim ³⁷, G. D'anniballe ^{73a,73b}, M. Danninger ¹⁴⁵, V. Dao ¹⁴⁸, G. Darbo ^{56b}, F. Dattola ⁴⁷, S. D'Auria ^{70a,70b}, A. D'Avanzo ^{71a,71b}, T. Davidek ¹³⁴, J. Davidson ¹⁶⁹, I. Dawson ⁹⁴, K. De ⁸, C. De Almeida Rossi ¹⁵⁸, N. De Biase ⁴⁷, S. De Castro ^{24b,24a}, N. De Groot ¹¹⁵, P. de Jong ¹¹⁶, H. De la Torre ¹¹⁷, A. De Maria ^{112a}, S. De Miranda Rimes ^{81d}, A. De Salvo ^{74a}, U. De Sanctis ^{75a,75b}, F. De Santis ^{69a,69b}, A. De Santo ¹⁴⁹, J.B. De Vivie De Regie ⁵⁹, K.G. De Vries ¹¹⁶, J. Debevc ⁹³, D.V. Dedovich ³⁸, J. Degens ⁹², A.M. Deiana ⁴⁴, J. Del Peso ⁹⁹, L. Delagrangé ²⁷, F. Deliot ¹³⁶, C.M. Delitzsch ⁴⁸, M. Della Pietra ^{71a,71b}, D. Della Volpe ⁵⁵, A. Dell'Acqua ³⁷, L. Dell'Asta ^{70a,70b}, M. Delmastro ⁴, C.C. Delogu ^{56b,56a}, P.A. Delsart ⁵⁹, S. Demers ¹⁷⁴, M. Demichev ³⁸, H. Denizli ^{22a,1}, M.G. Depala ⁹², L. D'Eramo ⁴⁰, D. Derendarz ⁸⁶, L. Derin ^{56b,56a}, F. Derue ¹²⁸, P. Dervan ^{92,*}, A.M. Desai ¹, K. Desch ²⁵, F.A. Di Bello ^{73a,73b}, A. Di Ciaccio ^{75a,75b}, L. Di Ciaccio ⁴, D. Di Croce ³⁷, C. Di Donato ^{71a,71b}, A. Di Girolamo ³⁷, G. Di Gregorio ⁶⁵, A. Di Luca ^{77a,77b}, B. Di Micco ^{76a,76b}, R. Di Nardo ^{76a,76b}, K.F. Di Petrillo ³⁹, M. Diamantopoulou ¹⁵⁴, F.A. Dias ¹¹⁶, M.A. Diaz ^{138a,138b}, A.R. Didenko ³⁸, M. Didenko ¹⁶⁵, S.D. Diefenbacher ^{18a}, E.B. Diehl ¹⁰⁶, S. Díez Cornell ⁴⁷, C. Díez Pardos ¹⁴⁴, C. Dimitriadi ¹⁴⁷, A. Dimitrievska ²¹, A. Dimri ¹⁴⁸, Y. Ding ⁶¹, J. Dingfelder ²⁵, T. Dingley ¹²⁷, I-M. Dinu ^{28b}, S.J. Dittmeier ^{62b}, F. Dittus ³⁷, M. Divisek ¹³⁴, B. Dixit ⁹², F. Djama ¹⁰², T. Djobava ^{152b}, C. Doglioni ^{101,98}, A. Dohnalova ^{29a}, Z. Dolezal ¹³⁴, K. Domijan ^{85a}, K.M. Dona ³⁹, M. Donadelli ^{81d}, B. Dong ¹⁰⁷, J. Donini ⁴⁰, A. D'Onofrio ^{71a,71b}, M. D'Onofrio ⁹², J. Dopke ¹³⁵, A. Doria ^{71a}, N. Dos Santos Fernandes ^{131a}, I.A. Dos Santos Luz ^{81e}, P. Dougan ⁴⁴, M.T. Dova ⁹⁰, A.T. Doyle ⁵⁸, M.P. Drescher ⁵⁴, E. Dreyer ¹⁷¹, I. Drivas-koulouris ¹⁰, M. Drnevich ¹¹⁸, D. Du ⁶¹, T. Du ³⁹, T.A. du Pree ¹¹⁶, Z. Duan ^{112a}, M. Dubau ⁴, F. Dubinin ³⁸, M. Dubovsky ^{29a}, E. Duchovni ¹⁷¹, G. Duckeck ¹⁰⁹, P.K. Duckett ⁹⁶, O.A. Ducu ^{28b}, D. Duda ⁵¹, A. Dudarev ³⁷, M.M. Dudek ⁸⁶, E.R. Duden ²⁷, M. D'uffizi ¹⁰¹, L. Duflost ⁶⁵, M. Dührssen ³⁷, I. Duminica ^{28g}, A.E. Dumitriu ^{28b}, M. Dunford ^{62a}, T. Duong ⁴, A. Duperrin ¹⁰², A.F. Duque Bran ⁴⁰, H. Duran Yildiz ^{3a}, A. Durglishvili ^{152b}, G.I. Dyckes ^{18a}, M. Dyndal ^{85a}, B.S. Dziedzic ³⁷, G.H. Eberwein ¹²⁷, B. Eckerova ^{29a}, J.C. Egan ⁹⁶, S. Eggebrecht ⁵⁴, E. Egidio Purcino De Souza ^{81e}, G. Eigen ¹⁷, K. Einsweiler ^{18a}, T. Ekelof ¹⁶³, P.A. Ekman ⁹⁸, S. El Farkh ^{36b}, Y. El Ghazali ⁶¹, H. El Jarrari ¹⁰⁴, A. El Moussaouy ^{36a}, I. Elbaz ¹⁵⁴, D. Elitez ³⁷, M. Ellert ¹⁶³, F. Ellinghaus ¹⁷³, T.A. Elliot ⁹⁵, J. Elmsheuser ³⁰, M. Elsayy ^{83b}, M. Elsing ³⁷, D. Emeliyanov ¹³⁵, Y. Enari ⁸², S. Epari ¹⁰⁸, D. Ernani Martins Neto ⁸⁶, F. Ernst ³⁷, M. Escalier ⁶⁵, C. Escobar ¹⁶⁵, R. Estevam De Paula ^{81c}, E. Etzion ¹⁵⁴, G. Evans ^{131a,131b}, H. Evans ⁶⁷, L.S. Evans ⁴⁷, S. Ezzarqtouni ^{36a}, F. Fabbri ^{24b,24a}, L. Fabbri ^{24b,24a}, G. Facini ⁹⁶, V. Fadeyev ¹³⁷, D. Fakoudis ¹⁰⁰, S. Falciano ^{74a}, L.F. Falda Ulhoa Coelho ²⁷, F. Fallavollita ¹¹⁰, G. Falsetti ^{43b,43a}, J. Faltova ¹³⁴, C. Fan ¹⁶⁴, K.Y. Fan ^{63b}, Y. Fan ¹⁴, Y. Fang ^{14,112c},

M. Fanti ^{70a,70b}, M. Faraj ^{68a,68c}, Z. Farazpay ⁹⁷, A. Farbin ⁸, A. Farilla ^{76a}, K. Farman ¹⁵¹,
J.N. Farr ¹⁷⁴, M.S. Farrington ⁶⁰, S.M. Farrington ^{135,51}, F. Fassi ^{36e}, D. Fassouliotis ⁹,
L. Fayard ⁶⁵, G. Fazzino ^{62b}, P. Federic ¹³⁴, P. Federicova ¹³², M. Feickert ¹⁷², L. Feligioni ¹⁰²,
D.E. Fellers ^{18a}, C. Feng ^{113b}, Y. Feng ¹⁴, Z. Feng ⁶⁵, B. Fernandez Barbadillo ⁹¹,
P. Fernandez Martinez ⁶⁶, C. Fernandez Ruiz ³³, J. Ferrando ⁹¹, A. Ferrari ¹⁶³, P. Ferrari ^{116,115},
R. Ferrari ^{72a}, D. Ferrere ⁵⁵, C. Ferretti ¹⁰⁶, M.P. Fewell ¹, D. Fiacco ^{74a,74b}, F. Fiedler ¹⁰⁰,
P. Fiedler ¹³³, S. Filimonov ³⁸, M.S. Filip ^{28b,s}, M. Filipig ^{68a,68c}, A. Filipčič ⁹³,
E.K. Filmer ^{159a}, F. Filthaut ¹¹⁵, M.C.N. Fiolhais ^{131a,131c,c}, L. Fiorini ¹⁶⁵, W.C. Fisher ¹⁰⁷,
T. Fitschen ¹⁰¹, I. Fleck ¹⁴⁴, P. Fleischmann ¹⁰⁶, T. Flick ¹⁷³, M. Flores ^{34d,ag},
L.R. Flores Castillo ^{63a}, M. Foll ¹²⁶, F.M. Follega ^{77a,77b}, N. Fomin ³³, J.H. Foo ¹⁵⁸,
A. Formica ¹³⁶, M. Fornasiero ¹⁴⁹, A.C. Forti ¹⁰¹, N. Forti ^{24b,24a}, E. Fortin ¹⁰²,
A.W. Fortman ^{18a}, L. Foster ^{18a}, L. Fountas ⁹, H. Fox ⁹¹, P. Francavilla ^{73a,73b},
S. Francescato ⁶⁰, S. Franchellucci ²⁰, M. Franchini ^{24b,24a}, S. Franchino ^{62a}, D. Francis ³⁷,
L. Franco ⁴⁷, L. Franconi ⁴⁷, M. Franklin ⁶⁰, G. Frattari ³⁷, Y.Y. Frid ¹⁵⁴, N. Fritzsche ³⁷,
A. Froch ⁵⁵, D. Froidevaux ³⁷, J.A. Frost ¹³⁵, Y. Fu ¹⁰⁷, S. Fuenzalida Garrido ^{138g},
Y.C. Fujikake ¹³⁷, M. Fujimoto ¹⁴⁸, K.Y. Fung ^{63a}, E. Furtado De Simas Filho ^{81e},
M. Furukawa ¹⁵⁶, M. Fuste Costa ⁴⁷, P. Fuste Martin ¹³, J. Fuster ¹⁶⁵, A. Gaa ⁵⁴,
A. Gabrielli ^{24b,24a}, A. Gabrielli ¹⁵⁸, G. Gagliardi ^{56b,56a}, L.G. Gagnon ^{18a}, S. Galantzan ¹⁵⁴,
J. Gallagher ¹, E.J. Gallas ¹²⁷, A.L. Gallen ¹⁶³, B.J. Gallop ¹³⁵, K.K. Gan ¹²⁰, Y. Gao ⁵¹,
Z. Gao ^{112a}, A. Garabaglu ¹⁴⁰, F.M. Garay Walls ^{138a,138b}, C. García ¹⁶⁵, A. Garcia Alonso ¹¹⁶,
A.G. Garcia Caffaro ¹⁷⁴, J.E. García Navarro ¹⁶⁵, M.A. Garcia Ruiz ^{23b}, M. Garcia-Sciveres ^{18a},
G.L. Gardner ¹²⁹, R.W. Gardner ³⁹, N. Garelli ¹⁶¹, R.B. Garg ¹⁴⁶, J.M. Gargan ³³, C.A. Garner ¹⁵⁸,
C.M. Garvey ^{34a}, V.K. Gassmann ¹⁶¹, G. Gaudio ^{72a}, A.J. Gavin ⁹⁴, J. Gavranovic ⁹³,
I.L. Gavrilenko ^{131a}, C. Gay ¹⁶⁶, G. Gaycken ¹²⁴, A. Gekow ¹²⁰, C. Gemme ^{56b}, M.H. Genest ⁵⁹,
A.D. Gentry ¹¹⁴, S. George ⁹⁵, T. Geralis ⁴⁵, A.A. Gerwin ¹²¹, P. Gessinger-Befurt ³⁷,
M. Ghani ¹⁶⁹, K. Ghorbanian ⁹⁴, A. Ghosal ¹⁴⁴, A. Ghosh ¹⁶², A. Ghosh ⁷, B. Giacobbe ^{24b},
S. Giagu ^{74a,74b}, A. Giannini ⁶¹, S.M. Gibson ⁹⁵, D.T. Gil ^{85b}, B.J. Gilbert ⁴¹, D. Gillberg ³⁵,
G. Gilles ¹¹⁶, D.M. Gingrich ^{2,aj}, M.P. Giordani ^{68a,68c}, P.F. Giraud ¹³⁶, G. Giugliarelli ^{68a,68c},
D. Giugni ^{70a}, F. Giuli ^{75a,75b,al}, I. Gkialas ^{9,i}, B.C. Gladwyn ¹²⁷, C. Glasman ⁹⁹,
M. Glazewska ²⁰, R.M. Gleason ¹⁶², G. Glemža ⁴⁷, I. Gnesi ^{24b,24a,am}, Y. Go ³⁰,
M. Goblirsch-Kolb ³⁷, B. Gocke ⁴⁸, D. Godin ¹⁰⁸, B. Gokturk ^{22a}, S. Goldfarb ¹⁰⁵, T. Golling ⁵⁵,
M.G.D. Gololo ^{34c}, A. Golub ¹⁴⁰, J.P. Gombas ¹⁰⁷, A. Gomes ^{131a,131b}, G. Gomes Da Silva ¹⁴⁴,
A.J. Gomez Delegido ³⁷, R. Gonçalves ^{131a}, A. Gongadze ^{152c}, F. Gonnella ²¹, J.L. Gonski ¹⁴⁶,
R.Y. González Andana ⁵¹, S. González de la Hoz ¹⁶⁵, M.V. Gonzalez Rodrigues ⁴⁷,
R. Gonzalez Suarez ¹⁶³, S. Gonzalez-Sevilla ⁵⁵, L. Goossens ³⁷, B. Gorini ³⁷, E. Gorini ^{69a,69b},
A. Gorišek ⁹³, T.C. Gosart ¹²⁹, A.T. Goshaw ⁵⁰, M.I. Gostkin ³⁸, S. Goswami ¹²²,
C.A. Gottardo ³⁷, S.A. Gotz ¹⁰⁹, M. Goughri ^{36b}, A.G. Goussiou ¹⁴⁰, N. Govender ^{34c},
R.P. Grabarczyk ¹²⁷, I. Grabowska-Bold ^{85a}, K. Graham ³⁵, E. Gramstad ¹²⁶,
S. Grancagnolo ^{69a,69b}, C.M. Grant ¹, P.M. Gravila ^{28f}, F.G. Gravili ^{69a,69b}, H.M. Gray ^{18a},
M. Greco ¹¹⁰, M.J. Green ¹, C. Grefe ²⁵, A.S. Grefsrud ¹⁷, I.M. Gregor ⁴⁷, K.T. Greif ¹⁶²,
P. Grenier ¹⁴⁶, S.G. Grewe ¹¹⁰, K. Grimm ³², S. Grinstein ^{13,x}, E. Gross ¹⁷¹, J. Grosse-Knetter ⁵⁴,
L.H. Grossman ^{18b}, L. Guan ¹⁰⁶, G. Guerrieri ³⁷, R. Guevara ¹²⁶, R. Gugel ¹⁰⁰,
J.A.M. Guhit ¹⁰⁶, A. Guida ¹⁹, E. Guilloton ¹⁶⁹, S. Guindon ³⁷, F. Guo ^{14,112c}, J. Guo ^{141a},
L. Guo ⁴⁷, L. Guo ^{112b,u}, Y. Guo ¹⁰⁶, Y. Guo ⁴¹, A. Gupta ⁴⁸, R. Gupta ¹³⁰, S. Gupta ²⁷,
S. Gurbuz ²⁵, S.S. Gurdasani ⁴⁷, G. Gustavino ^{74a,74b}, P. Gutierrez ¹²¹,
L.F. Gutierrez Zagazeta ¹²⁹, M. Gutsche ⁴⁹, C. Gutschow ⁹⁶, W. Guérin ⁸⁹, C. Gwenlan ¹²⁷,
C.B. Gwilliam ⁹², E.S. Haaland ¹²⁶, A. Haas ¹¹⁸, M. Habedank ⁵⁸, C. Haber ^{18a},

R.J. Haberle ¹⁷¹, H.K. Hadavand ⁸, A. Haddad ⁴⁰, A. Hadeef ⁴⁹, A.I. Hagan ⁹¹, J.J. Hahn ¹⁴⁴, M. Haleem ¹⁶⁸, J. Haley ¹²², G.D. Hallelwell ¹⁰², J.A. Hallford ⁴⁷, K. Hamano ¹⁶⁷, H. Hamdaoui ¹⁶³, M. Hamer ²⁵, S.E.D. Hammoud ⁶⁵, E.J. Hampshire ⁹⁵, L. Han ^{112a}, L. Han ⁶¹, S. Han ¹⁴, K. Hanagaki ⁸², M. Hance ¹³⁷, D.A. Hangal ⁴¹, H. Hanif ¹⁴⁵, M.D. Hank ¹²⁹, J.B. Hansen ⁴², P.H. Hansen ⁴², T. Harenberg ¹⁷³, S. Harkusha ¹⁷⁵, M.L. Harris ¹⁰³, Y.T. Harris ²⁵, J. Harrison ¹³, P.F. Harrison ¹⁶⁹, M.L.E. Hart ⁹⁶, N.M. Hartman ¹¹⁰, N.M. Hartmann ¹⁰⁹, R.Z. Hasan ^{95,135}, Y. Hasegawa ¹⁴³, D. Hashimoto ¹¹¹, F. Haslbeck ³⁷, S. Hassan ¹²⁶, R. Hauser ¹⁰⁷, M. Haviernik ¹³⁴, C.M. Hawkes ²¹, R.J. Hawkings ³⁷, Y. Hayashi ¹⁵⁶, D. Hayden ¹⁰⁷, R.L. Hayes ¹¹⁶, C.P. Hays ¹²⁷, J.M. Hays ⁹⁴, H.S. Hayward ⁹², M. He ^{14,112c}, Y. He ⁴⁷, Y. He ⁹⁶, V. Hedberg ⁹⁸, J. Heilman ³⁵, S. Heim ⁴⁷, T. Heim ^{18a}, J.J. Heinrich ¹²⁴, L. Heinrich ¹¹⁰, J. Hejbal ¹³², M. Helbig ⁴⁹, A. Held ¹⁷², S. Hellesund ¹⁷, C.M. Helling ¹⁶⁶, F.N.E. Henry ⁵⁸, H. Herde ⁹⁸, Y. Hernández Jiménez ¹⁴⁸, G. Hertén ⁵³, R. Herténberger ¹⁰⁹, L. Hervás ³⁷, M.E. Hespings ¹⁰⁰, N.P. Hessey ^{159a}, J. Hessler ¹¹⁰, R. Hicks ¹²⁹, M. Hidaoui ^{36b}, N. Hidic ¹³⁴, E. Hill ¹⁵⁸, T.S. Hillersoy ¹⁷, S.J. Hillier ²¹, J.R. Hinds ¹⁰⁷, F. Hinterkeuser ²⁵, M. Hirose ¹²⁵, S. Hirose ¹⁶⁰, D. Hirschbuehl ¹⁷³, B. Hiti ⁹³, J. Hobbs ¹⁴⁸, R. Hobincu ^{28e}, N. Hod ¹⁷¹, A.M. Hodges ¹⁶⁴, M.C. Hodgkinson ¹⁴², B.H. Hodgkinson ¹²⁷, A. Hoecker ³⁷, D.D. Hofer ¹⁰⁶, J. Hofer ¹⁶⁵, J. Hofner ¹⁰⁰, M. Holzbock ³⁷, L.B.A.H. Hommels ³³, V. Homsak ¹²⁷, J.J. Hong ⁶⁷, T.M. Hong ¹³⁰, R. Honscheid ¹²⁷, B.H. Hooberman ¹⁶⁴, W.H. Hopkins ⁶, M.C. Hoppesch ¹⁶⁴, Y. Horii ¹¹¹, M.E. Horstmann ¹¹⁰, M.M. Horzela ⁵⁴, S. Hou ¹⁵¹, M.R. Housenga ¹⁶⁴, J. Howarth ⁵⁸, J. Hoya ⁶, M. Hrabovsky ¹²³, T. Hryn'ova ⁴, P.J. Hsu ⁶⁴, S.-C. Hsu ¹⁴⁰, T. Hsu ⁶⁵, M. Hu ^{18a}, P. Hu ^{63b}, Q. Hu ⁶¹, S. Huang ³³, X. Huang ^{14,112c}, Y. Huang ¹³⁴, Y. Huang ^{112b}, Y. Huang ¹⁴, Z. Huang ⁶⁵, Z. Hubacek ¹³³, F. Huegging ²⁵, T.B. Huffman ¹²⁷, M. Hufnagel Maranha De Faria ^{81a}, C.A. Hugli ⁴⁷, M. Huhtinen ³⁷, S.K. Huiberts ¹⁷, R. Hulsken ¹⁰⁴, C.E. Hultquist ^{18a}, D.L. Humphreys ¹⁰³, N. Huseynov ¹², J. Huston ¹⁰⁷, B. Huth ³⁷, J. Huth ⁶⁰, L. Huth ⁴⁷, R. Hyneman ⁷, G. Iacobucci ⁵⁵, G. Iakovidis ³⁰, L. Iconomidou-Fayard ⁶⁵, J.P. Iddon ³⁷, P. Iengo ^{71a,71b}, Y. Iiyama ¹⁵⁶, T. Iizawa ¹⁵⁶, Y. Ikegami ⁸², D. Iliadis ¹⁵⁵, N. Ilic ¹⁵⁸, H. Imam ^{36a}, G. Inacio Goncalves ^{81d}, S.A. Infante Cabanas ^{138c}, T. Ingebretsen Carlson ^{46a,46b}, J.M. Inglis ⁹⁴, G. Introzzi ^{72a,72b}, M. Iodice ^{76a}, V. Ippolito ^{74a,74b}, R.K. Irwin ⁹², M. Ishino ¹⁵⁶, W. Islam ¹⁷², C. Issever ¹⁹, O.N. Istantia ^{65,b}, S. Istin ^{22a,ar}, K. Itabashi ¹²⁵, H. Ito ¹⁷⁰, R. Iuppa ^{77a,77b}, A. Ivina ¹⁷¹, F. Ivone ³⁷, S. Izumiyama ¹¹¹, V. Izzo ^{71a}, P. Jacka ¹³³, P. Jackson ¹, P.R. Jacobson ⁵⁰, P. Jain ⁴⁷, K. Jakobs ⁵³, J. Jamieson ⁵⁸, W. Jang ¹⁵⁶, S. Jankovych ¹¹⁶, B.K. Jashal ¹³⁵, M. Javurkova ¹⁰³, P. Jawahar ¹⁰¹, L. Jeanty ¹²⁴, J. Jejelava ^{152a,ae}, P. Jenni ^{53,f}, L. Jerala ⁹³, C.E. Jessiman ³⁵, H. Jia ¹⁶⁶, J. Jia ¹⁴⁸, K. Jia ¹⁴⁶, X. Jia ^{110,112c}, C. Jiang ⁵¹, Q. Jiang ^{63b}, S. Jiggins ⁴⁷, M. Jimenez Ortega ¹⁶⁵, J. Jimenez Pena ¹³, S. Jin ^{112a}, A. Jinaru ^{28b}, O. Jinnouchi ¹³⁹, P. Johansson ¹⁴², K.A. Johns ⁷, J.W. Johnson ¹³⁷, F.A. Jolly ⁴⁷, D.M. Jones ¹⁴⁹, E. Jones ⁴⁷, P. Jones ³³, R.W.L. Jones ⁹¹, T.J. Jones ⁹², H.L. Joos ³⁷, R. Joshi ¹²⁰, J. Jovicevic ¹⁶, X. Ju ^{18a}, J.J. Junggeburth ³⁷, T. Junkermann ^{62a}, A. Juste Rozas ^{13,x}, M.K. Juzek ⁸⁶, S. Kabana ^{138f}, A. Kaczmarska ⁸⁶, S.A. Kadir ¹⁴⁶, M. Kado ¹¹⁰, H. Kagan ¹²⁰, M. Kagan ¹⁴⁶, A. Kahn ¹²⁹, C. Kahra ¹⁰⁰, T. Kaji ¹⁵⁶, E. Kajomovitz ¹⁵³, N. Kakati ¹⁷¹, N. Kakoty ¹³, S. Kandel ⁸, E. Kanellaki ⁴⁵, N. Kanellos ¹⁰, S. Kang ⁵⁰, D. Kar ^{34j,*}, E. Karentzos ²⁵, K. Karki ⁸, O. Karkout ¹¹⁶, S.N. Karpov ³⁸, Z.M. Karpova ³⁸, V. Kartvelishvili ^{91,152b}, E. Kasimi ¹⁵⁵, J. Katzy ⁴⁷, S. Kaur ³⁵, R. Kavak ¹⁶⁴, K. Kawade ¹⁴³, M.P. Kawale ¹²¹, C. Kawamoto ⁸⁷, E.F. Kay ³⁷, S. Kazakos ¹⁰⁷, K. Kazakova ¹⁰², J.M. Keaveney ^{34a}, R. Keeler ¹⁶⁷, G.V. Kehris ⁶⁰, J.S. Keller ³⁵, J.M. Kelly ¹⁶⁷, J.I. Kelsey ¹⁶⁴, J.J. Kempster ¹⁴⁹, O. Kepka ¹³², J. Kerr ^{159b}, B.P. Kerridge ¹³⁵, B.P. Kerševan ⁹³, L. Keszeghova ^{29a}, R.A. Khan ¹³⁰, A. Khanov ¹²², M. Kholodenko ^{131a},

T.J. Khoo ¹⁹, G. Khoraiuli ¹⁶⁸, Y. Khoulaki ^{36a}, Y.A.R. Khwaira ¹²⁸, D. Kim ⁶, D.W. Kim ^{18b},
Y.K. Kim ³⁹, N. Kimura ⁹⁶, M.K. Kingston ⁵⁴, F. Kirfel ²⁵, J. Kirk ¹³⁵, A.E. Kiryunin ¹¹⁰,
S. Kita ¹⁶⁰, O. Kivernyk ²⁵, M. Klassen ³⁷, C. Klein ³⁵, L. Klein ¹⁶⁸, M.H. Klein ⁴⁴,
S.B. Klein ⁵⁵, U. Klein ⁹², A. Klimentov ³⁰, P. Kluit ¹¹⁶, S. Kluth ¹¹⁰, E. Kneringer ⁷⁸,
T.M. Knight ¹⁵⁸, A. Knue ⁴⁸, M. Kobel ⁴⁹, D. Kobylianskii ¹⁷¹, S.F. Koch ³⁷, M. Kocian ¹⁴⁶,
P. Kodyš ¹³⁴, D.M. Koeck ¹²⁴, T. Koffas ³⁵, K. Kojima ⁸², O. Kolay ⁴⁹, I. Koletsou ⁴,
T. Komarek ⁸⁶, S. Kondo ¹⁵⁶, K. Köneke ⁵⁴, A.X.Y. Kong ¹, T. Kono ¹¹⁹, N. Konstantinidis ⁹⁶,
P. Kontaxakis ⁵⁵, B. Konya ⁹⁸, R. Kopeliansky ⁴¹, S. Koperny ^{85a}, R. Koppenhofer ⁵³,
I. Kopsalis ¹⁰, K. Korcyl ⁸⁶, K. Kordas ^{155,d}, A. Korn ⁹⁶, S. Korn ⁵⁴, I. Korolkov ¹³,
O. Kortner ¹¹⁰, S. Kortner ¹¹⁰, W.H. Kostecka ¹¹⁷, M. Kostov ^{29a}, V.V. Kostyukhin ¹⁴⁴,
A. Kotsokechagia ³⁷, A. Kotwal ⁵⁰, A. Koulouris ³⁷, A. Kourkoumeli-Charalampidi ^{72a,72b},
O. Kovanda ¹²⁴, R. Kowalewski ¹⁶⁷, W. Kozanecki ¹²⁴, G. Kramberger ⁹³, P. Kramer ²⁵,
A. Krasznahorkay ¹⁰³, A.C. Kraus ¹¹⁷, J.W. Kraus ¹⁷³, J.A. Kremer ⁴⁷, N.B. Krengel ¹⁴⁴,
T. Kresse ¹⁵⁸, L. Kretschmann ¹⁷³, J. Kretzschmar ⁹², P. Krieger ¹⁵⁸, K. Krizka ²¹,
K. Kroeninger ⁴⁸, H. Kroha ¹¹⁰, J. Kroll ¹³², J. Kroll ¹²⁹, K.S. Krowpman ¹⁰⁷, U. Kruchonak ³⁸,
H. Krüger ²⁵, N. Krumnack ⁷⁹, J. Krupa ¹⁴⁶, M.C. Kruse ⁵⁰, O. Kuchinskaia ³⁸, S. Kuday ^{3a},
S. Kuehn ³⁷, R. Kuesters ⁵³, T. Kuhl ⁴⁷, V. Kukhtin ³⁸, Y. Kulchitsky ³⁸, S. Kuleshov ^{138d,138b},
J. Kull ¹, E.V. Kumar ¹⁰⁹, M. Kumar ^{34j}, N. Kumari ⁴⁷, P. Kumari ^{159b}, A. Kupco ¹³²,
O. Kuprash ⁵³, H. Kurashige ⁸⁴, L.L. Kurchaninov ^{159a}, O. Kurdysh ⁴, M. Kuze ¹³⁹,
A.K. Kvam ¹⁰³, J. Kvita ¹²³, N.G. Kyriacou ¹⁴⁰, M. Laassiri ³⁰, C. Lacasta ¹⁶⁵, H. Lacker ¹⁹,
D. Lacour ¹²⁸, E. Ladygin ³⁸, A. Lafarge ⁴⁰, B. Laforge ¹²⁸, T. Lagouri ¹⁷⁴, F.Z. Lahbabi ^{36a},
S. Lai ⁵⁴, W.S. Lai ⁹⁶, I.K. Lakomic ⁵⁴, J.E. Lambert ¹⁶⁷, S. Lammers ⁶⁷, W. Lampl ⁷,
C. Lampoudis ¹⁵⁵, G. Lamprinoudis ¹⁶⁸, A.N. Lancaster ¹¹⁷, U. Landgraf ⁵³, M.P.J. Landon ⁹⁴,
V.S. Lang ⁵³, A.J. Lankford ¹⁶², F. Lanni ³⁷, C.S. Lantz ¹⁶⁴, K. Lantzsch ²⁵, A. Lanza ^{72a},
M. Lanzac Berrocal ¹⁶⁵, T. Lari ^{70a}, D. Larsen ¹⁷, L. Larson ¹¹, F. Lasagni Manghi ^{24b},
M. Lassnig ³⁷, H.C. Lau ¹⁶⁷, S.D. Lawlor ¹⁴², R. Lazaridou ¹⁶², M. Lazzaroni ^{70a,70b},
E.T.T. Le ¹⁶², H.D.M. Le ¹⁰⁷, E.M. Le Boulicaut ¹⁷⁴, D.O. Le Guennec ¹³⁶, L.T. Le Pottier ^{18a},
B. Leban ^{24b,24a}, F. Ledroit-Guillon ⁵⁹, T.F. Lee ^{159b}, L.L. Leeuw ^{34h}, M. Lefebvre ¹⁶⁷,
C. Leggett ^{18a}, L.M. Lehmann ¹¹⁶, W.A. Leight ¹⁰³, W. Leinonen ¹¹⁵, A. Leisos ^{155,t},
M.A.L. Leite ^{81c}, C.E. Leitgeb ¹⁹, R. Leitner ¹³⁴, E. Lelak ¹³⁴, K.J.C. Leney ⁴⁴, T. Lenz ²⁵,
S. Leone ^{73a}, C. Leonidopoulos ⁵¹, A. Leopold ¹⁴⁷, J. LePage-Bourbonnais ³⁵, R. Les ¹⁰⁷,
C.G. Lester ³³, J. Levêque ⁴, L.J. Levinson ¹⁷¹, G. Levrini ^{24b,24a}, M.P. Lewicki ⁸⁶,
C. Lewis ¹⁴⁰, D.J. Lewis ⁴, L. Lewitt ¹⁴², A. Li ³⁰, B. Li ^{113b}, C. Li ¹⁰⁶, C-Q. Li ¹¹⁰, H. Li ^{113b},
H. Li ¹⁰¹, H. Li ¹⁵, H. Li ⁶¹, H. Li ^{113b}, J. Li ^{141a}, L. Li ^{141a}, R. Li ¹⁷⁴, S. Li ^{141b,141a}, T. Li ⁵,
Y. Li ¹⁴, Z. Li ^{14,112c}, Z. Li ⁶¹, S. Liang ^{14,112c}, Z. Liang ¹⁴, M. Liberatore ¹³⁶, B. Liberti ^{75a},
G.B. Libotte ^{81d}, K. Lie ^{63c}, J. Lieber Marin ^{81e}, H. Lien ⁶⁷, H. Lin ¹⁰⁶, S.F. Lin ¹⁴⁸,
L. Linden ¹⁰⁹, R.E. Lindley ⁷, J.H. Lindon ³⁷, J. Ling ⁶⁰, E. Lipeles ¹²⁹, A. Lipniacka ¹⁷,
A. Lister ¹⁶⁶, J.D. Little ⁶⁷, B. Liu ^{113a}, B.X. Liu ^{112b}, D. Liu ¹⁵³, D. Liu ¹³⁷, E.H.L. Liu ²¹,
H. Liu ^{112b}, J.K.K. Liu ¹¹⁸, K. Liu ^{141b}, K. Liu ^{141b}, M. Liu ⁶¹, M.Y. Liu ⁶¹, P. Liu ^{113b},
Q. Liu ¹⁴⁶, S. Liu ¹⁴⁸, X. Liu ^{113b}, Y. Liu ^{112b,112c}, Y. Liu ¹⁶⁴, Y.L. Liu ^{113b}, Y.W. Liu ⁶¹,
Z. Liu ^{65j}, S.L. Lloyd ⁹⁴, E.M. Lobodzinska ⁴⁷, P. Loch ⁷, E. Lodhi ¹⁵⁸, K. Lohwasser ¹⁴²,
E. Loiacono ¹²², J.D. Lomas ²¹, I. Longarini ¹⁶², R. Longo ^{24b,24a,am}, A. Lopez Solis ¹³,
N.A. Lopez-canelas ⁷, N. Lorenzo Martinez ⁴, A.M. Lory ¹⁰⁹, M. Losada ^{83b},
G. Löschke Centeno ⁴, X. Lou ^{14,112c}, P.A. Love ⁹¹, H. Lu ¹⁴, M. Lu ⁶⁵, S. Lu ¹²⁹,
Y.J. Lu ¹⁵¹, H.J. Lubatti ¹⁴⁰, C. Luci ^{74a,74b}, F.L. Lucio Alves ^{112a}, J.A. Lue ¹²⁴, F. Luehring ⁶⁷,
B.S. Lunday ¹²⁹, O. Lundberg ¹⁴⁷, J. Lunde ³⁷, N.A. Luongo ⁶, M.S. Lutz ¹⁵⁸, A.B. Lux ²⁶,
D. Lynn ³⁰, R. Lysak ¹³², V. Lysenko ¹³³, E. Lytken ⁹⁸, V. Lyubushkin ³⁸, T. Lyubushkina ³⁸,

M.M. Lyukova ¹⁴⁸, H. Ma ³⁰, K. Ma ⁶¹, L.L. Ma ^{113b}, W. Ma ⁶¹, Y. Ma ^{113b},
P.C. Machado De Abreu Farias ^{81e}, D. Macina ³⁷, R. Madar ⁴⁰, T. Madula ⁹⁶, J. Maeda ⁸⁴,
T. Maeno ³⁰, P.T. Mafa ^{34f}, G. Magni ⁶⁵, H. Maguire ¹⁴², M. Maheshwari ³³, V. Maiboroda ⁶⁵,
G. Maineri ^{70a,70b}, A. Maio ^{131a,131b,131d}, K. Maj ^{85a}, O. Majersky ⁴⁷, S. Majewski ¹²⁴,
A. Makita ¹⁵⁶, N. Makovec ⁶⁵, V. Maksimovic ¹⁶, B. Malaescu ¹²⁸, J. Malamant ¹²⁶,
Pa. Malecki ⁸⁶, F. Malek ^{59,n}, M. Mali ⁹³, D. Malito ⁹⁵, A. Maloizel ⁵, A. Malvezzi Lopes ^{81d},
S. Malyukov ³⁸, J. Mamuzic ⁹³, G. Mancini ⁵², M.N. Mancini ²⁷, G. Manco ^{72a,72b},
S.S. Mandarray ¹⁴⁹, I. Mandić ⁹³, L. Manhaes de Andrade Filho ^{81a}, I.M. Maniatis ¹⁷¹,
J. Manjarres Ramos ⁸⁹, D.C. Mankad ¹⁷¹, A. Mann ¹⁰⁹, T. Manoussos ³⁷, M.N. Mantinan ³⁹,
S. Manzoni ³⁷, L. Mao ^{141a}, X. Mapekula ^{34c}, A. Marantis ¹⁵⁵, R.R. Marcelo Gregorio ¹,
G. Marchiori ⁵, C. Marcon ^{70a}, E. Maricic ¹⁶, M. Marinescu ⁴⁷, S. Marium ⁴⁷,
M. Marjanovic ¹²¹, A. Markhoos ⁵³, M. Markovitch ⁶⁵, M.K. Maroun ¹⁰³, M.C. Marr ¹⁴⁵,
T.L. Marsault ¹³⁶, G.T. Marsden ¹⁰¹, Z. Marshall ^{18a}, S. Marti-Garcia ¹⁶⁵, J. Martin ⁹⁶,
T.A. Martin ¹³⁵, V.J. Martin ⁵¹, B. Martin dit Latour ¹⁷, L. Martinelli ^{74a,74b},
V.I. Martinez Outschoorn ¹⁰³, P. Martinez Suarez ³⁷, S. Martin-Haugh ¹³⁵, G. Martinovicova ¹³⁴,
V.S. Martoiu ^{28b}, A. Martone ⁸⁹, A.C. Martyniuk ⁹⁶, A. Marzin ³⁷, D. Mascione ^{77a,77b},
L. Masetti ¹⁰⁰, J. Masik ¹⁰¹, A.L. Maslennikov ³⁸, S.L. Mason ⁴¹, P. Massarotti ^{71a,71b},
P. Mastrandrea ^{73a,73b}, A. Mastroberardino ^{43b,43a}, R. Mastrofrancesco ^{72a,72b}, T. Masubuchi ¹²⁵,
T.T. Mathew ¹²⁴, J. Matousek ¹³⁴, D.M. Mattern ⁴⁸, K. Mauer ⁴⁷, J. Maurer ^{28b}, T. Maurin ⁵⁸,
B. Maček ⁹³, C. Mavungu Tsava ¹⁰², A.E. May ¹⁰¹, E. Mayer ⁴⁰, R. Mazini ^{34j}, S.M. Mazza ¹³⁷,
E. Mazzeo ³⁷, J.P. Mc Gowan ¹⁶⁷, S.P. Mc Kee ¹⁰⁶, C.C. McCracken ¹⁶⁶, E.F. McDonald ¹⁰⁵,
L.F. Mcelhinney ⁹¹, J.A. Mcfayden ¹⁴⁹, R.P. McGovern ¹⁶⁷, R.P. Mckenzie ^{34j},
D.J. McLaughlin ⁹⁶, S.J. McMahon ¹³⁵, C.M. Mcpartland ⁹², R.A. McPherson ^{167,ab},
S. Mehlhase ¹⁰⁹, A. Mehta ⁹², D. Melini ¹⁶⁵, B.R. Mellado Garcia ^{14,ah}, A.H. Melo ⁵⁴,
F. Meloni ⁴⁷, A.M. Mendes Jacques Da Costa ¹⁰¹, L. Meng ⁹¹, S. Menke ¹¹⁰, M. Mentink ³⁷,
E. Meoni ^{43b,43a}, G. Mercado ¹¹⁷, S. Merianos ¹⁵⁵, C. Merlassino ^{68a,68c}, C. Meroni ^{70a,70b},
J. Metcalfe ⁶, A.S. Mete ⁶, E. Meuser ¹⁰⁰, C. Meyer ⁶⁷, J-P. Meyer ¹³⁶, O. Mezhska ^{29b},
Y. Miao ^{112a}, R.P. Middleton ¹³⁵, M. Mihovilovic ⁶⁵, L. Mijović ⁵¹, G. Mikenberg ¹⁷¹,
M. Mikestikova ¹³², M. Mikuž ⁹³, H. Mildner ¹⁰⁰, A. Milic ³⁷, D.W. Miller ³⁹, E.H. Miller ¹⁴⁶,
A. Milov ¹⁷¹, D.A. Milstead ^{46a,46b}, T. Min ^{112a}, I.A. Minashvili ^{152b}, A.I. Mincer ¹¹⁸, B. Mindur ^{85a},
M. Mineev ³⁸, Y. Mino ⁸⁷, L.M. Mir ¹³, M. Miralles Lopez ⁵⁸, M. Mironova ^{18a}, M. Missio ⁴⁰,
A. Mitra ¹⁶⁹, V.A. Mitsou ¹⁶⁵, Y. Mitsumori ¹¹¹, P.S. Miyagawa ⁹⁴, R. Mizuhiki ⁸⁴,
T. Mkrtchyan ³⁷, M. Mlinarevic ⁹⁶, T. Mlinarevic ⁹⁶, M. Mlynarikova ¹³⁴, L. Mlynarska ^{85a},
C. Mo ^{141a}, H. Mobius ⁴⁷, S. Mobius ²⁰, M.H. Mohamed Farook ¹¹⁴, S. Mohapatra ⁴¹,
M.F. Mohd Soberi ⁵¹, S. Mohiuddin ¹²², G. Mokgatitwane ^{34j}, R. Mole ²¹, L. Moleri ¹⁷¹,
U. Molinatti ¹²⁷, M.E. Mollerach ³¹, L.G. Mollier ²⁰, L. Monaco ^{37,58}, B. Mondal ¹³²,
S. Mondal ¹³⁴, K. Mönig ⁴⁷, E. Monnier ¹⁰², L. Monsonis Romero ¹⁶⁵, A. Montella ^{46a,46b},
M. Montella ¹²⁰, F. Montekali ^{76a,76b}, F. Monticelli ⁹⁰, S. Monzani ^{68a,68c}, M.E.E. Moors ²⁵,
A. Morancho Tarda ⁴², N. Morange ⁶⁵, M. Moreno Llácer ¹⁶⁵, C. Moreno Martinez ⁵⁵,
J.M. Moreno Perez ^{23b}, P. Morettini ^{56b}, S. Morgenstern ^{62a}, M. Morii ⁶⁰, M. Morinaga ¹⁵⁶,
F. Morodei ^{74a,74b}, P. Moschovakos ³⁷, B. Moser ⁵³, M. Mosidze ^{152b}, T. Moskalets ⁴⁴,
P. Moskvitina ¹¹⁵, C.J. Mosomane ^{34b}, J. Moss ³², T. Motta Quirino ^{81d}, A. Moussa ^{36d},
Y. Moyal ^{171,k}, H. Moyano Gomez ¹³, E.J.W. Moyse ¹⁰³, T.G. Mroz ⁸⁶, S. Muanza ¹⁰²,
M. Mucha ²⁵, J. Mueller ¹³⁰, D. Muller ¹⁴⁴, G.A. Mullier ¹⁶³, A.J. Mullin ³³, J.J. Mullin ⁵⁰,
A.C. Mullins ⁴⁴, A.E. Mulski ⁶⁰, D.P. Mungo ¹⁵⁸, D. Munoz Perez ¹²², F.J. Munoz Sanchez ¹⁰¹,
W.J. Murray ^{169,135}, E. Musajan ⁶¹, M. Muškinja ⁹³, C. Mwewa ⁴⁷, A.J. Myers ⁸, G. Myers ¹⁰⁶,
M. Myska ¹³³, B.P. Nachman ¹⁴⁶, I.A. Nadas ^{28d}, K. Nagai ¹²⁷, K. Nagano ⁸², R. Nagasaka ¹⁵⁶,

J.L. Nagle ^{30,ao}, E. Nagy ¹⁰², A.M. Nairz ³⁷, T. Nakagawa ⁸⁷, Y. Nakahama ⁸², K. Nakamura ⁸²,
 K. Nakkalil ⁵, A. Nandi ^{62b}, H. Nanjo ¹²⁵, E.A. Narayanan ⁴⁴, Y. Narukawa ¹⁵⁶,
 L. Nasella ^{70a,70b}, S. Nasri ^{83c}, C. Nass ²⁵, G. Navarro ^{23a}, A. Nayaz ¹⁹, S. Nechaeva ^{24b,24a},
 F. Nechansky ¹³², L. Nedic ¹²⁷, A. Negri ^{72a,72b}, M. Negrini ^{24b}, C. Nellist ¹¹⁶, C. Nelson ¹⁰⁴,
 K. Nelson ¹⁰⁶, S. Nemecek ¹³², M. Nessi ^{37,g}, M.S. Neubauer ¹⁶⁴, J. Newell ⁹², P.R. Newman ²¹,
 Y.W.Y. Ng ¹⁶⁴, B. Ngair ^{83b}, H.D.N. Nguyen ¹⁰⁸, J.D. Nichols ¹²¹, R. Nicolaidou ¹³⁶,
 J. Nielsen ¹³⁷, M. Niemeyer ⁵⁴, J. Niermann ³⁷, N. Nikiforou ³⁷, I. Nikolic-Audit ¹²⁸,
 P. Nilsson ³⁰, G. Ninio ¹⁵⁴, A. Nisati ^{74a}, D. Nishimura ¹⁵⁶, R. Nisius ¹¹⁰, N. Nitika ¹⁷¹,
 E.K. Nkadimeng ^{34b}, T. Nobe ¹⁵⁶, D. Noll ¹⁴⁶, T. Nommensen ¹⁵⁰, M.B. Norfolk ¹⁴²,
 B.J. Norman ³⁵, L.C. Nosler ^{18a}, M. Noury ^{36a}, J. Novak ⁹³, T. Novak ⁹³, P. Novotny ¹⁷¹,
 R. Novotny ¹³³, L. Nozka ¹²³, K. Ntekas ³⁷, D. Ntounis ¹⁴⁶, N.M.J. Nunes De Moura Junior ^{81b},
 J. Ocariz ¹²⁸, I. Ochoa ^{131a}, A. Odella Rodriguez ¹³, S. Oerdek ⁴⁷, J.T. Offermann ³⁹,
 A. Ogrodnik ⁸⁶, A. Oh ¹⁰¹, C.C. Ohm ¹⁴⁷, H. Oide ⁸², M.L. Ojeda ³⁷, Y. Okumura ¹⁵⁶,
 L.F. Oleiro Seabra ^{131a}, I. Oleksiyuk ⁵⁵, G. Oliveira Correa ¹³, D. Oliveira Damazio ³⁰,
 J.L. Oliver ¹, R. Omar ⁶⁷, A.P. O'Neill ²⁰, Y. Onoda ¹³⁹, A. Onofre ^{131a,131e,e}, P.U.E. Onyisi ¹¹,
 M.J. Oreglia ³⁹, D. Orestano ^{76a,76b}, R. Orlandini ^{76a,76b}, R.S. Orr ¹⁵⁸, L.M. Osojnak ⁴¹,
 Y. Osumi ¹¹¹, G. Otero y Garzón ³¹, H. Otono ⁸⁸, M. Ouchrif ^{36d}, F. Ould-Saada ¹²⁶,
 T. Ovsianikova ¹⁴⁰, M. Owen ⁵⁸, R.E. Owen ¹³⁵, S.A. Oyeniran ¹¹⁴, V.E. Ozcan ^{22a},
 F. Ozturk ⁸⁶, N. Ozturk ⁸, S. Ozturk ⁸⁰, H.A. Pacey ¹²⁷, K. Pachal ^{159a}, A. Pacheco Pages ¹³,
 C. Padilla Aranda ¹³, G. Padovano ^{74a,74b}, S. Pagan Griso ^{18a}, L. Pagani ^{75a,75b}, J. Pampel ²⁵,
 D.K. Panchal ¹¹, C.E. Pandini ⁵⁹, J.G. Panduro Vazquez ¹³⁵, H.D. Pandya ¹, H. Pang ¹³⁶,
 P. Pani ⁴⁷, G. Panizzo ^{68a,68c}, L. Panwar ^{128,w}, L. Paolozzi ²¹, S. Parajuli ¹⁶⁴, A. Paramonov ⁶,
 C. Paraskevopoulos ⁵², D. Paredes Hernandez ^{63b}, S.R. Paredes Saenz ⁵¹, A. Pareti ^{72a,72b},
 K.R. Park ⁴¹, T.H. Park ¹¹⁰, F. Parodi ^{56b,56a}, J.A. Parsons ⁴¹, J.A. Partridge ¹³⁷, U. Parzefall ⁵³,
 B.A. Paschen ^{18a}, B. Pascual Dias ⁴⁰, L. Pascual Dominguez ⁹⁹, E. Pasqualucci ^{74a},
 S. Passaggio ^{56b}, F. Pastore ⁹⁵, P. Patel ⁸⁶, U.M. Patel ⁵⁰, J.R. Pater ¹⁰¹, T. Pauly ³⁷,
 A. Paunovic ¹⁶, F. Pauwels ¹³⁴, C.I. Pazos ¹⁶¹, M. Pedersen ¹²⁶, R. Pedro ^{131a}, O. Penc ¹³²,
 C.C. Penelaud ¹²⁸, S. Peng ¹⁵, G.D. Penn ¹⁷⁴, B.S. Peralva ^{81d}, A.P. Pereira Peixoto ¹⁴⁰,
 L. Pereira Sanchez ¹⁴⁶, D.V. Perepelitsa ^{30,ao}, G. Perera ¹⁰³, E. Perez Codina ³⁷, M. Perganti ¹⁰,
 H. Pernegger ³⁷, S. Perrella ^{74a,74b}, K. Peters ⁴⁷, R.F.Y. Peters ¹⁰¹, B.A. Petersen ³⁷,
 T.C. Petersen ⁴², E. Petit ¹⁰², V. Petousis ¹³³, A.R. Petri ^{70a,70b}, T. Petru ¹³⁴, M. Pettee ^{18a},
 A. Petukhov ⁸⁰, K. Petukhova ³⁷, R. Pezoa ^{138g}, L. Pezzotti ^{24b,24a}, G. Pezzullo ¹⁷⁴,
 L. Pfaffenbichler ³⁷, A.J. Pflieger ⁷⁸, T.M. Pham ¹⁷², T. Pham ¹⁰⁵, P.W. Phillips ¹³⁵,
 G. Piacquadio ¹⁴⁸, E. Pianori ^{18a}, F. Piazza ¹²⁴, R. Piegai ³¹, D. Pietreanu ^{28b},
 A.D. Pilkington ¹⁰¹, T. Pilusa ^{34j}, M. Pinamonti ^{68a,68c}, J.L. Pinfeld ², G. Pinheiro Matos ⁴¹,
 B.C. Pinheiro Pereira ^{131a}, J. Pinol Bel ¹³, A.E. Pinto Pinoargote ¹²⁸, L. Pintucci ^{68a,68c},
 K.M. Piper ¹⁴⁹, A. Pirttikoski ⁵⁵, D.A. Pizzi ³⁵, L. Pizzimento ^{63b}, A. Plebani ³³,
 M.-A. Pleier ³⁰, V. Pleskot ¹³⁴, E. Plotnikova ³⁸, G. Poddar ⁹⁴, R. Poettgen ⁹⁸, L. Poggioli ¹²⁸,
 S. Polacek ¹³⁴, G. Polesello ^{72a}, A. Poley ¹⁴⁵, A. Polini ^{24b}, C.S. Pollard ¹⁶⁹, Z.B. Pollock ¹²⁰,
 E. Pompa Pacchi ¹²¹, N.I. Pond ⁹⁶, D. Ponomarenko ⁶⁷, L. Pontecorvo ³⁷, S. Popa ^{28a},
 G.A. Popeneciu ^{28d}, A. Poreba ³⁷, D.M. Portillo Quintero ^{159a}, S. Pospisil ¹³³, M.A. Postill ¹⁴²,
 P. Postolache ^{28c}, K. Potamianos ¹⁶⁹, P.A. Potepa ^{85a}, I.N. Potrap ³⁸, C.J. Potter ³³, H. Potti ¹⁵⁰,
 J. Poveda ¹⁶⁵, M.E. Pozo Astigarraga ³⁷, R. Pozzi ³⁷, A. Prades Ibanez ^{75a,75b}, S.R. Pradhan ¹⁴²,
 J. Pretel ¹⁶⁷, D. Price ¹⁰¹, M. Primavera ^{69a}, L. Primomo ^{68a,68c}, M.A. Principe Martin ⁹⁹,
 R. Privara ¹²³, T. Procter ^{85b}, M.L. Proffitt ¹⁴⁰, N. Proklova ¹²⁹, K. Prokofiev ^{63c}, G. Proto ¹¹⁰,
 J. Proudfoot ⁶, M. Przybycien ^{85a}, W.W. Przygoda ^{85b}, A. Psallidas ⁴⁵, D. Pudzha ⁵², P. Puhl ⁵⁷,
 H.I. Purnell ¹, D. Pyatizbyantseva ¹¹⁵, J. Qian ¹⁰⁶, R. Qian ¹⁰⁷, D. Qichen ¹²⁷, Y. Qin ¹³,

T. Qiu ⁵¹, A. Quadt ⁵⁴, M. Queitsch-Maitland ¹⁰¹, G. Quetant ⁵⁵, R.P. Quinn ¹⁶⁶,
 D. Rafanoharana ¹¹⁰, J.L. Rainbolt ³⁹, S. Rajagopalan ³⁰, E. Ramakoti ³⁸, L. Rambelli ^{56b,56a},
 I.A. Ramirez-Berend ³⁵, K. Ran ^{106,112c}, S.D. Randles ⁹², D.S. Rankin ¹²⁹, N.P. Raphecha ^{34j},
 H. Rasheed ^{28b}, A. Rastogi ^{18a}, S. Rave ¹⁰⁰, S. Ravera ^{56b,56a}, B. Ravina ³⁷, I. Ravinovich ¹⁷¹,
 M. Raymond ³⁷, A.L. Read ¹²⁶, N.P. Readioff ¹⁴², D.M. Rebuzzi ^{72a,72b}, A.S. Reed ⁵⁸,
 K. Reeves ²⁷, D. Reikher ³⁷, T. Reisch ⁵⁵, A. Rej ⁴⁸, H. Ren ⁶¹, M. Renda ^{28b}, F. Renner ⁴⁷,
 A.G. Rennie ⁵⁸, M. Repik ⁵⁵, A.L. Rescia ^{43b,43a}, S. Resconi ^{70a}, M. Ressegotti ^{56b},
 S. Rettie ¹¹⁶, W.F. Rettie ³⁵, M.M. Revering ³³, O.L. Rezanova ³⁸, P. Reznicek ¹³⁴, H. Riani ^{36d},
 N. Ribaric ³⁷, B. Ricci ^{68a,68c}, E. Ricci ^{77a,77b}, R. Richter ¹¹⁰, E. Richter-Was ^{85b}, M. Ridel ¹²⁸,
 S. Ridouani ^{36d}, P. Riedler ³⁷, E.M. Riefel ^{46a,46b}, J.O. Rieger ¹¹⁶, M. Rimoldi ^{34c},
 L. Rinaldi ^{24b,24a}, P. Rincke ^{163,54}, G. Ripellino ¹⁶³, I. Riu ¹³, J.C. Rivera Vergara ¹⁶⁷,
 F. Rizatdinova ¹²², E. Rizvi ⁹⁴, B.R. Roberts ³⁹, S.S. Roberts ¹³⁷, D. Robinson ³³, A. Robson ⁵⁸,
 A. Rocchi ^{75a,75b}, C. Roda ^{73a,73b}, F.A. Rodriguez ¹¹⁷, S. Rodriguez Bosca ³⁷,
 Y. Rodriguez Garcia ^{23a}, A.M. Rodríguez Vera ¹¹⁷, S. Roe ³⁷, J.T. Roemer ³⁷, O. Røhne ¹²⁶,
 R.A. Rojas ³⁷, Z. Rokavec ⁹³, C.P.A. Roland ¹²⁸, A. Romaniouk ⁷⁸, E. Romano ^{72a,72b},
 M. Romano ^{24b}, N. Rompotis ⁹², L. Roos ¹²⁸, S. Rosati ^{74a}, L. Roscher ⁴⁷, B.J. Rosser ³⁹,
 E. Rossi ¹²⁷, E. Rossi ^{71a,71b}, L.P. Rossi ⁶⁰, L. Rossini ⁵³, R. Rosten ¹²⁰, M. Rotaru ^{28b},
 R. Roth ³⁷, F.A. Rothen ⁵⁵, D. Rousseau ⁶⁵, D. Rousso ⁴⁷, S. Roy-Garand ⁵⁵, A. Rozanov ¹⁰²,
 Z.M.A. Rozario ⁵⁸, Y. Rozen ¹⁵³, A. Rubio Jimenez ¹⁶⁵, V.H. Ruelas Rivera ¹⁹, T.A. Ruggeri ¹,
 A. Ruggiero ¹²⁷, A. Ruiz-Martinez ¹⁶⁵, A. Rummler ³⁷, G.B. Rupnik Boero ³⁷,
 N.A. Rusakovich ³⁸, S. Ruscelli ⁴⁸, H.L. Russell ¹⁶⁷, G. Russo ¹³⁷, J.P. Rutherford ⁷,
 S. Rutherford Colmenares ¹¹⁸, M. Rybar ¹³⁴, P. Rybczynski ^{85a}, A. Ryzhov ⁴⁴, M.A.E. Saadawy ⁴⁴,
 F. Safai Tehrani ^{74a}, S. Saha ¹, B. Sahoo ¹⁷¹, B.T. Saifuddin ¹²¹, M. Saimpert ¹³⁶,
 I. Sainz Saenz Diez ^{62a}, G.T. Saito ^{81c}, M. Saito ¹⁵⁶, T. Saito ¹⁵⁶, A. Sala ^{70a,70b}, O.T. Salin ⁶⁵,
 A. Salnikov ¹⁴⁶, J. Salt ¹⁶⁵, A. Salvador Salas ¹⁵⁴, F. Salvatore ¹⁴⁹, A. Salzburger ³⁷,
 D. Sammel ⁵³, E. Sampson ⁹¹, D. Sampsonidis ^{155,d}, D. Sampsonidou ¹²⁴, M.A.A. Samy ⁵⁸,
 J. Sánchez ¹⁶⁵, V. Sanchez Sebastian ¹⁶⁵, H. Sandaker ¹²⁶, C.O. Sander ⁴⁷, J.A. Sandesara ¹⁷²,
 M. Sandhoff ¹⁷³, C. Sandoval ^{23b}, L. Sanfilippo ^{62a}, D.P.C. Sankey ¹³⁵, T. Sano ⁸⁷,
 A. Sansar ^{22c}, A. Sansoni ⁵², M. Santana Queiroz ^{18b}, L. Santi ³⁷, C. Santoni ⁴⁰, G. Santoro ^{43b,43a},
 H. Santos ^{131a,131b}, L. Santos Pereira Trigo ⁴⁷, E. Sanzani ^{24b,24a}, K.A. Saoucha ^{83d},
 J.G. Saraiva ^{131a,131d}, J. Sardain ⁷, S. Sarkar ⁵⁰, O. Sasaki ⁸², K. Sato ¹⁶⁰, C. Sauer ³⁷,
 E. Sauvan ⁴, P. Savard ^{158,aj}, M. Savic ¹⁶⁴, R. Sawada ¹⁵⁶, C. Sawyer ¹³⁵, L. Sawyer ⁹⁷,
 A.M. Sayed ²⁷, C. Sbarra ^{24b}, A. Sbrizzi ^{24b,24a}, R. Scaglioni ^{72a,72b}, T. Scanlon ⁹⁶,
 J. Schaarschmidt ¹⁴⁰, U. Schäfer ¹⁰⁰, A.C. Schaffer ^{65,44}, D. Schaile ¹⁰⁹, R.D. Schamberger ¹⁴⁸,
 C. Scharf ¹⁹, M.M. Schefer ²⁰, D. Scheirich ¹³⁴, M. Schernau ^{138f}, C. Scheulen ⁵⁵,
 C. Schiavi ^{56b,56a}, M. Schioppa ^{43b,43a}, S. Schlenker ³⁷, T. Schlomer ⁵⁴, J. Schmeing ¹⁷³,
 C.R. Schmidt ⁴⁹, E. Schmidt ¹¹⁰, M.A. Schmidt ¹⁷³, K. Schmieden ²⁵, C. Schmitt ¹⁰⁰,
 N. Schmitt ¹⁰⁰, S. Schmitt ⁴⁷, N.A. Schneider ¹⁰⁹, L. Schoeffel ¹³⁶, A. Schoening ^{62b},
 P.G. Scholer ³⁵, E. Schopf ¹⁴⁴, M. Schott ²⁵, S. Schramm ⁵⁵, T. Schroer ⁵⁵,
 H-C. Schultz-Coulon ^{62a}, M. Schumacher ⁵³, B.A. Schumm ¹³⁷, Ph. Schune ¹³⁶, H.R. Schwartz ⁷,
 A. Schwartzman ¹⁴⁶, T.A. Schwarz ¹⁰⁶, Ph. Schwemling ¹³⁶, R. Schwienhorst ¹⁰⁷,
 F.G. Sciacca ²⁰, A. Sciandra ³⁰, G. Sciolla ²⁷, S.A. Scoville ¹³⁰, F. Scuri ^{73a}, C.D. Sebastiani ³⁷,
 K. Sedlaczek ¹¹⁷, A. Sehrawat ^{138b}, S.C. Seidel ¹¹⁴, B.D. Seidlitz ⁴¹, C. Seitz ⁴⁷,
 J.M. Seixas ^{81b}, G. Sekhniaidze ^{71a}, L. Selem ¹²⁸, N. Semprini-Cesari ^{24b,24a}, A. Semushin ¹⁷⁵,
 V. Senthilkumar ¹¹⁶, L. Serin ⁶⁵, M. Sessa ^{71a,71b}, H. Severini ¹²¹, F. Sforza ^{56b,56a}, A. Sfyrla ⁵⁵,
 Q. Sha ¹⁴, H. Shaddix ¹¹⁷, A.H. Shah ³³, R. Shaheen ¹⁴⁷, J.D. Shahinian ¹²⁹, M. Shamim ³⁷,
 L.Y. Shan ¹⁴, M. Shapiro ^{18a}, A. Sharma ³⁷, A.S. Sharma ¹⁶⁶, P. Sharma ³⁰, K. Shaw ¹⁴⁹,

S.M. Shaw ¹⁰¹, D. Shemyakin ¹⁷¹, Q. Shen ¹⁴, D.J. Sheppard ¹⁴⁵, P. Sherwood ⁹⁶, L. Shi ^{112b}, X. Shi ¹⁴, E.B. Shields ¹⁷¹, S. Shimizu ⁸², S. Shirabe ⁸⁸, M. Shiyakova ^{38,z}, M.J. Shochet ³⁹, D.R. Shope ¹²⁶, B. Shrestha ¹²¹, S. Shrestha ^{120,aq}, I. Shreyber ³⁸, M.J. Shroff ¹⁰⁴, P. Sicho ¹³², A.M. Sickles ¹⁶⁴, E. Sideras Haddad ^{34j}, A.C. Sidley ¹¹⁶, A. Sidoti ^{24b}, F. Siegert ⁴⁹, Dj. Sijacki ¹⁶, F. Sili ⁶¹, J.M. Silva ⁵¹, I. Silva Ferreira ^{81b}, M.V. Silva Oliveira ³⁰, S.B. Silverstein ^{46a}, S. Simion ⁶⁵, R. Simoniello ³⁷, E.L. Simpson ¹⁰¹, H. Simpson ¹⁴⁹, L.R. Simpson ⁶, S. Simsek ⁸⁰, S. Sindhu ⁵⁴, S.N. Singh ²⁷, S. Singh ³⁰, S. Sinha ⁴⁷, S. Sinha ¹⁰¹, M. Sioli ^{24b,24a}, K. Sioulas ⁹, I. Siral ³⁷, E. Sitnikova ⁴⁷, J. Sjölin ^{46a,46b}, A. Skaf ⁵⁴, E. Skorda ²¹, P. Skubic ¹²¹, M. Slawinska ⁸⁶, I. Slazyk ¹⁷, I. Sliusar ¹²⁶, V. Smakhtin ¹⁷¹, B.H. Smart ¹³⁵, S. Yu. Smirnov ^{138b}, Y. Smirnov ^{34c}, O. Smirnova ⁹⁸, J.L. Smith ¹⁰¹, M.B. Smith ³⁵, R. Smith ¹⁴⁶, H. Smitmanns ¹⁰⁰, M. Smizanska ⁹¹, K. Smolek ¹³³, P. Smolyanskiy ¹³³, A.A. Snesarev ³⁸, H.L. Snoek ¹¹⁶, R.M. Snyder ⁵⁰, S. Snyder ³⁰, R. Sobie ^{167,ab}, A. Soffer ¹⁵⁴, C.A. Solans Sanchez ³⁷, E. Yu. Soldatov ³⁸, U. Soldevila ¹⁶⁵, A.A. Solodkov ^{34j}, S. Solomon ²⁷, A. Soloshenko ³⁸, O.V. Solovyanov ⁴⁰, P. Sommer ⁴⁹, A. Sopczak ¹³³, A.L. Sopio ⁵¹, F. Sopkova ^{29b}, J.D. Sorenson ¹¹⁴, I.R. Sotarriva Alvarez ¹³⁹, V. Sothilingam ^{62a}, O.J. Soto Sandoval ^{138c,138b}, S. Sottocornola ⁶⁷, R. Soualah ^{83a}, D. South ⁴⁷, N. Soybelman ¹⁷¹, S. Spagnolo ^{69a,69b}, A.S. Spellman ¹²⁴, D. Sperlich ⁵³, B. Spisso ^{71a,71b}, L. Splendori ¹⁰², M. Spousta ¹³⁴, E.J. Staats ³⁵, R. Stamen ^{62a}, E. Stanecka ⁸⁶, W. Stanek-Maslouska ⁴⁷, M.V. Stange ⁴⁹, B. Stanislaus ^{18a}, M.M. Stanitzki ⁴⁷, G.H. Stark ¹³⁷, J. Stark ⁸⁹, P. Staroba ¹³², P. Starovoitov ^{83d}, R. Staszewski ⁸⁶, C. Stauch ¹⁰⁹, G. Stavropoulos ⁴⁵, A. Steff ³⁷, A. Stein ¹⁰⁰, P. Steinberg ³⁰, B. Stelzer ^{145,159a}, H.J. Stelzer ¹³⁰, O. Stelzer ^{159a}, H. Stenzel ⁵⁷, T.J. Stevenson ¹⁴⁹, G.A. Stewart ⁴⁷, G. Stoicea ^{28b}, M. Stolarski ^{131a}, S. Stonjek ¹¹⁰, A. Straessner ⁴⁹, J. Strandberg ¹⁴⁷, S. Strandberg ^{46a,46b}, M. Stratmann ¹⁷³, M. Strauss ¹²¹, T. Strebler ¹⁰², P. Strizenec ^{29b}, R. Ströhmer ¹⁶⁸, D.M. Strom ¹²⁴, R. Stroynowski ⁴⁴, A. Strubig ^{46a,46b}, S.A. Stucci ³⁰, B. Stugu ¹⁷, J. Stupak ¹²¹, N.A. Styles ⁴⁷, D. Su ¹⁴⁶, S. Su ⁶¹, X. Su ⁶¹, D. Suchy ^{29a}, A.D. Sudhakar Ponnu ⁵⁴, L. Sudit ¹⁷¹, Y. Sue ⁸², K. Sugizaki ¹²⁹, D.M.S. Sultan ¹²⁷, L. Sultanaliyeva ²⁵, S. Sultansoy ^{3b}, S. Sun ¹⁷², W. Sun ¹⁴, S. Sundar Raman ¹⁶⁶, N. Sur ⁹⁸, J.P. Surdutovich ¹²⁰, N. Suri Jr ¹⁷⁴, M.R. Sutton ¹⁴⁹, M. Svatos ¹³², P.N. Swallow ³³, S.N. Swatman ³⁷, M. Swiatlowski ^{159a}, A. Swoboda ³⁷, I. Sykora ^{29a}, M. Sykora ¹³⁴, T. Sykora ¹³⁴, D. Ta ¹⁰⁰, K. Tackmann ^{47,y}, A. Taffard ¹⁶², R. Tafirout ^{159a}, Y. Takubo ⁸², M. Talby ¹⁰², N.M. Tamir ¹⁵⁴, A. Tanaka ¹⁵⁶, J. Tanaka ¹⁵⁶, R. Tanaka ⁶⁵, M. Tanasini ¹⁴⁸, Z. Tao ¹⁶⁶, S. Tapia Araya ^{138g}, S. Tapprogge ¹⁰⁰, A. Tarek Abouelfadl Mohamed ³⁷, S. Tarem ¹⁵³, K. Tariq ¹⁴, G. Tarna ³⁷, G.F. Tartarelli ^{70a}, M.J. Tartarin ^{141b}, P. Tas ¹³⁴, M. Tasevsky ¹³², E. Tassi ^{43b,43a}, A.C. Tate ¹⁶⁴, Y. Tayalati ^{36e,aa}, G.N. Taylor ¹⁰⁵, W. Taylor ^{159b}, R.J. Taylor Vara ¹⁶⁵, A.S. Tegetmeier ⁸⁹, P. Teixeira-Dias ⁹⁵, J.J. Teoh ¹⁵⁸, K. Terashi ¹⁵⁶, J. Terron ⁹⁹, S. Terzo ¹³, M. Testa ⁵², R.J. Teuscher ^{158,ab}, A. Thaler ⁷⁸, T. Thevenaux-Pelzer ¹⁰², J.P. Thomas ²¹, E.A. Thompson ^{18a}, P.D. Thompson ²¹, E. Thomson ¹²⁹, R.E. Thornberry ³⁰, T.M. Thory-Rao ²¹, C.N. Thotamuna Wijewardhana ¹⁴⁸, C. Tian ⁶¹, Y. Tian ⁵⁵, V. Tikhomirov ⁸⁰, Yu.A. Tikhonov ³⁸, D. Timoshyn ¹³⁴, E.X.L. Ting ¹, P. Tipton ¹⁷⁴, A. Tishelman-Charny ³⁰, K. Todome ¹³⁹, S. Todorova-Nova ¹³⁴, L. Toffolin ^{68a,68c}, M. Togawa ⁸², J. Tojo ⁸⁸, S. Tokár ^{29a}, O. Toldaiev ⁶⁷, A.J. Toler ¹⁰³, G. Tolkachev ¹⁰², M. Tomoto ⁸², L. Tompkins ¹⁴⁶, E. Torrence ¹²⁴, H. Torres ⁸⁹, D.I. Torres Arza ^{138g}, E. Torres Reoyo ¹⁶⁵, E. Torró Pastor ¹⁶⁵, M. Toscani ³¹, C. Tosciri ³⁹, M. Tost ¹¹, D.R. Tovey ¹⁴², T. Trefzger ¹⁶⁸, P.M. Tricarico ¹³, A. Tricoli ³⁰, I.M. Trigger ^{159a}, S. Trincaz-Duvoid ¹²⁸, D.A. Trischuk ¹⁶⁷, A. Tropina ³⁸, D. Truncali ^{75a,75b}, L. Truong ^{34c}, M. Trzebinski ⁸⁶, A. Trzupek ⁸⁶, F. Tsai ¹⁴⁸, A. Tsiamis ¹⁵⁵, P.V. Tsiareshka ³⁸, S. Tsigaridas ^{159a}, A. Tsirigotis ^{155,t}, V. Tsiskaridze ^{152a}, E.G. Tskhadadze ^{152a}, H.F. Tsoi ¹²⁹, Y. Tsujikawa ⁸⁷, V. Tsulaia ^{18a},

K. Tsuru ¹¹⁹, D. Tsybychev ¹⁴⁸, Y. Tu ^{63b}, A. Tudorache ^{28b}, V. Tudorache ^{28b}, S.B. Tuncay ¹²⁷,
 S. Turchikhin ^{56b,56a}, I. Turk Cakir ^{3a}, R. Turra ^{70a}, T. Turtuvshin ^{38,ac}, P.M. Tuts ⁴¹,
 Y. Uematsu ⁸², F. Ukegawa ¹⁶⁰, P.A. Ulloa Poblete ^{138c,138b}, G. Unal ³⁷, A. Undrus ³⁰,
 J. Urban ^{29b}, P. Urrejola ^{138e}, G. Usai ⁸, R. Ushioda ¹⁵⁷, M. Usman ¹⁰⁸, F. Ustuner ⁵¹,
 Z. Uysal ⁸⁰, V. Vacek ¹³³, B. Vachon ¹⁰⁴, T. Vafeiadis ³⁷, A. Vaitkus ⁹⁶, C. Valderanis ¹⁰⁹,
 E. Valdes Santurio ^{46a,46b}, M. Valente ³⁷, S. Valentinetti ^{24b,24a}, A. Valero ¹⁶⁵,
 E. Valiente Moreno ¹⁶⁵, A. Vallier ⁸⁹, J.A. Valls Ferrer ¹⁶⁵, D.R. Van Arneman ¹¹⁶,
 R. Van Den Broucke ¹²⁸, A. Van Der Graaf ⁴⁸, H.Z. Van Der Schyf ^{34j}, P. Van Gemmeren ⁶,
 M. Van Rijnbach ³⁷, S. Van Stroud ⁹⁶, I. Van Vulpen ¹¹⁶, P. Vana ¹³⁴, M. Vanadia ^{75a,75b},
 U.M. Vande Voorde ¹⁴⁷, W. Vandelli ³⁷, E.R. Vandewall ¹⁴⁶, D. Vannicola ¹⁵⁴, R. Vari ^{74a},
 M. Varma ¹⁷⁴, E.W. Varnes ⁷, C. Varni ^{85a}, D. Varouchas ⁶⁵, L. Varriale ¹⁶⁵, K.E. Varvell ¹⁵⁰,
 M.E. Vasile ^{28b}, A. Vasileiadou ⁹, L. Vaslin ⁸², M.D. Vassilev ¹⁴⁶, A. Vasyukov ³⁸,
 L.M. Vaughan ¹²², R. Vavricka ¹³⁴, T. Vazquez Schroeder ¹³, J. Veatch ³², V. Vecchio ¹⁰¹,
 M.J. Veen ¹⁰³, I. Veliscek ³⁰, I. Velkovska ⁹³, L.M. Veloce ¹⁵⁸, F. Veloso ^{131a,131c},
 A.G. Veltman ⁵¹, S.H. Venetianer ¹⁶¹, S. Veneziano ^{74a}, A. Ventura ^{69a,69b}, A. Verbytskyi ¹¹⁰,
 M. Verducci ^{73a,73b}, C. Vergis ⁹⁴, M. Verissimo De Araujo ^{81b}, W. Verkerke ¹¹⁶,
 J.C. Vermeulen ¹¹⁶, C. Vernieri ¹⁴⁶, M. Vessella ¹⁶², M.C. Vetterli ^{145,aj}, A. Vgenopoulos ¹⁰⁰,
 N. Viaux Maira ^{138g,af}, L. Vicens ¹³³, T. Vickey ¹⁴², O.E. Vickey Boeriu ¹⁴²,
 G.H.A. Viehhauser ¹²⁷, L. Vigani ^{62b}, M. Vigil ¹¹⁰, M. Villa ^{24b,24a}, M. Villaplana Perez ¹⁶⁵,
 E.M. Villhauer ³⁹, E. Vilucchi ⁵², M. Vincent ¹⁶⁵, M.G. Vincter ³⁵, A. Visibile ¹¹⁶, A. Visive ¹¹⁶,
 C. Vittori ^{24b,24a}, I. Vivarelli ^{24b,24a}, M.I. Vivas Alborno ⁴⁷, E. Voevodina ¹¹⁰, F. Vogel ¹⁰⁹,
 J.C. Voigt ⁴⁹, P. Vokac ¹³³, Yu. Volkotrub ^{85b}, L. Vomberg ²⁵, E. Von Toerne ²⁵,
 B. Vormwald ³⁷, K. Vorobev ⁵⁰, M. Vos ¹⁶⁵, K. Voss ¹⁴⁴, M. Vozak ³⁷, L. Vozdecky ¹²¹,
 N. Vranjes ¹⁶, M. Vranjes Milosavljevic ¹⁶, M. Vreeswijk ¹¹⁶, N.K. Vu ^{112a}, R. Vuillermet ³⁷,
 I. Vukotic ³⁹, I.K. Vyas ³⁵, J.F. Wack ³³, A. Wada ¹¹¹, S. Wada ¹⁶⁰, C. Wagner ¹⁴⁶,
 J.M. Wagner ^{18a}, W. Wagner ¹⁷³, S. Wahdan ¹⁷³, H. Wahlberg ⁹⁰, C.H. Waits ¹²¹, J. Walder ¹³⁵,
 R. Walker ¹⁰⁹, K. Walkingshaw Pass ⁵⁸, W. Walkowiak ¹⁴⁴, A. Wall ¹²⁹, E.J. Wallin ⁹⁸,
 T. Wamorkar ¹⁴⁶, K. Wandall-Christensen ¹⁶⁵, A. Wang ⁶¹, A.Z. Wang ¹³⁷, C. Wang ⁴⁷,
 C. Wang ¹¹, H. Wang ^{18a}, J. Wang ^{63c}, P. Wang ¹⁰¹, P. Wang ⁹⁶, R. Wang ⁶⁰, R. Wang ¹⁰⁶,
 R. Wang ⁶, S.M. Wang ¹⁵¹, S. Wang ^{14,an}, T. Wang ¹¹⁵, T. Wang ⁶¹, W.T. Wang ¹²⁷,
 W. Wang ^{113c}, X. Wang ¹⁶⁴, X. Wang ^{141a}, X. Wang ⁴⁷, Y. Wang ¹⁴⁸, Y. Wang ¹¹⁴, Z. Wang ¹⁴,
 Z. Wang ^{63b}, C. Wanotayaroj ⁸², A. Warburton ¹⁰⁴, A.L. Warnerbring ¹⁴⁴, S. Waterhouse ⁹⁶,
 A.T. Watson ²¹, H. Watson ⁵¹, M.F. Watson ²¹, E. Watton ³⁷, G. Watts ¹⁴⁰, B.M. Waugh ⁹⁶,
 J.M. Webb ⁵³, C. Weber ³⁰, M.S. Weber ²⁰, C. Wei ⁶¹, Y. Wei ⁵³, A.R. Weidberg ¹²⁷,
 E.J. Weik ¹¹⁸, J. Weingarten ⁴⁸, C. Weiser ⁵³, C.J. Wells ⁴⁷, P.S. Wells ³⁷, T. Wenaus ³⁰,
 T. Wengler ³⁷, N.S. Wenke ¹¹⁰, N. Wermes ²⁵, D. Werner ⁴⁷, M. Wessels ^{62a}, A.M. Wharton ⁹¹,
 A.S. White ³⁷, A. White ⁸, M.J. White ¹, D. Whiteson ¹⁶², L. Wickremasinghe ¹²⁵,
 W. Wiedenmann ¹⁷², M. Wielers ¹³⁵, R. Wierda ¹⁴⁷, C. Wiglesworth ⁴², H.G. Wilkens ³⁷,
 J.J.H. Wilkinson ³³, S. Williams ³³, S. Willocq ¹⁰³, D.J. Wilson ¹⁰¹, P.J. Windischhofer ³⁹,
 F.I. Winkel ³¹, F. Winklmeier ¹²⁴, B.T. Winter ⁵³, M. Wittgen ¹⁴⁶, M. Wobisch ⁹⁷, T. Wojtkowski ⁵⁹,
 Z. Wolfs ¹¹⁶, J. Wollrath ³⁷, M.W. Wolter ⁸⁶, H. Wolters ^{131a,131c}, M.C. Wong ¹³⁷,
 E.L. Woodward ⁴¹, S.D. Worm ⁴⁷, B.K. Wosiek ⁸⁶, K.A. Wozniak ⁵⁵, K.W. Woźniak ⁸⁶,
 S. Wozniewski ⁵⁴, K. Wraight ⁵⁸, C. Wu ¹⁵⁸, J. Wu ¹⁵⁶, M. Wu ^{112b}, M. Wu ¹¹⁵, S.L. Wu ¹⁷²,
 S. Wu ^{14,an}, X. Wu ⁶¹, Y.Q. Wu ¹⁵⁸, Y. Wu ⁶¹, Z. Wu ¹⁰², Z. Wu ^{112a}, J. Wuerzinger ¹¹⁰,
 T.R. Wyatt ¹⁰¹, B.M. Wynne ⁵¹, S. Xella ⁴², L. Xia ^{112a}, M. Xie ⁶¹, A. Xiong ¹²⁴,
 I. Xioidis ³⁷, D. Xu ¹⁴, H. Xu ⁶¹, L. Xu ⁶¹, R. Xu ¹²⁹, T. Xu ¹⁰⁶, W. Xu ^{112a}, Y. Xu ¹⁴⁰,
 Z. Xu ⁵¹, R. Xue ¹³⁰, B. Yabsley ¹⁵⁰, S. Yacoob ¹¹, Y. Yamaguchi ⁸², E. Yamashita ¹⁵⁶,

H. Yamauchi ¹⁶⁰, T. Yamazaki ^{18a}, Y. Yamazaki ⁸⁴, S. Yan ⁵⁸, Z. Yan ¹⁰³, C. Yang ^{18a}, H.J. Yang ^{141a}, H.T. Yang ⁶¹, S. Yang ⁶¹, X. Yang ³⁷, X. Yang ¹⁴, Y. Yang ¹⁵⁶, Y. Yang ⁶¹, W-M. Yao ^{18a}, C.L. Yardley ¹⁴⁹, J. Ye ¹⁴, S. Ye ³⁰, X. Ye ⁶¹, I. Yeletsikh ³⁸, B. Yeo ^{18b}, M.R. Yexley ⁹⁶, T.P. Yildirim ¹²⁷, K. Yorita ¹⁷⁰, C.J.S. Young ³⁷, C. Young ¹⁴⁶, I.N.L. Young ⁵⁸, N.D. Young ¹²⁴, D. Yu ^{141b,5}, Y. Yu ⁶¹, J. Yuan ^{14,112c,an}, M. Yuan ¹⁰⁶, R. Yuan ^{141b}, L. Yue ⁹⁶, M. Zaazoua ⁶¹, B. Zabinski ⁸⁶, I. Zahir ^{36a}, Q.U.A. Zahoor ⁵¹, A. Zaio ^{56b,56a}, Z.K. Zak ⁸⁶, T. Zakareishvili ¹⁶⁵, S. Zambito ⁵⁵, J. Zang ¹⁵⁶, R. Zanzottera ^{70a,70b}, O. Zaplatilek ¹³³, I. Zatocilova ⁵³, E. Zaya ¹⁴⁷, C. Zeitnitz ¹⁷³, H. Zeng ¹⁴, D.T. Zenger Jr ²⁷, T. Ženiš ^{29a}, S. Zenz ⁹⁴, W. Zhan ⁶¹, B. Zhang ¹⁶⁹, D.F. Zhang ¹⁴², G. Zhang ^{14,an}, J. Zhang ^{113b}, J. Zhang ⁶, L. Zhang ⁶¹, L. Zhang ^{112a}, P. Zhang ^{14,112c}, R. Zhang ^{112a}, S. Zhang ¹⁴, Y. Zhang ¹⁴⁰, Y. Zhang ⁹⁶, Y. Zhang ⁶¹, Y. Zhang ^{112a}, Z. Zhang ¹⁴⁹, Z. Zhang ¹⁰¹, Z. Zhang ^{18a}, Z. Zhang ^{113b}, Z. Zhang ⁶⁵, H. Zhao ¹⁴⁰, T. Zhao ^{113b}, Y. Zhao ³⁵, Z. Zhao ⁶¹, Z. Zhao ⁶¹, A. Zhemchugov ³⁸, J. Zheng ^{112a}, K. Zheng ¹⁶⁴, L. Zheng ^{113b}, X. Zheng ⁶¹, Z. Zheng ¹⁴⁶, D. Zhong ¹⁶⁴, B. Zhou ¹⁰⁶, B. Zhou ^{141b,141a}, N. Zhou ^{141a}, Y. Zhou ¹⁵, Y. Zhou ^{112a}, Y. Zhou ⁷, Z. Zhou ⁶¹, J. Zhu ¹⁰⁶, X. Zhu ^{141b}, Y. Zhu ^{141a}, X. Zhuang ¹⁴, K. Zhukov ⁶⁷, P. Ziakas ⁴, N.I. Zimine ³⁸, J. Zinsser ^{62b}, M. Ziolkowski ¹⁴⁴, L. Živković ¹⁶, A. Zoccoli ^{24b,24a}, K. Zoch ³⁷, A. Zografos ³⁷, T.G. Zorbas ¹⁴², L. Zwalinski ³⁷.

¹Department of Physics, University of Adelaide, Adelaide; Australia.

²Department of Physics, University of Alberta, Edmonton AB; Canada.

^{3(a)}Department of Physics, Ankara University, Ankara; ^(b)Division of Physics, TOBB University of Economics and Technology, Ankara; Türkiye.

⁴LAPP, Université Savoie Mont Blanc, CNRS/IN2P3, Annecy; France.

⁵APC, Université Paris Cité, CNRS/IN2P3, Paris; France.

⁶High Energy Physics Division, Argonne National Laboratory, Argonne IL; United States of America.

⁷Department of Physics, University of Arizona, Tucson AZ; United States of America.

⁸Department of Physics, University of Texas at Arlington, Arlington TX; United States of America.

⁹Physics Department, National and Kapodistrian University of Athens, Athens; Greece.

¹⁰Physics Department, National Technical University of Athens, Zografou; Greece.

¹¹Department of Physics, University of Texas at Austin, Austin TX; United States of America.

¹²Institute of Physics, Azerbaijan Academy of Sciences, Baku; Azerbaijan.

¹³Institut de Física d'Altes Energies (IFAE), Barcelona Institute of Science and Technology, Barcelona; Spain.

¹⁴Institute of High Energy Physics, Chinese Academy of Sciences, Beijing; China.

¹⁵Physics Department, Tsinghua University, Beijing; China.

¹⁶Institute of Physics, University of Belgrade, Belgrade; Serbia.

¹⁷Department for Physics and Technology, University of Bergen, Bergen; Norway.

^{18(a)}Physics Division, Lawrence Berkeley National Laboratory, Berkeley CA; ^(b)University of California, Berkeley CA; United States of America.

¹⁹Institut für Physik, Humboldt Universität zu Berlin, Berlin; Germany.

²⁰Albert Einstein Center for Fundamental Physics and Laboratory for High Energy Physics, University of Bern, Bern; Switzerland.

²¹School of Physics and Astronomy, University of Birmingham, Birmingham; United Kingdom.

^{22(a)}Department of Physics, Bogazici University, Istanbul; ^(b)Department of Physics Engineering, Gaziantep University, Gaziantep; ^(c)Department of Physics, Istanbul University, Istanbul; Türkiye.

^{23(a)}Facultad de Ciencias y Centro de Investigaciones, Universidad Antonio Nariño, Bogotá; ^(b)Departamento de Física, Universidad Nacional de Colombia, Bogotá; Colombia.

- ^{24(a)}Dipartimento di Fisica e Astronomia A. Righi, Università di Bologna, Bologna; ^(b)INFN Sezione di Bologna; Italy.
- ²⁵Physikalisches Institut, Universität Bonn, Bonn; Germany.
- ²⁶Department of Physics, Boston University, Boston MA; United States of America.
- ²⁷Department of Physics, Brandeis University, Waltham MA; United States of America.
- ^{28(a)}Transilvania University of Brasov, Brasov; ^(b)Horia Hulubei National Institute of Physics and Nuclear Engineering, Bucharest; ^(c)Department of Physics, Alexandru Ioan Cuza University of Iasi, Iasi; ^(d)National Institute for Research and Development of Isotopic and Molecular Technologies, Physics Department, Cluj-Napoca; ^(e)National University of Science and Technology Politehnica, Bucharest; ^(f)West University in Timisoara, Timisoara; ^(g)Faculty of Physics, University of Bucharest, Bucharest; Romania.
- ^{29(a)}Faculty of Mathematics, Physics and Informatics, Comenius University, Bratislava; ^(b)Department of Subnuclear Physics, Institute of Experimental Physics of the Slovak Academy of Sciences, Kosice; Slovak Republic.
- ³⁰Physics Department, Brookhaven National Laboratory, Upton NY; United States of America.
- ³¹Universidad de Buenos Aires, Facultad de Ciencias Exactas y Naturales, Departamento de Física, y CONICET, Instituto de Física de Buenos Aires (IFIBA), Buenos Aires; Argentina.
- ³²California State University, CA; United States of America.
- ³³Cavendish Laboratory, University of Cambridge, Cambridge; United Kingdom.
- ^{34(a)}Department of Physics, University of Cape Town, Cape Town; ^(b)iThemba Labs, Western Cape; ^(c)Department of Mechanical Engineering Science, University of Johannesburg, Johannesburg; ^(d)National Institute of Physics, University of the Philippines Diliman (Philippines); ^(e)Department of Physics, Stellenbosch University, Matieland; ^(f)University of KwaZulu-Natal, School of Agriculture and Science, Mathematics, Westville; ^(g)University of South Africa, Department of Physics, Pretoria; ^(h)University of Pretoria, Department of Mechanical and Aeronautical Engineering, Pretoria; ⁽ⁱ⁾University of Zululand, KwaDlangezwa; ^(j)School of Physics, University of the Witwatersrand, Johannesburg; South Africa.
- ³⁵Department of Physics, Carleton University, Ottawa ON; Canada.
- ^{36(a)}Faculté des Sciences Ain Chock, Université Hassan II de Casablanca; ^(b)Faculté des Sciences, Université Ibn-Tofail, Kénitra; ^(c)Faculté des Sciences Semlalia, Université Cadi Ayyad, LPHEA-Marrakech; ^(d)LPMR, Faculté des Sciences, Université Mohamed Premier, Oujda; ^(e)Faculté des sciences, Université Mohammed V, Rabat; ^(f)Institute of Applied Physics, Mohammed VI Polytechnic University, Ben Guerir; Morocco.
- ³⁷CERN, Geneva; Switzerland.
- ³⁸Affiliated with an international laboratory covered by a cooperation agreement with CERN.
- ³⁹Enrico Fermi Institute, University of Chicago, Chicago IL; United States of America.
- ⁴⁰LPC, Université Clermont Auvergne, CNRS/IN2P3, Clermont-Ferrand; France.
- ⁴¹Nevis Laboratory, Columbia University, Irvington NY; United States of America.
- ⁴²Niels Bohr Institute, University of Copenhagen, Copenhagen; Denmark.
- ^{43(a)}Dipartimento di Fisica, Università della Calabria, Rende; ^(b)INFN Gruppo Collegato di Cosenza, Laboratori Nazionali di Frascati; Italy.
- ⁴⁴Physics Department, Southern Methodist University, Dallas TX; United States of America.
- ⁴⁵National Centre for Scientific Research "Demokritos", Agia Paraskevi; Greece.
- ^{46(a)}Department of Physics, Stockholm University; ^(b)Oskar Klein Centre, Stockholm; Sweden.
- ⁴⁷Deutsches Elektronen-Synchrotron DESY, Hamburg and Zeuthen; Germany.
- ⁴⁸Fakultät Physik, Technische Universität Dortmund, Dortmund; Germany.
- ⁴⁹Institut für Kern- und Teilchenphysik, Technische Universität Dresden, Dresden; Germany.
- ⁵⁰Department of Physics, Duke University, Durham NC; United States of America.

- ⁵¹SUPA - School of Physics and Astronomy, University of Edinburgh, Edinburgh; United Kingdom.
- ⁵²INFN e Laboratori Nazionali di Frascati, Frascati; Italy.
- ⁵³Physikalisches Institut, Albert-Ludwigs-Universität Freiburg, Freiburg; Germany.
- ⁵⁴II. Physikalisches Institut, Georg-August-Universität Göttingen, Göttingen; Germany.
- ⁵⁵Département de Physique Nucléaire et Corpusculaire, Université de Genève, Genève; Switzerland.
- ⁵⁶(^a) Dipartimento di Fisica, Università di Genova, Genova; (^b) INFN Sezione di Genova; Italy.
- ⁵⁷II. Physikalisches Institut, Justus-Liebig-Universität Giessen, Giessen; Germany.
- ⁵⁸SUPA - School of Physics and Astronomy, University of Glasgow, Glasgow; United Kingdom.
- ⁵⁹LPSC, Université Grenoble Alpes, CNRS/IN2P3, Grenoble INP, Grenoble; France.
- ⁶⁰Laboratory for Particle Physics and Cosmology, Harvard University, Cambridge MA; United States of America.
- ⁶¹Department of Modern Physics and State Key Laboratory of Particle Detection and Electronics, University of Science and Technology of China, Hefei; China.
- ⁶²(^a) Kirchhoff-Institut für Physik, Ruprecht-Karls-Universität Heidelberg, Heidelberg; (^b) Physikalisches Institut, Ruprecht-Karls-Universität Heidelberg, Heidelberg; Germany.
- ⁶³(^a) Department of Physics, Chinese University of Hong Kong, Shatin, N.T., Hong Kong; (^b) Department of Physics, University of Hong Kong, Hong Kong; (^c) Department of Physics and Institute for Advanced Study, Hong Kong University of Science and Technology, Clear Water Bay, Kowloon, Hong Kong; China.
- ⁶⁴Department of Physics, National Tsing Hua University, Hsinchu; Taiwan.
- ⁶⁵IJCLab, Université Paris-Saclay, CNRS/IN2P3, 91405, Orsay; France.
- ⁶⁶Centro Nacional de Microelectrónica (IMB-CNM-CSIC), Barcelona; Spain.
- ⁶⁷Department of Physics, Indiana University, Bloomington IN; United States of America.
- ⁶⁸(^a) INFN Gruppo Collegato di Udine, Sezione di Trieste, Udine; (^b) ICTP, Trieste; (^c) Dipartimento Politecnico di Ingegneria e Architettura, Università di Udine, Udine; Italy.
- ⁶⁹(^a) INFN Sezione di Lecce; (^b) Dipartimento di Matematica e Fisica, Università del Salento, Lecce; Italy.
- ⁷⁰(^a) INFN Sezione di Milano; (^b) Dipartimento di Fisica, Università di Milano, Milano; Italy.
- ⁷¹(^a) INFN Sezione di Napoli; (^b) Dipartimento di Fisica, Università di Napoli, Napoli; Italy.
- ⁷²(^a) INFN Sezione di Pavia; (^b) Dipartimento di Fisica, Università di Pavia, Pavia; Italy.
- ⁷³(^a) INFN Sezione di Pisa; (^b) Dipartimento di Fisica E. Fermi, Università di Pisa, Pisa; Italy.
- ⁷⁴(^a) INFN Sezione di Roma; (^b) Dipartimento di Fisica, Sapienza Università di Roma, Roma; Italy.
- ⁷⁵(^a) INFN Sezione di Roma Tor Vergata; (^b) Dipartimento di Fisica, Università di Roma Tor Vergata, Roma; Italy.
- ⁷⁶(^a) INFN Sezione di Roma Tre; (^b) Dipartimento di Matematica e Fisica, Università Roma Tre, Roma; Italy.
- ⁷⁷(^a) INFN-TIFPA; (^b) Università degli Studi di Trento, Trento; Italy.
- ⁷⁸Universität Innsbruck, Department of Astro and Particle Physics, Innsbruck; Austria.
- ⁷⁹Department of Physics and Astronomy, Iowa State University, Ames IA; United States of America.
- ⁸⁰Istinye University, Sariyer, Istanbul; Türkiye.
- ⁸¹(^a) Departamento de Engenharia Elétrica, Universidade Federal de Juiz de Fora (UFJF), Juiz de Fora; (^b) Universidade Federal do Rio De Janeiro COPPE/EE/IF, Rio de Janeiro; (^c) Instituto de Física, Universidade de São Paulo, São Paulo; (^d) Rio de Janeiro State University, Rio de Janeiro; (^e) Federal University of Bahia, Bahia; Brazil.
- ⁸²KEK, High Energy Accelerator Research Organization, Tsukuba; Japan.
- ⁸³(^a) Khalifa University of Science and Technology, Abu Dhabi; (^b) New York University Abu Dhabi, Abu Dhabi; (^c) United Arab Emirates University, Al Ain; (^d) University of Sharjah, Sharjah; United Arab Emirates.
- ⁸⁴Graduate School of Science, Kobe University, Kobe; Japan.

- ^{85(a)} AGH University of Krakow, Faculty of Physics and Applied Computer Science, Krakow; ^(b) Marian Smoluchowski Institute of Physics, Jagiellonian University, Krakow; Poland.
- ⁸⁶ Institute of Nuclear Physics Polish Academy of Sciences, Krakow; Poland.
- ⁸⁷ Faculty of Science, Kyoto University, Kyoto; Japan.
- ⁸⁸ Research Center for Advanced Particle Physics and Department of Physics, Kyushu University, Fukuoka ; Japan.
- ⁸⁹ L2IT, Université de Toulouse, CNRS/IN2P3, UPS, Toulouse; France.
- ⁹⁰ Instituto de Física La Plata, Universidad Nacional de La Plata and CONICET, La Plata; Argentina.
- ⁹¹ Physics Department, Lancaster University, Lancaster; United Kingdom.
- ⁹² Oliver Lodge Laboratory, University of Liverpool, Liverpool; United Kingdom.
- ⁹³ Department of Experimental Particle Physics, Jožef Stefan Institute and Department of Physics, University of Ljubljana, Ljubljana; Slovenia.
- ⁹⁴ Department of Physics and Astronomy, Queen Mary University of London, London; United Kingdom.
- ⁹⁵ Department of Physics, Royal Holloway University of London, Egham; United Kingdom.
- ⁹⁶ Department of Physics and Astronomy, University College London, London; United Kingdom.
- ⁹⁷ Louisiana Tech University, Ruston LA; United States of America.
- ⁹⁸ Fysiska institutionen, Lunds universitet, Lund; Sweden.
- ⁹⁹ Departamento de Física Teórica C-15 and CIAFF, Universidad Autónoma de Madrid, Madrid; Spain.
- ¹⁰⁰ Institut für Physik, Universität Mainz, Mainz; Germany.
- ¹⁰¹ School of Physics and Astronomy, University of Manchester, Manchester; United Kingdom.
- ¹⁰² CPPM, Aix-Marseille Université, CNRS/IN2P3, Marseille; France.
- ¹⁰³ Department of Physics, University of Massachusetts, Amherst MA; United States of America.
- ¹⁰⁴ Department of Physics, McGill University, Montreal QC; Canada.
- ¹⁰⁵ School of Physics, University of Melbourne, Victoria; Australia.
- ¹⁰⁶ Department of Physics, University of Michigan, Ann Arbor MI; United States of America.
- ¹⁰⁷ Department of Physics and Astronomy, Michigan State University, East Lansing MI; United States of America.
- ¹⁰⁸ Group of Particle Physics, University of Montreal, Montreal QC; Canada.
- ¹⁰⁹ Fakultät für Physik, Ludwig-Maximilians-Universität München, München; Germany.
- ¹¹⁰ Max-Planck-Institut für Physik (Werner-Heisenberg-Institut), München; Germany.
- ¹¹¹ Graduate School of Science and Kobayashi-Maskawa Institute, Nagoya University, Nagoya; Japan.
- ^{112(a)} Department of Physics, Nanjing University, Nanjing; ^(b) School of Science, Shenzhen Campus of Sun Yat-sen University; ^(c) University of Chinese Academy of Science (UCAS), Beijing; China.
- ^{113(a)} School of Physics, Nankai University, Tianjin; ^(b) Institute of Frontier and Interdisciplinary Science and Key Laboratory of Particle Physics and Particle Irradiation (MOE), Shandong University, Qingdao; ^(c) School of Physics, Zhengzhou University; China.
- ¹¹⁴ Department of Physics and Astronomy, University of New Mexico, Albuquerque NM; United States of America.
- ¹¹⁵ Institute for Mathematics, Astrophysics and Particle Physics, Radboud University/Nikhef, Nijmegen; Netherlands.
- ¹¹⁶ Nikhef National Institute for Subatomic Physics and University of Amsterdam, Amsterdam; Netherlands.
- ¹¹⁷ Department of Physics, Northern Illinois University, DeKalb IL; United States of America.
- ¹¹⁸ Department of Physics, New York University, New York NY; United States of America.
- ¹¹⁹ Ochanomizu University, Otsuka, Bunkyo-ku, Tokyo; Japan.
- ¹²⁰ Ohio State University, Columbus OH; United States of America.
- ¹²¹ Homer L. Dodge Department of Physics and Astronomy, University of Oklahoma, Norman OK; United

States of America.

¹²²Department of Physics, Oklahoma State University, Stillwater OK; United States of America.

¹²³Palacký University, Joint Laboratory of Optics, Olomouc; Czech Republic.

¹²⁴Institute for Fundamental Science, University of Oregon, Eugene, OR; United States of America.

¹²⁵Graduate School of Science, University of Osaka, Osaka; Japan.

¹²⁶Department of Physics, University of Oslo, Oslo; Norway.

¹²⁷Department of Physics, Oxford University, Oxford; United Kingdom.

¹²⁸LPNHE, Sorbonne Université, Université Paris Cité, CNRS/IN2P3, Paris; France.

¹²⁹Department of Physics, University of Pennsylvania, Philadelphia PA; United States of America.

¹³⁰Department of Physics and Astronomy, University of Pittsburgh, Pittsburgh PA; United States of America.

¹³¹(^a) Laboratório de Instrumentação e Física Experimental de Partículas - LIP, Lisboa; (^b) Departamento de Física, Faculdade de Ciências, Universidade de Lisboa, Lisboa; (^c) Departamento de Física, Universidade de Coimbra, Coimbra; (^d) Centro de Física Nuclear da Universidade de Lisboa, Lisboa; (^e) Departamento de Física, Escola de Ciências, Universidade do Minho, Braga; (^f) Departamento de Física Teórica y del Cosmos, Universidad de Granada, Granada (Spain); (^g) Departamento de Física, Instituto Superior Técnico, Universidade de Lisboa, Lisboa; Portugal.

¹³²Institute of Physics of the Czech Academy of Sciences, Prague; Czech Republic.

¹³³Czech Technical University in Prague, Prague; Czech Republic.

¹³⁴Charles University, Faculty of Mathematics and Physics, Prague; Czech Republic.

¹³⁵Particle Physics Department, Rutherford Appleton Laboratory, Didcot; United Kingdom.

¹³⁶IRFU, CEA, Université Paris-Saclay, Gif-sur-Yvette; France.

¹³⁷Santa Cruz Institute for Particle Physics, University of California Santa Cruz, Santa Cruz CA; United States of America.

¹³⁸(^a) Departamento de Física, Pontificia Universidad Católica de Chile, Santiago; (^b) Millennium Institute for Subatomic physics at high energy frontier (SAPHIR), Santiago; (^c) Instituto de Investigación Multidisciplinario en Ciencia y Tecnología, y Departamento de Física, Universidad de La Serena; (^d) Universidad Andres Bello, Department of Physics, Santiago; (^e) Universidad San Sebastian, Recoleta; (^f) Instituto de Alta Investigación, Universidad de Tarapacá, Arica; (^g) Departamento de Física, Universidad Técnica Federico Santa María, Valparaíso; Chile.

¹³⁹Department of Physics, Institute of Science, Tokyo; Japan.

¹⁴⁰Department of Physics, University of Washington, Seattle WA; United States of America.

¹⁴¹(^a) State Key Laboratory of Dark Matter Physics, School of Physics and Astronomy, Shanghai Jiao Tong University, Key Laboratory for Particle Astrophysics and Cosmology (MOE), SKLPPC, Shanghai; (^b) State Key Laboratory of Dark Matter Physics, Tsung-Dao Lee Institute, Shanghai Jiao Tong University, Shanghai; China.

¹⁴²Department of Physics and Astronomy, University of Sheffield, Sheffield; United Kingdom.

¹⁴³Department of Physics, Shinshu University, Nagano; Japan.

¹⁴⁴Department Physik, Universität Siegen, Siegen; Germany.

¹⁴⁵Department of Physics, Simon Fraser University, Burnaby BC; Canada.

¹⁴⁶SLAC National Accelerator Laboratory, Stanford CA; United States of America.

¹⁴⁷Department of Physics, Royal Institute of Technology, Stockholm; Sweden.

¹⁴⁸Departments of Physics and Astronomy, Stony Brook University, Stony Brook NY; United States of America.

¹⁴⁹Department of Physics and Astronomy, University of Sussex, Brighton; United Kingdom.

¹⁵⁰School of Physics, University of Sydney, Sydney; Australia.

¹⁵¹Institute of Physics, Academia Sinica, Taipei; Taiwan.

- ^{152(a)}E. Andronikashvili Institute of Physics, Iv. Javakhishvili Tbilisi State University, Tbilisi; ^(b)High Energy Physics Institute, Tbilisi State University, Tbilisi; ^(c)University of Georgia, Tbilisi; Georgia.
- ¹⁵³Department of Physics, Technion, Israel Institute of Technology, Haifa; Israel.
- ¹⁵⁴Raymond and Beverly Sackler School of Physics and Astronomy, Tel Aviv University, Tel Aviv; Israel.
- ¹⁵⁵Department of Physics, Aristotle University of Thessaloniki, Thessaloniki; Greece.
- ¹⁵⁶International Center for Elementary Particle Physics and Department of Physics, University of Tokyo, Tokyo; Japan.
- ¹⁵⁷Graduate School of Science and Technology, Tokyo Metropolitan University, Tokyo; Japan.
- ¹⁵⁸Department of Physics, University of Toronto, Toronto ON; Canada.
- ^{159(a)}TRIUMF, Vancouver BC; ^(b)Department of Physics and Astronomy, York University, Toronto ON; Canada.
- ¹⁶⁰Division of Physics and Tomonaga Center for the History of the Universe, Faculty of Pure and Applied Sciences, University of Tsukuba, Tsukuba; Japan.
- ¹⁶¹Department of Physics and Astronomy, Tufts University, Medford MA; United States of America.
- ¹⁶²Department of Physics and Astronomy, University of California Irvine, Irvine CA; United States of America.
- ¹⁶³Department of Physics and Astronomy, University of Uppsala, Uppsala; Sweden.
- ¹⁶⁴Department of Physics, University of Illinois, Urbana IL; United States of America.
- ¹⁶⁵Instituto de Física Corpuscular (IFIC), Centro Mixto Universidad de Valencia - CSIC, Valencia; Spain.
- ¹⁶⁶Department of Physics, University of British Columbia, Vancouver BC; Canada.
- ¹⁶⁷Department of Physics and Astronomy, University of Victoria, Victoria BC; Canada.
- ¹⁶⁸Fakultät für Physik und Astronomie, Julius-Maximilians-Universität Würzburg, Würzburg; Germany.
- ¹⁶⁹Department of Physics, University of Warwick, Coventry; United Kingdom.
- ¹⁷⁰Waseda University, Tokyo; Japan.
- ¹⁷¹Department of Particle Physics and Astrophysics, Weizmann Institute of Science, Rehovot; Israel.
- ¹⁷²Department of Physics, University of Wisconsin, Madison WI; United States of America.
- ¹⁷³Fakultät für Mathematik und Naturwissenschaften, Fachgruppe Physik, Bergische Universität Wuppertal, Wuppertal; Germany.
- ¹⁷⁴Department of Physics, Yale University, New Haven CT; United States of America.
- ¹⁷⁵Yerevan Physics Institute, Yerevan; Armenia.
- ^a Also at Affiliated with an institute formerly covered by a cooperation agreement with CERN.
- ^b Also at An-Najah National University, Nablus; Palestine.
- ^c Also at Borough of Manhattan Community College, City University of New York, New York NY; United States of America.
- ^d Also at Center for Interdisciplinary Research and Innovation (CIRI-AUTH), Thessaloniki; Greece.
- ^e Also at Centre of Physics of the Universities of Minho and Porto (CF-UM-UP); Portugal.
- ^f Also at CERN, Geneva; Switzerland.
- ^g Also at Département de Physique Nucléaire et Corpusculaire, Université de Genève, Genève; Switzerland.
- ^h Also at Departament de Física de la Universitat Autònoma de Barcelona, Barcelona; Spain.
- ⁱ Also at Department of Financial and Management Engineering, University of the Aegean, Chios; Greece.
- ^j Also at Department of Modern Physics and State Key Laboratory of Particle Detection and Electronics, University of Science and Technology of China, Hefei; China.
- ^k Also at Department of Physics, Ben Gurion University of the Negev, Beer Sheva; Israel.
- ^l Also at Department of Physics, Bolu Abant İzzet Baysal University, Bolu; Türkiye.
- ^m Also at Department of Physics, King's College London, London; United Kingdom.
- ⁿ Also at Department of Physics, Stellenbosch University; South Africa.

- ^o Also at Department of Physics, University of Fribourg, Fribourg; Switzerland.
- ^p Also at Department of Physics, University of Thessaly; Greece.
- ^q Also at Department of Physics, Westmont College, Santa Barbara; United States of America.
- ^r Also at Faculty of Physics, Sofia University, 'St. Kliment Ohridski', Sofia; Bulgaria.
- ^s Also at Faculty of Physics, University of Bucharest; Romania.
- ^t Also at Hellenic Open University, Patras; Greece.
- ^u Also at Henan University; China.
- ^v Also at Imam Mohammad Ibn Saud Islamic University; Saudi Arabia.
- ^w Also at Indian Institute of Technology (IIT), Jodhpur; India.
- ^x Also at Institutio Catalana de Recerca i Estudis Avancats, ICREA, Barcelona; Spain.
- ^y Also at Institut für Experimentalphysik, Universität Hamburg, Hamburg; Germany.
- ^z Also at Institute for Nuclear Research and Nuclear Energy (INRNE) of the Bulgarian Academy of Sciences, Sofia; Bulgaria.
- ^{aa} Also at Institute of Applied Physics, Mohammed VI Polytechnic University, Ben Guerir; Morocco.
- ^{ab} Also at Institute of Particle Physics (IPP); Canada.
- ^{ac} Also at Institute of Physics and Technology, Mongolian Academy of Sciences, Ulaanbaatar; Mongolia.
- ^{ad} Also at Institute of Physics, Azerbaijan Academy of Sciences, Baku; Azerbaijan.
- ^{ae} Also at Institute of Theoretical Physics, Iliia State University, Tbilisi; Georgia.
- ^{af} Also at Millennium Institute for Subatomic physics at high energy frontier (SAPHIR), Santiago; Chile.
- ^{ag} Also at National Institute of Physics, University of the Philippines Diliman (Philippines); Philippines.
- ^{ah} Also at School of Physics, University of the Witwatersrand, Johannesburg; South Africa.
- ^{ai} Also at The Collaborative Innovation Center of Quantum Matter (CICQM), Beijing; China.
- ^{aj} Also at TRIUMF, Vancouver BC; Canada.
- ^{ak} Also at Università di Napoli Parthenope, Napoli; Italy.
- ^{al} Also at Università degli Studi Link; Italy.
- ^{am} Also at University and INFN Torino, Torino; Italy.
- ^{an} Also at University of Chinese Academy of Sciences (UCAS), Beijing; China.
- ^{ao} Also at University of Colorado Boulder, Department of Physics, Colorado; United States of America.
- ^{ap} Also at University of Siena; Italy.
- ^{aq} Also at Washington College, Chestertown, MD; United States of America.
- ^{ar} Also at Yeditepe University, Physics Department, Istanbul; Türkiye.
- * Deceased